View Article Online
View Journal

Green Chemistry

Cutting-edge research for a greener sustainable future

Accepted Manuscript

This article can be cited before page numbers have been issued, to do this please use: B. P. P. Chang, A. Gupta, R. Muthuraj and T. Mekonnen, *Green Chem.*, 2021, DOI: 10.1039/D1GC01115D.

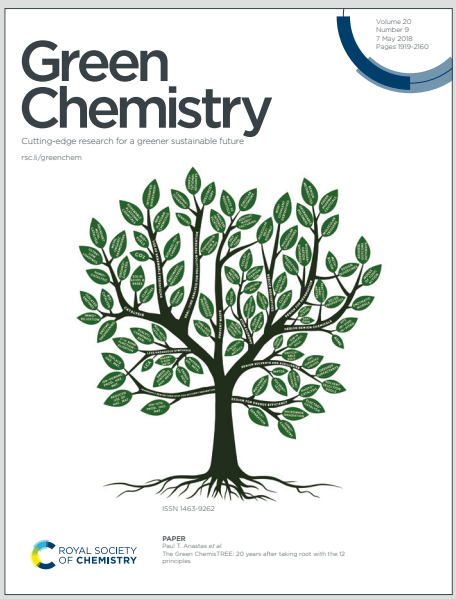

View Article Online
DOI: 10.1039/D1GC01115D

Bioresourced fillers for rubber composites sustainability: Current development and future opportunities

Boon Peng Chang[a], Arvind Gupta[a], Rajendran Muthuraj[d], Tizazu H. Mekonnen[a,b,c]*

[a] Department of Chemical Engineering, University of Waterloo, 200 University Avenue, Engineering 6, N2L 3G1 Canada, Waterloo, ON, Canada;
[b]Institute of Polymer Research, University of Waterloo, Waterloo, ON, Canada
[c]Waterloo Institute for Nanotechnology, University of Waterloo, Waterloo, ON, Canada
[d] Worn Again Technologies Ltd, Bio City, Pennyfoot St, Nottingham, NG1 1GF, United Kingdom

*Corresponding author email: tmekonnen@uwaterloo.ca

Abstract

Ending the fossil fuel era towards a sustainable future will require high-performing renewable materials with a low environmental impact. Carbon black, produced by partial combustion or thermal decomposition of petroleum hydrocarbons, is by far the most dominant filler of rubber composites, followed by mineral fillers (e.g. silica, talc, clay, calcium carbonate, etc.). However, the manufacture of carbon black has a considerable carbon footprint. Similarly, the mineral fillers do not also come without a challenge including poor compatibility with rubber matrices and high density. Consequently, the need for sustainable and green fillers with low or even zero carbon footprint has dramatically increased. In recent years, plant derived sustainable materials, such as cellulose nanocrystals, natural fibers, lignin, biochar, polysaccharides, etc. are extensively investigated as a substitute or complementary fillers of rubbers. In this work, we critically reviewed the recent developments in the innovation and utilization of sustainable biofillers for rubber composite applications, emphasizing the effect of the filler on the structure-processing-property relationship in rubber composites. A wide range of biofillers with an array of structure, morphology, and physico-chemical properties and their various attributes in different rubbers are intensively reviewed and discussed. Effective fabrication strategies and surface modifications platforms on the different biofillers to develop a high-performance sustainable rubber

View Article Online
DOI: 10.1039/D1GC01115D

biocomposites were critically reviewed. Finally, future perspectives for biofillers in rubber composite applications and challenges are discussed.

Keywords: Rubber; Composites; Cellulose; Lignin; Natural fibers, Bioresources

List of Abbreviation

BC	Bacterial cellulose
CNT	Carbon nanotubes
MWCNT	Multiwall carbon nanotubes
CB	Carbon black
GF	Glass fiber
GO	Graphene oxide
CF	Carbon fiber
CNC	Cellulose nanocrystalline
CNF	Cellulose nanofiber
PP	Polypropylene
phr	Mass parts per hundred parts of rubber
VOC	Volatile organic compounds
TiO_2	Titanium dioxide
PLA	Poly(lactic acid)
ZnO	Zinc oxide
PMMA	Poly(methyl methacrylate)
EVA	Polyethylene-co-vinyl acetate
NF	Natural fiber
GTR	Ground tires rubber
MA	Maleic anhydride
MCC	Microcrystalline cellulose
EPDM	Ethylenepropylene-diene monomer
CTE	Coefficient of linear thermal expansion
BR	Polybutadiene rubber
SBR	Styrene butadiene rubber
C-SBR	Carboxylated styrene butadiene rubber
CO_2	Carbon dioxide
$CaCO_3$	Calcium carbonate
SEM	Scanning electron microscopy
$ScCO_2$	Supercritical carbon dioxide
TEM	Transmission electron microscopy
ANBR	Acrylonitrile-butadiene rubber
NBR	Nitrile rubber
NR	Natural rubber
ENR	Epoxidized natural rubber
XNBR	Carboxylated nitrile rubber
WVP	Water vapor permeation

View Article Online
DOI: 10.1039/D1GC01115D

1. Introduction

Renewable and sustainable biobased composites (biocomposites) innovation is among the best solutions to deal with environmental pollution, climate change, and the gradual depletion of finite petroleum resources associated with materials development. From the encouragement and enforcement of government bodies around the globe, biocomposites design and fabrication have become an enticing research topic and new scientific vision in both industry and academia. Industries have started to pursue eco-friendlier alternative materials for consumer products and advanced material fabrications.

Biocomposites are composite materials that are made from at least one biosourced component, i.e., either matrix or filler or both. Biosourced materials include all range of plant fibers, biomasses, and agricultural wastes such as rice husk, sugar beet, starch, sawdust, corn stalk, etc. Presently, natural fibers (NF) are the most widely explored and established biosource constituent for biocomposites fabrication. Due to the lightweight and high specific mechanical properties of NF, the application of NF-based biocomposites in the automotive industry is rapidly increasing in recent years [1, 2]. The substitution of synthetic fiber (e.g., glass fiber (GF)) reinforced composites with NF-reinforced biocomposites can reduce the overall weight of cars, which leads to fuel efficiency and less carbon footprint. In addition, the production of NF-based biocomposites is generally 30% less energy consumptive compared to the traditional synthetic GF-based composites [3].

Biobased fibers extracted from sisal, hemp, jute, kenaf, coir, date-palm, and flax are some of the popular natural fillers for green composites fabrication. Recently, agricultural wastes and co-products are being extensively used to develop biocomposites because of their low to negative cost, availability, and acceptable performances. A large amount of wastes is produced from

View Article Online
DOI: 10.1039/D1GC01115D

agroforestry and agricultural harvesting every year. Most of these wastes end-up in landfill and/or incineration, which are detrimental to the environment. The diversion of and effectively utilizing these waste biomass into value-added products can promote the circular economy concept (waste-to-resources). **Fig. 1** shows the current popular biobased waste fillers that can be utilized as additives or reinforcing agents for biocomposites fabrication after further processing and purification. These waste-derived materials are abundant and possess great potential as multifunctional green biofillers for different polymer systems including rubber.

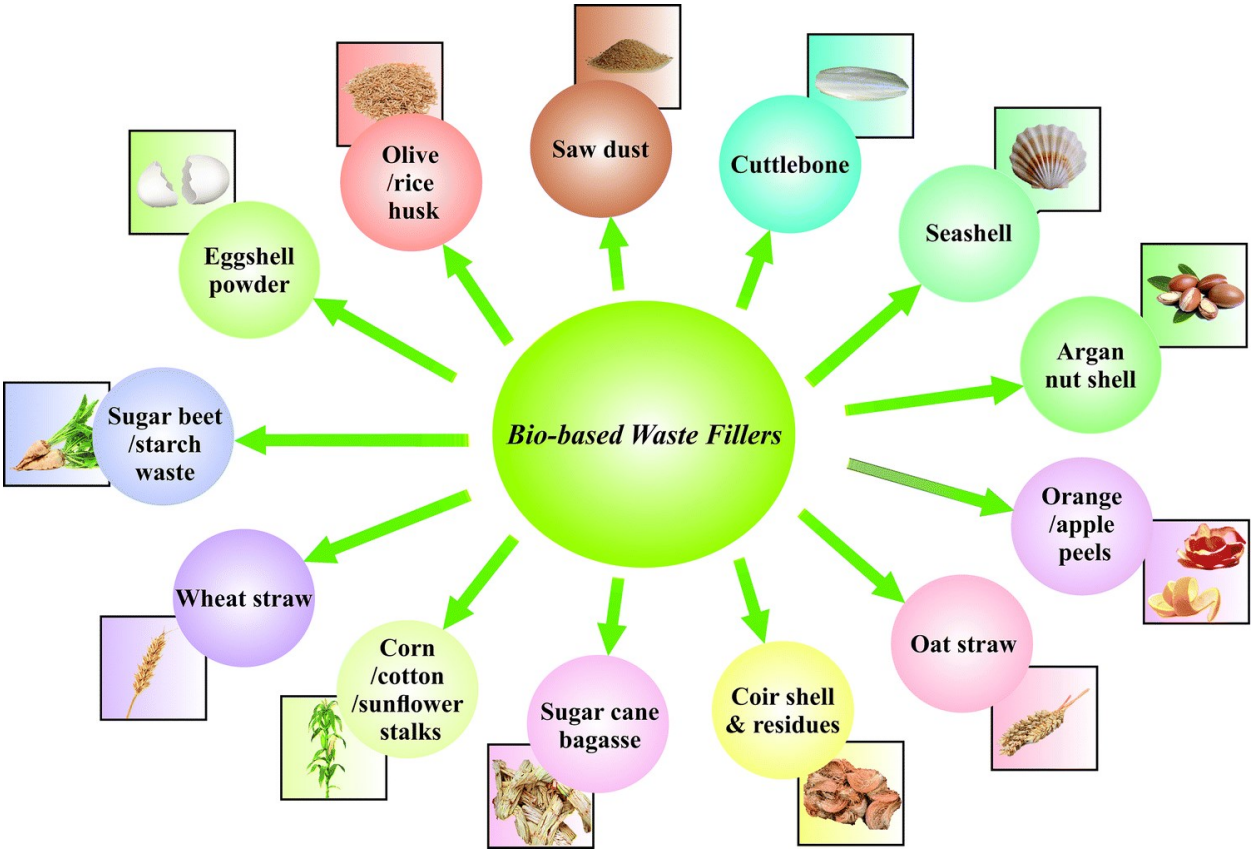

Fig. 1. Various commonly used biosourced fillers and bio-wastes from biomass feedstock for polymer composites applications. Figure adapted with permission from ref. [4]. Copyright Springer, 2019.

Natural rubber (NR) is a natural product produced from rubber plants (*Hevea brasiliensis*) latex and it is one of the essential materials that have been with humans since ancient civilization. It is composed of a complex mixture of different chemical components including, hydrocarbons,

View Article Online
DOI: 10.1039/D1GC01115D

water, starch, proteins, sugars, gums, alkaloids, lipids, and inorganic substances. The latex undergoes a coagulation process upon exposure to air, or through pH adjustment or thermal treatment. Rubber crumb recovered as such has interesting properties, including unique elasticity, good dynamic mechanical performance, and excellent energy absorption that no or few other materials can provide. The expansion of its application in the modern rubber industry started since the discovery of rubber vulcanization with sulfur by Charles Goodyear in the early 19 centuries. Some of the irreplaceable important NR-based products are boots, early tires, gaskets, belts, etc. With the increasing demand for rubber products, non-renewable synthetic rubbers were produced starting from the 20th century (e.g. styrene butadiene rubber (SBR), polybutadiene rubber (BR), polychloroprene (CR), nitrile butadiene rubber (NBR) etc.). In 2018, the global consumption of rubber was around 30 million tonnes of which 13.7 million tonnes were NR [5].

Rubbers, also commonly referred as elastomers, are important class of polymers. Because of their large free volume content, rubber usually requires appropriate additives and reinforcements to obtain useful material properties for different applications. The mechanical strength and stiffness of the rubber filled composites can be enhanced significantly by improving filler-rubber interactions and optimizing the filler dispersion. Currently, carbon black (CB) and silane modified silica are the most commonly used reinforcing filler in rubber composites because of their strong reinforcing effects. Other additives such as crosslinking agents, activators, antioxidants, heat stabilizers, dyes, pigments, plasticizers, etc are also introduced in rubber composites to improve the overall performances.

To date, CB is by far the most applied reinforcing filler in rubber product manufacturing [5]. Over 90% of the worldwide production of CB is used in rubber products such as tires, belts, sidewalls, inner liners, conveyor belts, footware, etc [6]. The good surface reactivity, homogeneity,

View Article Online
DOI: 10.1039/D1GC01115D

and the hierarchical structure of CB make it a promising filler for rubber composite materials [7, 8]. The consumption of CB exceeded one million tons per year in the United States' tire industry alone [9]. However, the production of CB is very energy-intensive and is not sustainable in the long term as it is derived from a finite resources [10]. On the other hand, silica is derived from minerals. Though it is not a petrochemical-based product, it also consumes a lot of energy during production [11]. Furthermore, both CB (~1.7-1.9 g/cm^3) and silica (2.5 g/cm^3) exhibited higher density as compared to the rubber matrix (1.1 g/cm^3) [12]. Therefore, tire manufacturers are looking for alternative light-weight and "greener" substitutes. **Table 1** presented important material properties of common incumbent rubbers fillers and some of the green fillers that can potentially be used in rubber composites applications. It can be noticed that the biobased fillers possesses diverse fundamental properties which exhibited huge potential to replace the existing traditional petroleum-based or mineral-based fillers with satisfactory modulus and high surface area. In addition, the biobased fillers are generally lighter in weight as compared to traditional fillers that can provide weight saving benefits to the rubber composites.

Table 1. Important material properties of some traditional fillers and sustainable biofillers that could be used for rubber composites applications.

Basic properties of various fillers														
Traditionally used fillers								**Relatively new (biobased fillers)**						
Filler	Carbon black	Clay	Silica	Calcium carbonate	Talc	Mica	TiO_2	Biochar	Cellulose nanocrystal (CNC)	Chitin	Eggshell	Kraft lignin	Starch	Natural fibers (Hemp)
Density (g/cm^3)	1.8-2.1	~2.5	~2.65	~2.71	~2.5-2.8	2.7-2.9	4.23	~1.3-1.4	~1.5	~1.43	~2.1	~1.3-1.4	1.5	1.2-1.6
Modulus (GPa)	4-30	2-250 MPa	60-80	70-90	56.25 Ref.[13]	57 Ref.[14]	~220	10-25 Ref[15]	70-134	150 Ref.[16]	41-86 Ref.[17]	4	2.7 Ref.[18]	30-70 Ref.[19]
Color	Black	Brown/ White	White	White	Gray/ White	White	White	Black	White	Brown/ White	Brown/ White	Brown	White	Brown
Surface area (m^2/g)	7-12 Ref.[20]	5.83 Ref.[21]	110-240 Ref.[22]	4.46 Ref.[21]	2.51 Ref.[23]	4.85	98.2 Ref.[24]	438 (Pyrolyzed at 600 °C) Ref.[25]	400-500 Ref.[26]	360 Ref.[27]	19.6 Ref.[28]	15.8 ± 2.5 Ref.[29]	0.9-1.3 Ref.[30]	0.5-1.0
Unique features	Black in color, good mechanical & abrasion resistance	Large ratio of surface area to volume, Good cation exchange capacities	Good optical, mechanical and thermal properties	Nontoxic, odorless, & thermal stable	Softness, lubricity	Platy layers structure	Unique optical, photo stability anti-oxidant & chemical resistance	Black in color, high surface area	Heat stability, customizable, high mechanical strength & high aspect ratio	Bio-compatibility, bio-degradability, non-toxicity	Low cost industrial byproduct, good mechanical properties	Abundant, Hydrophobic, UV protection	Biodegradable, non-toxic, low cost	Light-weight, good thermal and acoustic insulating, biodegradable, processing friendly

Note: Most of the presented information are estimates value that based on the authors current knowledge. They can be varying from the different grades available from the producer in the market around the globe.

View Article Online
DOI: 10.1039/D1GC01115D

In order to reduce the environmental pollution and global warming, there is increasing interest to replace CB and other inorganic mineral-based fillers in rubber materials with more sustainable biobased fillers as an alternative. Biobased fillers including lignin [31], cellulose nanocrystals (CNC) or cellulose nanofibers (CNF)[32], starch [33], eggshell [34, 35], pistachio shell [36], soy protein [37], etc have been explored as reinforcement in the rubber composites.

In alignment with global environmental concerns, industries have shifted their focus into sustainable development in terms of raw materials, energy efficiency, and product recycling. Part of this aim can be achieved by using renewable materials that are derived from various biomass feedstocks or through recycling of agricultural industry wastes. This has accelerated the biocomposites innovation and development as an alternative to traditional synthetic composites. NF and other agro-forestry derived biomass resources have the advantages of being renewable and sustaianble as compared to inorganic traditional fillers. The main challenge of these biobased fillers is their ability to fulfill cost and performance attributes that can be on-par to the current existing traditional fillers. The cellulose incorporated rubber composites were found to improve wear resistance [36], reduced Payne effect [12], and enhance biodegradability of rubber in soil [38]. Composites made from these materials are beneficial to the environment, which can contribute to sustainable development in the future. **Fig. 2** shows the closed loop sustainable approach to produce NR composites with micro-and nano-structured renewable fillers extracted from different biomasses.

View Article Online
DOI: 10.1039/D1GC01115D

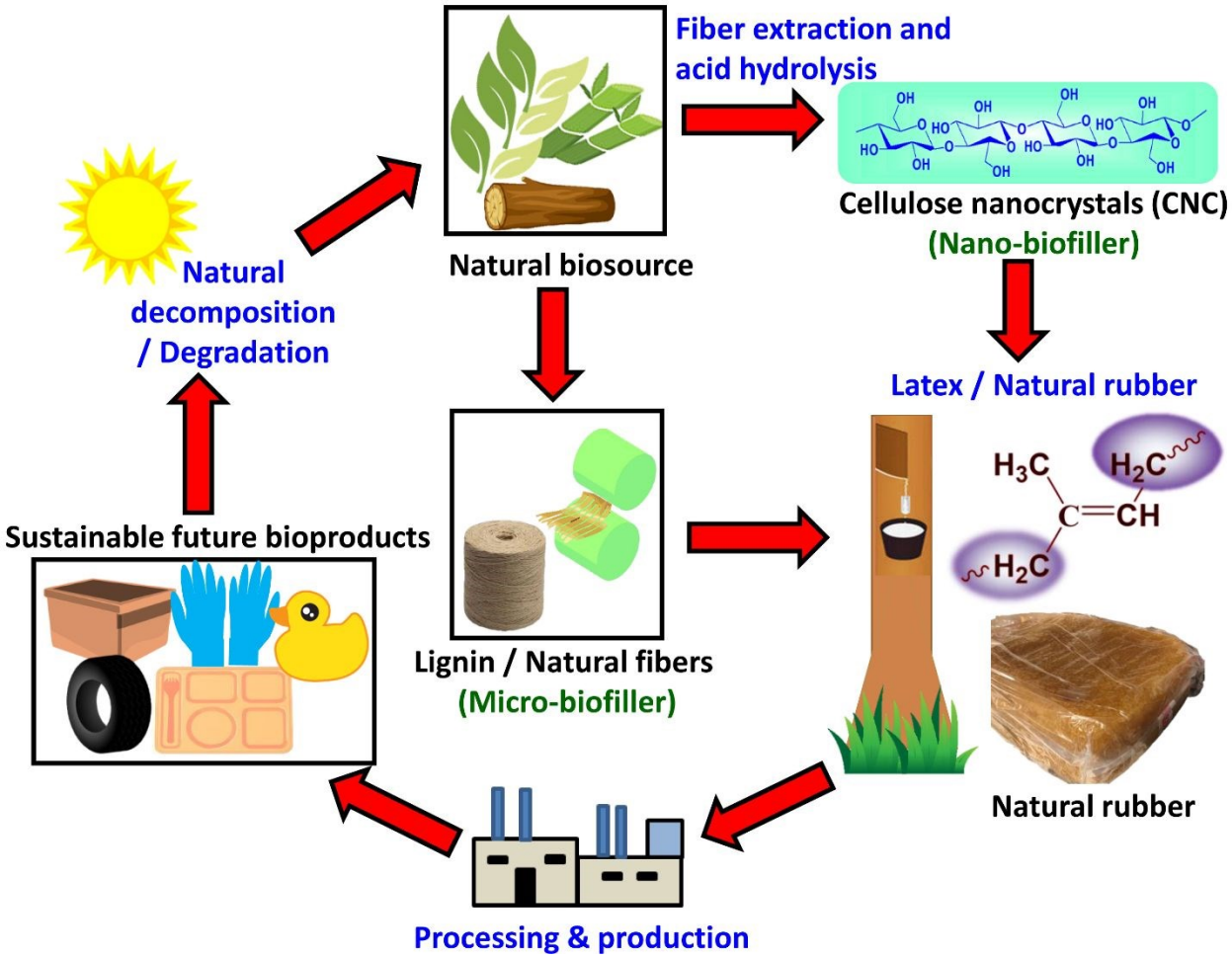

Fig. 2. Schematic diagram of a promising closed loop sustainable approach to develop renewable and sustainable NR-based micro-and nano-biocomposites consumer products.

It is widely accepted that the use of sustainable biofillers for rubber products provides long term environmental benefits; however, the specific performance attributes of these biofillers must be properly evaluated to ensure that they fulfill industrial requirements for specific application. Overall, there is an increasing interest in biomass derived filler reinforced rubber composites for various industrial applications as an alternative to CB or mineral-filled rubber composites. At the same time, biomass supply chain in conjuncture with the performance attributes of the biofillers are among the critical challenges for the successful development of rubber composites with enhanced sustainability and performance. Biomass properties can often vary based on their harvesting time and methods, collection, transport and storage mechanisms, and

View Article Online
DOI: 10.1039/D1GC01115D

extraction/processing methodologies. These variabilities need to be addressed by developing protocols for the effective utilization of biosourced fibers/filler in industrial applications. In many cases, the polarity difference between the natural filler/fibers and rubber matrix typically results in inferior composite performance. The insufficient compatibility between the renewable fibers/fillers and rubber can be overcome by modifying the fibers/fillers or matrix or combination of the two. Hybrid fillers strategy and appropriate processing methods are also important factors to achieve desired properties for specific end-use industrial applications. Another challenge in rubber biocomposites is the recyclability, durability, and service life requirements for engineering applications.

This review presented the recent developments achieved in the use of renewable and sustainable biofillers in rubber composites based on NR, synthetic rubbers, and thermoplastic elastomer matrices. A comprehensive and critical review of the scientific literature, patents, and market studies were carried out. The effect of various fillers on the structure–property of rubber composites and their potential to replace or complement traditional rubber fillers in both lightly crosslinked rubber goods (e.g. gloves) and highly crosslinked rubber products (e.g. tires) are reviewed. **Scheme 1** presents the structure and scope of the review. Finally, future perspective and challenges are discussed.

View Article Online
DOI: 10.1039/D1GC01115D

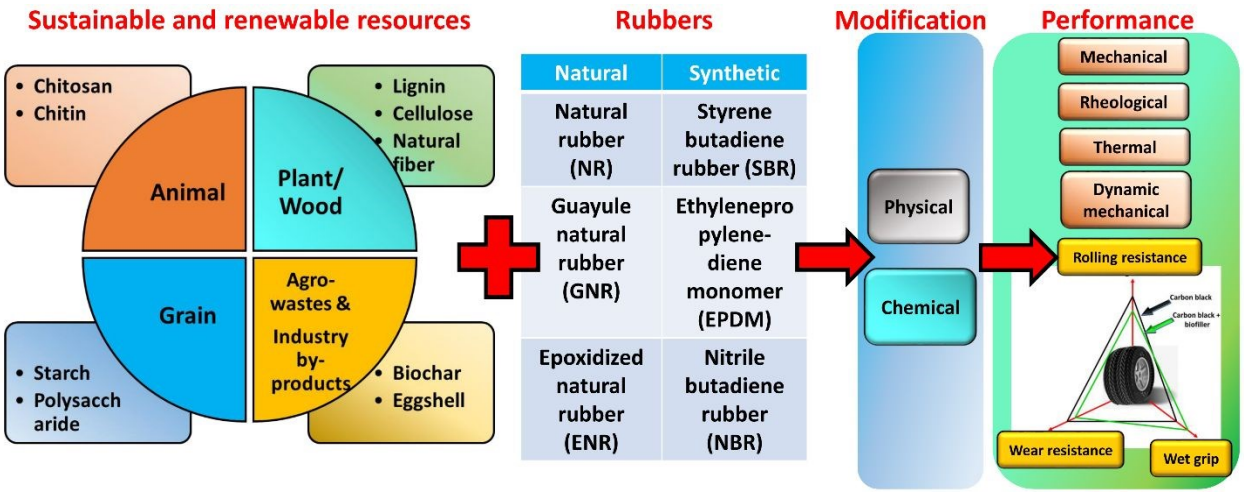

Scheme 1. The complete structure and scope of this review.

2. Towards environmentally friendly green rubber composites

Rubbers are extensively used in several commodity and advanced material applications due to their excellent dynamic and static mechanical properties. Pristine NR develops a crystalline domain due to the realignment of rubber chains when subject to a large strain. These crystalline units work as reinforcement which ultimately enhances mechanical properties at applied high strain [39]. However, to enhance the mechanical properties of the rubber at room temperature, filler mediated reinforcement is usually required.

Rubber compositions are typically filled with particulates such as CB, calcium carbonate ($CaCO_3$), aluminum silicates, talc, mica, and fumed silica to improve the performance and reduce cost [40, 41]. Such compositions are extensively used in various rubber applications, such as tires, conveyor and power transmission belts, foot wares, hoses, gaskets, seals, coatings, mattings, construction, etc. This is because fillers provide excellent mechanical, thermal, and physical properties that would not otherwise be achieved. Depending on their effect on the mechanical performance of rubber compositions, fillers can be classified as reinforcing, semi-reinforcing, or

View Article Online
DOI: 10.1039/D1GC01115D

non-reinforcing. While reinforcing fillers improve the mechanical and abrasion resistance properties of rubber compositions, non-reinforcing fillers simply act as diluents, and semi-reinforcing fillers perform both functions to some extent [42].

The effect of fillers on rubber compositions is related to the intrinsic properties of the filler including particle size, shape, aspect ratio, and interfacial interaction between the rubber elastomer and the filler. CB is the dominant filler used in the tire industry due to its excellent compatibility with common rubbers used in tires, which translates into reinforcement in the form of enhanced dynamic and static mechanical properties. Other fillers such as $CaCO_3$, clays, silica, silicates, talc, and titanium dioxide (TiO_2) are also used as partial substitute of CB usually to impart some performance benefits and improve the cost structure of the rubber [40, 41, 43].

Although CB has been used in the rubber industry for many decades, the carbon footprint of its processing and production is extremely high due to the partial combustion of hydrocarbons. It has been reported that 2.5 tons of CO_2 are emitted during the production of one ton of CB [44]. In addition, studies have found that CB is carcinogenic to humans. Excessive inhalation of this ultra-fine powder causes malignant lung tumors [45] and cell inflammatory [46].

The tire industry is keen on developing rubber compositions that provide low rolling resistance, high wet traction, and long-lifetime to tires, mainly by complementing or replacing a portion of CB fillers or fine-tuning the formulations. Formulations that provide cost-saving, and energy savings through better processability or light-weighting without compromising the performance attributes are of interest as well.

Polysaccharides such as starch [47], cellulose [48], microcrystalline cellulose or cellulose microcrystals (MCC) [11, 49, 50], nanocrystalline and nanofibrillated cellulose [32], cellulose esters [51, 52] are among the promising candidates that are being extensively investigated as potential renewable

View Article Online
DOI: 10.1039/D1GC01115D

reinforcing fillers of rubber, with various degrees of success. Wu et al. [47] reported the use of gelatinized starch as a filler in SBR with an *in situ* compatibilization and results exhibited reinforcing effect in the developed formulation. However, sensitivity to moisture could be a major challenge for starch-based incorporated rubber formulations, owing to the hydrophilic nature of the starch. Replacement of CB with CNC (10 phr, mass parts per hundred parts of rubber) in a ternary blend of NR/butyl rubber/SBR matrix was also shown to improve dynamic and static mechanical performance as compared to the control [32].

2.1. Cellulose fibers

There are growing interests in the scientific community and industries to replace non-sustainable filler with renewable agents without compromising the performances. Due to cost, availability, and performance attributes, cellulose fiber reinforcement of rubber gained substantial attention. The properties of the reinforced rubber composites can be fine-tuned by varying the amount and dimensions of the cellulose [53]. Cellulose (cellulosic fibers) possess relatively high tensile modulus (20-70 GPa) and tensile strength (□1 GPa) depending on their fibril orientation, high aspect ratio (50-200), good flexibility (better than glass fibers), and relatively low cost which makes it an attractive filler material in rubber composites[54].

Bai and Li [11] reported the partial replacement of silica with microcrystalline cellulose (MCC) in rubber composites. They found that the MCC did not adversely affect the mechanical performance of the rubber with up to 18% substitution of silica. The composites with MCC reduced Mooney viscosity and improved heat resistance. However, the tear strength was reduced as compared to the silica-based rubber composites.

Homogeneous dispersion of the filler and favorable thermodynamic interaction between rubber matrix and filler can provide less surface defects with enhanced properties [55]. Different

View Article Online
DOI: 10.1039/D1GC01115D

physical and chemical treatments, such as alkaline treatment, benzylation, etc.,[54] can be taken into consideration in order to enhance the adhesion between fibers and matrix. Physical modifications, such as plasma treatment and electron irradiation can also be used to graft cellulose fibers to NR molecules. Ahlblad and his group[56] have carried out a 5 min plasma treatment of 10 phr cellulose fibers in the presence of butadiene and/or divinylbenzene and found a reduction in hydrophilicity with no water absorption due to the grafting phenomenon. The same research group[57] have employed another physical method called electron irradiation. Results of this study demonstrated the reduction in the hydrophilicity, enhancement in the adhesion and dispersion of cellulose fibers in the rubber matrix, which led to an effective transfer of load between the matrix and cellulose fibers that ultimately improve mechanical properties of rubber.

Another strategy to improve the dispersion of cellulose fibers in rubber, adopted by Reis-Nunes et al. [39, 58] is precipitation/coagulation of NR latex solution with regenerated cellulose (10% aqueous solution of cellulose xanthate) in an acidic medium followed by vulcanization. The homogeneous dispersion of 25% cellulose in the NR matrix led to an enhancement in the tensile strength and tear strength by 64% and 175%, respectively. Also, the addition of cellulose fibers in natural rubber results in reduced gas transport. It is known that the natural and synthetic rubber is available in the form of water suspension (latex), which makes filler dispersion relatively easy. As dispersed cellulose fibers contain primary and secondary hydroxyl moieties, it can react with rubber during the vulcanization and curing process to form chemical bonds[55, 59]. Reinforcing rubber with cellulose powder can result in the improvement of tensile properties and hardness by strain-induced crystallization during stretching which causes the orientation of rubber and cellulose molecules [48].

View Article Online
DOI: 10.1039/D1GC01115D

Although regenerated cellulose is a low-cost potential alternative reinforcing filler in rubbers, properties of produced rubber composites were found to be less than CB-filled rubber composites [60]. Overall, the effect of the reinforcing agent on the rubber depends on the fillers intrinsic properties such as shape, particle size, size distribution, etc. It is anticipated that the nanocomposite of rubber and nanocellulose may result in improved properties [61] as filler's size, shape, aspect ratio, surface characteristics positively affects rubber properties (**Fig. 3**). Nano-sized cellulose (nanocellulose) expected to enhance rubber properties significantly due to its nanoscale morphology that can interact with the elastomer chains at molecular level, enhanced available reactive hydroxyl functional groups, high crystallinity, etc. Nano-sized cellulose can be fabricated from cellulosic fibers using acid hydrolysis which generates 3-50 nm cross-section and submicron length. A brief report about production and application of CNC and cellulose nanofibers is given elsewhere [62-64]. The effect of nanocellulose species on the properties of rubber is discussed in the subsequent section.

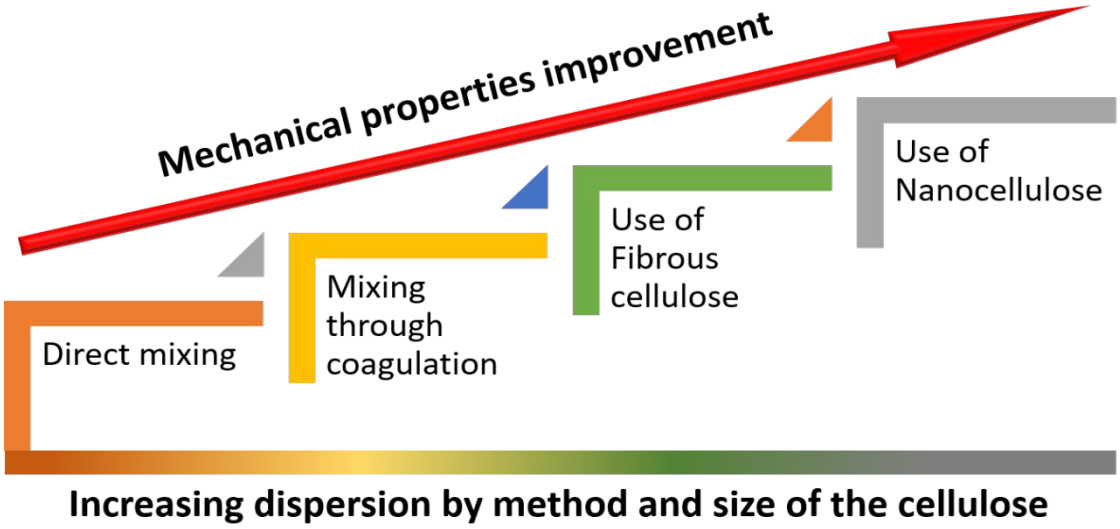

Fig. 3. Effect of different mixing methods and size of cellulose species on rubber mechanical properties.

View Article Online
DOI: 10.1039/D1GC01115D

2.2. Cellulose nanocrystals and cellulose nanofibers

Cellulose nanocrystals (CNC) and cellulose nanofibers (CNF) are the most researched nanocellulose species as a filler for biocomposites including rubber [65]. The main advantages of these CNCs against other nano-fillers are their renewability, abundance, low density, availability of reactive groups, low energy consumption during processing, etc. [66]. They can be extracted from plants using various physical and chemical processes [67]. CNC (also referred as cellulose nanowhiskers) are needle-like or rod-shaped nanoparticles with a size of 10-20 nm in width and several hundred nanometers in length [68], while CNF are nano-size in diameter with micron size in length. **Fig. 4** presents the microscopic images and the main characteristic differences between CNC and CNF and their extraction techniques.

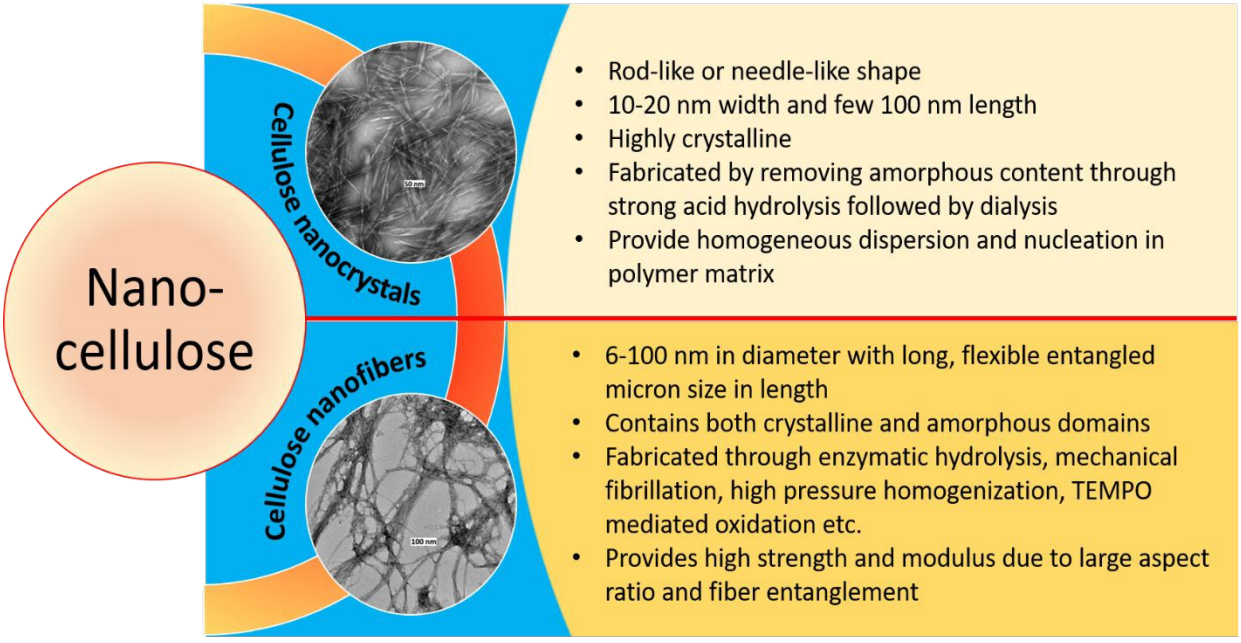

Fig. 4. Microscopic images of both CNC and CNF and main characteristic differences between CNC and CNF and their extraction techniques. Data and TEM image adapted and reproduced from ref. [68]. Copyright ACS, 2013.

Different from the micron sized microcrystalline cellulose (MCC), the nano-size CNCs can maintain the transparency of the parent composites depending on the fabrication technique. Due

View Article Online
DOI: 10.1039/D1GC01115D

to their nano size, CNCs have inherently high surface area among other types of cellulose derivatives. This high specific surface area of nanocellulose exhibited high potential to be used as green and stiff reinforcing agent in different types of polymers for biobased nanocomposites development. The tensile strength and modulus of CNC are estimated to be approximately □14-29 GPa [69] and □143 GPa (measured by Raman spectroscopy on an epoxy/CNC composite), respectively[70]. The crystalline nature of CNCs makes it □1300% stronger with 100-600% higher modulus than the native cellulose. Besides its high specific strength, low density and very low coefficient of thermal expansion (CTE) [71] are also its extra merits for composite applications, especially light-weight auto parts.

At 20 phr loading of CNCs, the tensile strength of nitrile rubber (NBR) has doubled due to enhanced crosslink density[69] resulting from homogeneous dispersion and strong interaction between CNC and NBR. Part of the good reinforcing effect of nanocellulose is due to their high aspect ratio and good interfacial bonding with polar rubber materials[72]. With an optimal CNC contents, a strong percolation network could form in the nanocomposites through hydrogen bonding linkages (interaction between hydroxyl and oxygen of the adjacent molecules) between the nanocellulosic molecules [38, 66, 73]. Also, it was found that CNCs can increase the crosslinking density of the carboxylated styrene butadiene rubber (C-SBR) through hydrogen bonding formation between the hydroxyl groups of CNC and carboxyl groups of C-SBR molecules [74]. Due to the good interfacial compatibility, good stress transfer was observed in the CNC/NBR nanocomposite foams, as shown in the gradual improvement in tensile strength, elongation at break and tear strength without any surface treatment [75].

Overall, the properties of the rubber composites can significantly vary depending on the source of the nanocellulose because the source decides the sequence length of crystalline and

View Article Online
DOI: 10.1039/D1GC01115D

amorphous domains ultimately affecting the dimension of nanocellulose species. Bamboo derived CNC reinforced NR nanocomposites showed better elongation at break than sisal CNC-reinforced NR nanocomposites [67, 76]. Moreover, the mechanical performance depends greatly on the nanocomposites preparation and the properties of the rubber matrix. Also, the unique network structures of nanocellulose allow it to hybridize with different nanoparticles in forming a strong hierarchical structure [77]. CNC can also be used in rubber along with other fillers such as graphene [78], CB [79, 80], silicon dioxide (SiO_2) [81] for different applications.

2.2.1. Effect of CNCs on the thermal properties of rubber

In terms of thermal stability, the onset degradation temperature of the CNC/rubber nanocomposites are usually lower than the neat rubber due to the early degradation of main CNC resulting from the decomposition of glycosyl and sulfate groups arising from the hydrolysis of CNCs[74]. However, there should not be a significant shift of the maximum decomposition temperature to a lower temperature if a strong crosslinking networks are formed in the rubber composites. For instance, a study reported the thermal stability enhancement of NR with the use of bamboo nanocellulose as a reinforcing filler[76]. The great vicinity on the nanocellulose-NR interphases forms a barrier in restricting the NR chain mobility resulting in reduced diffusion of degradation products. Similarly, no adverse effect of CNC extracted from pine pulp on NR composites was found [82]. The strong network formation in the CNC/rubber nanocomposites (e.g. nitrile rubber) can also be reflected in the enhancement of the storage modulus before glass transition temperature and the glass transition temperature could shift to higher temperatures. In other words, enhancement in the glass transition can also be a measure of the degree of interaction between components. Interaction of cellulosic nanoparticles with polychloroprene rubber results in reduction in free volume and ultimately suppress the rubber chains mobility causing upshift in

View Article Online
DOI: 10.1039/D1GC01115D

glass transition temperature [83]. However, studies also reported that there is no significant changes in the glass transition in case of NR after the incorporation of CNCs [38].

2.2.2. Effect of CNCs on static and dynamic mechanical properties of rubber

Pasquini et al.[84] observed that the incorporation of cassava bagasse CNC in NR enhanced the tensile storage modulus significantly, which increased with the increase in the CNC loading levels. Similarly, when 15 phr CNC, produced using cottonseed linter pulp, was used to reinforce C-SBR matrix, the storage modulus below the glass transition has increased by as much as 55% [74]. Strong filler to filler interaction also called percolation structure and interaction with C-SBR plays a major role in the increase in storage modulus. Bacterial cellulose (BC), which is a nano-fibrous cellulose produced by bacteria, could also be used as reinforcing biofillers in NR. Comparison of the stress-strain curve of neat NR with 2.5% of BC filled NR, the properties did not display noticeable change at such low levels of filler loading. However, high amount of BC (around 5-10%) enhanced the tensile strength and modulus of the NR by 80% and around 900%, respectively while making the NR brittle and relatively less stretchable. Incorporation of 5% CNC, extracted from pine pulp, in pre-vulcanized NR results in increased tensile strength (38%) and modulus (433%) along with storage modulus. Conversely, ductility was found to reduce (~16%) due to reinforcing effect of CNC [82].

A peculiar phenomenon of CNC fibers is that the inter and intra-molecular hydrogen bonding leads to high modulus in dry conditions whereas disintegration of the molecular network and weakened filler-filler interaction happens upon exposure to water resulting in reduction in modulus [85]. This repetitive change in modulus due to moisture interaction can make CNC and its composite a water/moisture responsive materials [86, 87]. Storage modulus of biocomposites of CNC with NR increase from 1.2 MPa to 2.6 MPa, whereas in case of epoxidized natural rubber (ENR)

View Article Online
DOI: 10.1039/D1GC01115D

and CNC based biocomposite, it increased to 25 MPa at 37 °C to be utilized for water responsive biomedical applications [88]. In the case of ENR, dual network formation, i.e. filler-filler and filler-matrix synergistically improve the modulus and show good reversibility in moisture triggered tunable mechanical behavior.

Rubber applications in specific industries require load bearing while maintaining low density. In such cases, rubber foams come handy as the foaming significantly reduces the density of matrix[89, 90]. However, pure rubber cannot provide the required load support on its own mechanical integrity [91]. The use of CNCs that provide reinforcement, while maintaining low density could be appealing in such cases. Moreover, the presence of hydroxyl groups on the surface of CNC promotes hydrogen bonding with some rubbers, such as NBR (**Fig. 5a**). Reinforcing NBR foam with 15 phr CNC greatly enhances the tensile strength (from 3.7 MPa to 6.5 MPa) and tear strength (around 10 kN/m to 15.8 kN/m) (**Fig. 5c**) [75]. This enhancement in the mechanical properties was the result of enhanced crosslink density which can be resulted from the increased volume fraction of the rubber (**Fig. 5b**). This possible physical crosslinking promoted by hydroxyl groups present on CNC and -C≡N group of NBR chain also led to doubling of the storage modulus (from 610 MPa to 1150 MPa) below the glass transition temperature of the NBR. As proposed by Blanchard et.al. [92], the formation of Zn-CNC complex implies that the CNCs assists in enhancing the dispersion of ZnO that results in higher crosslinking density though the sulfur quantity (crosslinking agent) was kept constant. Consequently, the enhanced crosslinking in conjuncture with the reinforcing capability of CNCs results in improved tensile strength, and modulus that increased from 2 MPa to 7 MPa, and 3 kPa to 11 kPa, respectively, with the use of only 5 phr CNCs.

View Article Online
DOI: 10.1039/D1GC01115D

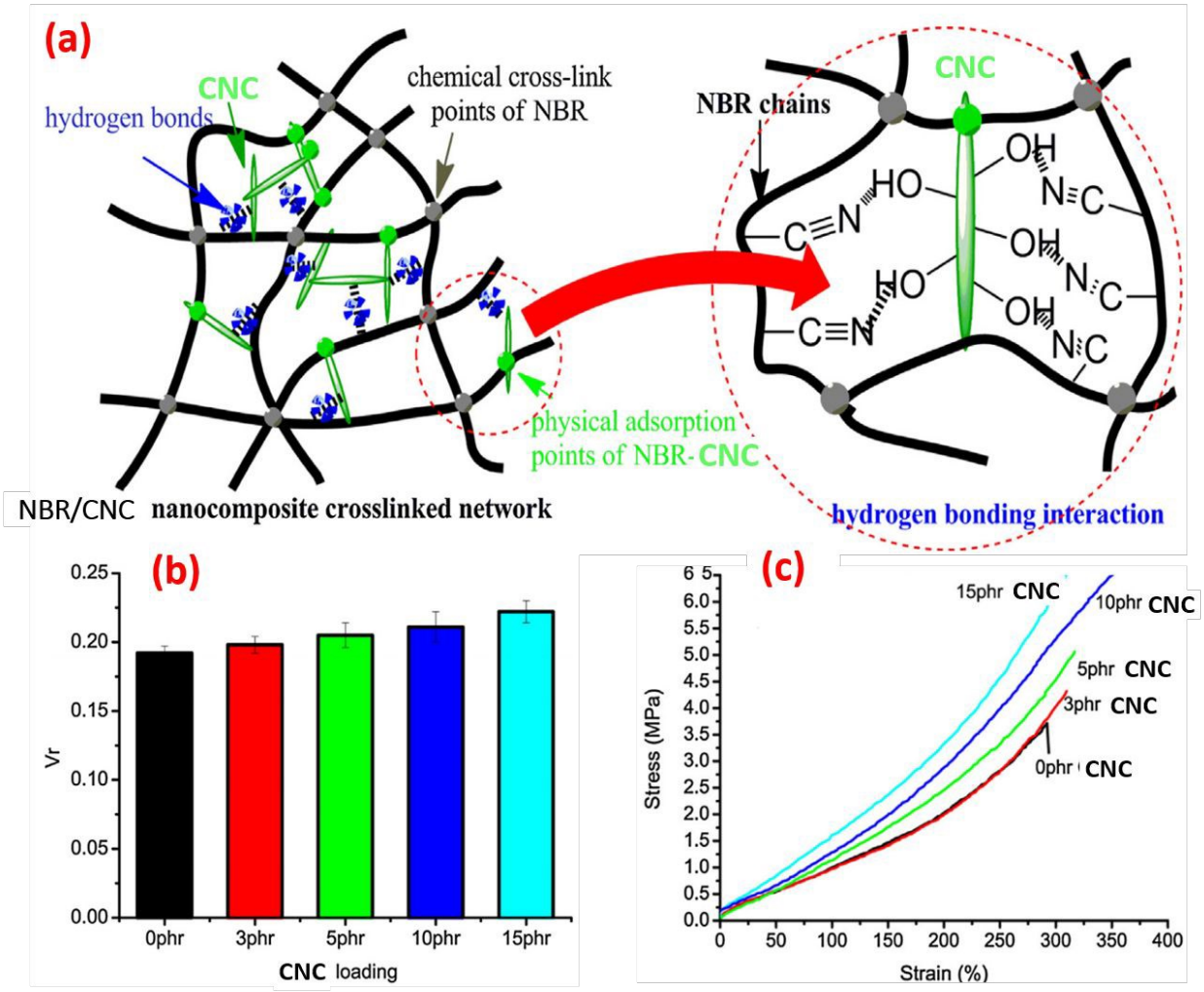

Fig. 5. (a) Possible hydrogen bonding mechanism of cellulose nanocrystals (CNC) with nitrile rubber (NBR), (b) its effect on volume fraction of rubber (V_r), and (c) stress-strain curve (phr, parts per hundred). Figure adapted and reproduced from ref. [75]. Copyright Elsevier, 2015.

Targeted chemical modification of CNCs and formation of chemical bond with elastomers can develop crosslink at the polymer interface and provide synergistic crosslinking and reinforcement effects[93-95]. Chemical modification of CNC using hydrocarbon chains containing thiol (-SH) groups and its dispersion in NR significantly improve the mechanical properties of rubber. Covalent bond or cross-linking between thiol groups and double bonds of rubber can be formed by photo-chemical reaction[96]. Kanoth et.al.[97] have fabricated a cross-linkable thiol modified CNC by esterification reaction with 11-mercaptoundecanoic acid and crosslinked with

View Article Online
DOI: 10.1039/D1GC01115D

NR via UV irradiation (**Fig. 6a**). The resulting covalent bond between the filler and matrix interface (10 phr modified CNC content) led to an increase in tensile strength, modulus, and strain at failure by 325%, 84%, 33%, respectively, in comparison to neat NR as shown in **Fig. 6 (b & c)**. Long hydrocarbon chain reduces the hydrophilicity of the CNCs and enhances its compatibility with and dispersion in NR, which ultimately enhance mechanical properties. It is also hypothesized that if the rubber network is crosslinked by a traditional vulcanization method, the reinforcing effect may give multifold improvement in mechanical properties [97]. In another work performed by Fumagalli et. al. [98], CNC was modified using palmitoyl chloride and 3,3`-Dithiodipropionic acid chloride (DTACL) to yield a hydrophobic CNC due to introduction of alkyl moieties and CNC with reactive surface due to incorporation of disulfide function, respectively. Incorporation of 17% modified CNC in SBR during melt processing, result in significant reinforcement (tensile strength increase from 2 MPa to 9 MPa, modulus increased from 10 MPa to 47 MPa) against neat SBR, whereas extensibility remained in the desired range (elongation was reduced from 368% to 329% only). The chemical reactive disulfide interaction bonding between DTACL modified CNC and SBR was responsible for the strain hardening effect.

In the case of hydrogenated acrylonitrile-butadiene rubber (ANBR), the use of 5% TEMPO (2,2,6,6-tetramethylpiperidine-1-oxyl radical) oxidized cellulose nanofibers (TOCN) produces high modulus (~45 MPa) composites [99]. Another researcher reported a tensile modulus of 63 MPa and a storage modulus of 112 MPa at 25°C with 5% TOCN hydrogenated ANBR [100]. Another method to enhance TOCN dispersion is proposed by Noguchi et. al. [101]. They reported that high-shear kneading can contribute to an improved dispersion of TOCN with greater homogeneity in the rubber matrix, which ultimately resulted in high tensile strength (~20 MPa), modulus (400 MPa), and storage modulus (>1200 MPa).

View Article Online
DOI: 10.1039/D1GC01115D

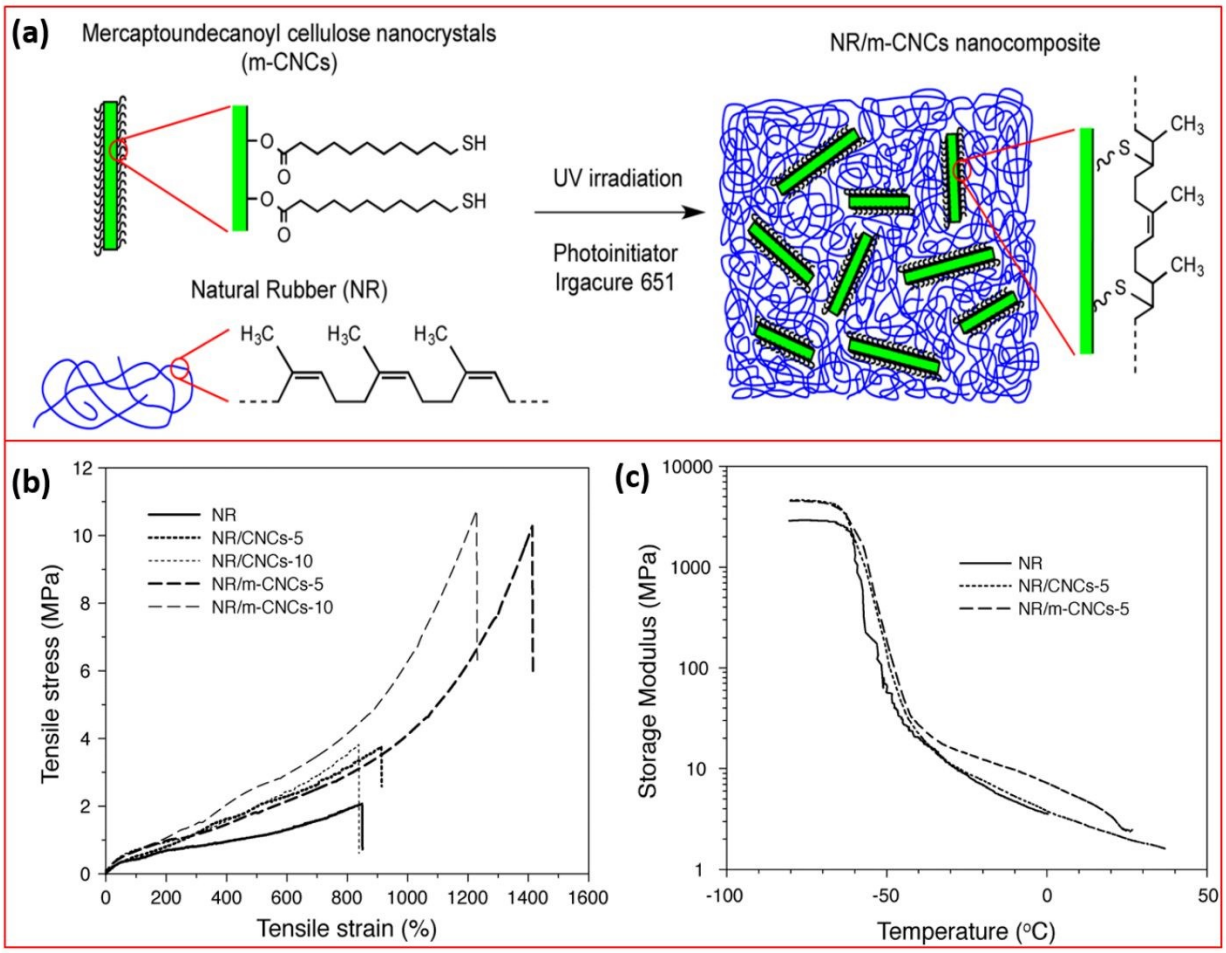

Fig. 6. Chemical modification of CNC with Thiol group and its photo initiated reaction with natural rubber (NR) that leads to its homogeneous dispersion (a) and its effect on tensile properties (b) and storage modulus (c). Figure adapted and reproduced from ref. [97]. Copyright ACS, 2015.

The Steglich esterification is a mild reaction that uses 1-ethyl-3-(3-dimethylaminopropyl)-carbodiimide (EDC) as a coupling reagent to produce ester from alcohol and carboxylic acid catalyzed by 4-dimethylaminopyridine (DMAP). In Steglich esterification technique, the functionalization of CNF with –SH or –C=C and its use in SBR as reinforcing agent was found to be more effective than CB. Tensile strength and modulus were improved from 3.2 to 12.3 MPa and 1.7 MPa to 27 MPa, respectively [102]. Modification of CNC via surface grafting with poly(lactic acid) with 3% total grafted PLA on the CNC improved the tensile strength and modulus of chloroprene rubber by 200% and 400%, respectively [103]. Grafting with lactic acid makes CNC

View Article Online
DOI: 10.1039/D1GC01115D

hydrophobic and improves the dispersion in the rubber matrix. Some other mechanical properties improvement related to different nanocellulose species and rubber composites are listed in **Table 2**. Further understaning of surface modification of CNC is condensed elsewhere [104].

2.2.3. Effect of CNCs on rubber rheology

Final product designing and processing is extremely depending on the viscoelastic characteristics of rubber and its blend and composites. Rheological evaluation of the materials is the most reliable technique to understand viscoelastic behavior of the composites before vulcanization. Rubbers have inherent crystallization behavior upon application of strain that results in higher tensile strength and viscosity. Before rubber processing, it is important to understand the vulcanization process which consists of different stages. Scorch time or cure induction time is an important parameter for rubber curing and processing. After completion of scorch time, crosslinking starts and rubber loses its fluidity. Optimization and understanding of such parameters decides the processing conditions and its different desired properties. After the induction time, crosslinking of rubber molecules starts drastically and a huge rise in elastic modulus (G') can be noticed in rheology data. Elastic modulus (G') is measure of energy storage by the material at particular temperature and its increment at low frequencies give information about rolling resistance of the rubber. This rise in elastic modulus continues until crosslinking completes and a plateau confirms the equilibrium curing. The use of fillers or reinforcing agents in rubbers can affect these parameters depending on the loading concentration, particle size, interfacial interaction and adhesion of filler and rubber chains.

A strong filler-polymer interfacial adhesion is crucial factor for reinforcement. Rubber matrix and filler interaction can be understood and quantified using rheological characteristics. The CNCs as fillers hinders the movement of rubber chains ultimately increasing the viscosity.

View Article Online
DOI: 10.1039/D1GC01115D

The crosslinked network structure formation during the vulcanization process immobilize CNC within cavities of crosslinked NR network. The complex formation between CNC-NR through curing agent and during curing process and filler-filler percolation network formation before curing results in the development of a homogeneously dispersed and robust structure, which has relatively high viscosity. Due to high aspect ratio and cylindrical shape of CNCs, increase in viscosity found to be a function of the amount of filler [105]. In order to enhance CNCs dispersion, oxidation of natural rubber can be another way which generates hydroxyl functional group on the backbone of NR that likely allow it to interact with CNC through hydrogen bonding. Such hydrogen bonding and filler-rubber interaction leads to enhanced viscosity at lower shear rate [106]. In the case of C-SBR, incorporation of CNCs promote the gelation and reduce induction time, which may be the result of hydrogen bonding between hydroxyl group of CNC and carboxylic acid groups of rubber upon mixing. It leads to the formation of a C-SBR rigid network loaded with CNC that have enhanced elastic modulus [107].

Contrary to elastic modulus, loss factor (tan δ) is the ratio of dissipated energy over stored energy. It is desired to have low tan δ at low frequencies because stored energy reduces rolling resistance. Whereas, high value of tan δ is needed at higher frequencies as energy loss enhances grip. Presence of CNC in C-SBR matrix cause higher tan δ which indicates enhanced viscous properties of C-SBR composites which improves the energy dissipation [107].

Another rheological property which is mainly observed in filler reinforced/filled rubbers called Payne effect, is related to softening of the rubber compound against induced strain. It describes the strength of filler network in repetitive low stain deformation and quantitatively it is the decrease in the elastic modulus of highly reinforced uncured rubber with increase in strain. It is related to the change in material's microstructure induced by repetitive deformation during low

View Article Online
DOI: 10.1039/D1GC01115D

amplitude dynamics. In other words, it can be ascribed to breakage and recovery of relatively week physical bonds which links neighboring filler aggregates under periodic loads. Increase in the strain induces typical reduction in elastic modulus and difference in the maximum and minimum G' can be used to quantify Payne effect and denoted as ΔG' at particular strain. For industrial production of tire, normally 350-400 kPa ΔG' is an acceptable range which indicate sufficient filler-filler interaction. Low amount (3 phr) of CNC in 30% silica filled natural rubber weaken the Payne effect confirming improved filler dispersion and filler-rubber interaction [108]. Normally, the addition of CNCs together with either silica or carbon black that are incorporated in rubber matrix as agglomerates can help improve their dispersion attributed to its nanostructure, high surface area, and high aspect ratio. The incorporation of a secondary reinforcing filler such as CNC may interrupts undesirable filler networks and reduce the Payne effect as depicted in **Fig. 7**. These usually have a positive impact in rubber composite materials (e.g. reducing rolling resistance of tires, thereby improving driving fuel efficiency).

View Article Online
DOI: 10.1039/D1GC01115D

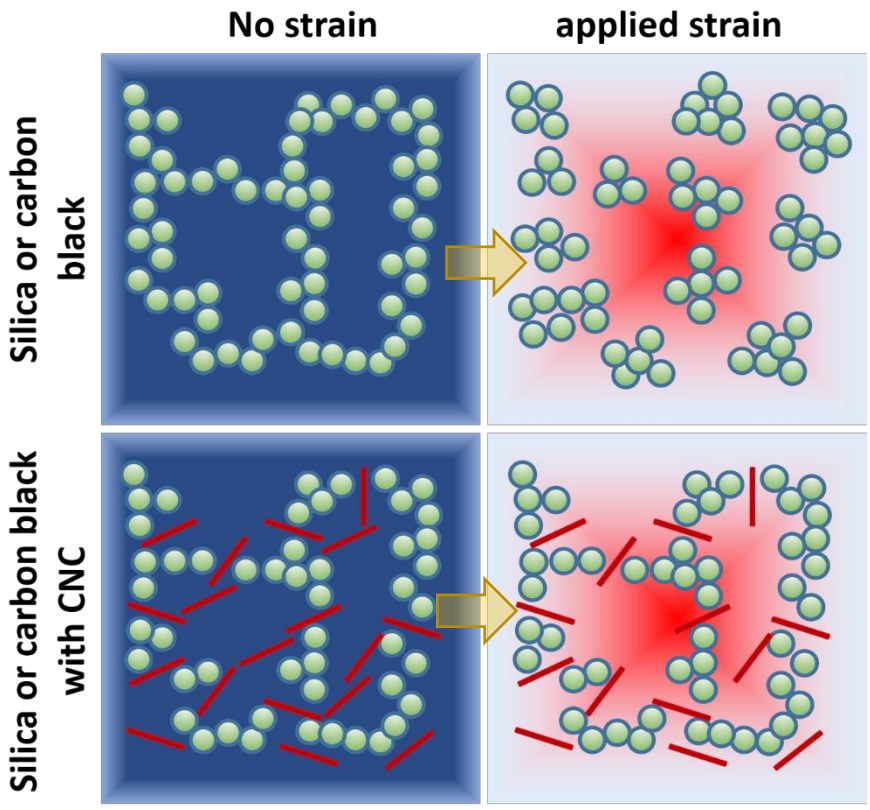

Fig. 7. Strain softening comparison between silica or carbon black-rubber formulation and hybrid network with CNC before and after applied strain.

2.2.4. CNC based rubber composites for packaging application

Barrier properties (both oxygen and water), moisture absorption, and degradation test are important attributes for materials to be used in packaging applications. The high crystallinity of CNCs provide positive effects on the water vapor permeation and barrier properties when a stable percolated cellulose network is established. The water vapor permeation (WVP) was found to increase with increasing CNC content initially [38]. However, the WVP of the rubber composites was reduced drastically when CNC loading was above 7.5 wt.% due to the formation of cellulose network. Similarly, moisture absorption reaches a plateau when optimum CNC loading is incorporated in rubber matrices[38]. Packaging films with very low gas permeability and relatively good tensile strength can be fabricated using nanocellulose-based NR composites. Also, the

View Article Online
DOI: 10.1039/D1GC01115D

incorporation of nanocellulose in NR matrix contributes to the enhancement in the biodegradability of the composites [109]. The use of CNF as filler in the NR matrix could also enhanced the grease resistance which makes this material more useful for packaging applications [110].

2.2.5. Biodegradation of CNC based rubber composites

Rubber films have been employed for a range of packing applications (foods, electronics, toys, etc.), which are typically utilized for single and short time use. After the short service life of such material is over, it can either be reused, repurposed, recycled, landfilled, or in some cases degraded to its constituents. Biodegradation of packaging materials, whereby materials are metabolized by microorganisms and converted into its basic components is another appealing end of life for polymers that reduces the ecological impact of plastics and elastomers [111]. Biodegradation of natural rubber is specifically of great interest as it is a natural product [112]. Many studies indicate that native natural rubber is biodegradable [112], however the crosslinking process that instils covalent bond between the chains limits its biodegradation.

The presence of nanocellulose could increase the rate of biodegradation of rubber in soil as the rate of biodegradation of cellulose is faster than rubber. Due to higher degradation rate of cellulose component in the nanocomposites films, microorganisms consumes cellulose faster than NR leading to increased porosity, void formation, and the loss of the integrity of the rubber matrix. The rubber matrix is then broken down into smaller particles with high surface area via the disintegration[38], which can promote its ultimate biodegradation. For instance, the presence of 12.5% CNF resulted in 71% biodegradation of NR within 4 weeks in soil [38]. Crosslinking of the NR may slow the rate of biodegradation even in presence of cellulose due to reduced accessibility for microorganisms [113]. Non-crosslinked NR/CNF nanocomposites promise a higher degree of

View Article Online
DOI: 10.1039/D1GC01115D

biodegradation, which is accelerated due to the presence of CNF [113] and possibly other types of cellulosic fillers.

Table 2. Some of the main mechanical properties improvement of cellulose nanocrystal reinforced rubber composites (only works published in recent 10 years are included).

Nanocellulose species	Rubber	Fiber treatment/ modification	Fiber loading	Highest TS achieved (MPa)	Highest E achieved (MPa)	EAB (%)	Other improvement	Ref.
CNF	NR	-No	2.5, 5, 7.5 & 10%	1.6 → 12.2 (at 10%)	1.3 → 9.6 (at 10%)	↓ with ↑ fiber content	CNF increased the rate of degradation of the composite when subjected to composting	113
CNC-RGO Hybrid	NR	CNC mediated assembly of graphene	1.25 & 2.08 vol.%	0.2 → 1.9 (at 2.08 vol.%)	Improved	440 → 550 (at 1.25 vol.%)	Significantly enhance electric conductivity and mechanical properties through 3D conductive network	78
Polyaniline-CNC Hybrid	NR	In situ polymerization of CNC with aniline	PANI-CNC/NR (15/10/100) wt.%	1.7 → 6.1	0.4 → 10.7	610 → 377	3D hierarchical structure significantly improved the electrical conductivity and	114

							mechanical properties simultaneously	
CNC/CB Hybrid	NR	CNC sonication with CB	2.5-7.5 phr	0.86 → 7.4	0.45 → 23.2	~450% vs 580% CB/NR vs CB/CNC/NR	Hybrid of CNC/CB 3D network enhance the electrical conductivity and mechanical properties simultaneously	115
CNC	Nitrile rubber foam	-No	3-15 phr	3.7 → 6.6 (at 15 phr)	N.A.	300 → 330 (at 10 phr)	Strong interfacial adhesion resulted in excellent reinforcement	75
CNC	C-SBR	-No	3-15 phr	16.9 → 24.1 (at 15 phr)	N.A.	~250 → 300 (at 10 phr)	Significant increase in tear strength with increasing CNC	74
CNC	Nitrile rubber	-No	5-20 phr	7.7 → 15.8	N.A.	↓ with ↑ fiber content	-Tear strength increases with increasing CNC -T_g shifted to a higher temp. with increasing CNC	69

CNP	NR	-Mechanical shearing -Enzymatic treatment -Acid hydrolysis	6 wt.%	0.56 → 6.6	0.50 → 109	576 → 849	-Different fiber treatment results in different mechanical properties enhancement	[67]
CNC	NR	3-aminopropyl-triethoxysilane	5-25 phr	Modified CNC showed ↑ TS	Modified CNC showed ↑ E	Modified CNC showed ↑ EAB	-Accelerated curing rate, reduced Payne effect -Improved tear strength hardness, & heat build-up	[12]
CNC	NR (crosslinked)	-No	2.5-10 wt.%	9.2 → 17.3 (at 10 wt.%)	1.7 → 3.8 (at 10 wt.%)	554 → 455 (at 10 wt.%)	Significant improvement on mechanical properties and thermal stability	[76]
CNC	NR	-No	2.5-12.5 wt.%	↑ 374%	↑ 530%	↓ EAB	-Optimal CNC loading exhibited positive impact on barrier properties	[38]

							-Presence of CNC increased the rate of degradation of rubber in soil.	

CNF: Cellulose nanofiber; CNC: Cellulose nanocrystal; CNP: Cellulose nanoparticles; RGO: Reduced graphene oxide; CB: Carbon black; TS: Tensile strength; E: Modulus; EAB: Elongation at break; N.A.: Not available; C-SBR: Carboxylated styrene-butadiene rubber; T_g: Glass transition temperature; Temp: Temperature, phr: parts per hundred.

View Article Online
DOI: 10.1039/D1GC01115D

3. Starch, nanostarch, and other polysaccharides

3.1. Starch and nanostarch

Starch is a class of polysaccharides, which are a highly functional renewable biopolymer extracted from the natural feedstock (e.g., potato and corn) and extensively used in a range of industrial goods in addition to the food industry [116]. It possesses a cyclic structure along with hydrogen bonding making it structurally rigid. Due to such rigidity and crystalline content, starch has a relatively high glass transition and melting temperature. Starch as a material retains several appealing attributes such as low density, availability, environmental friendliness, and low cost that make it a potentially promising biofiller for rubber composite applications. However, it has high polarity associated with the surface –OH moieties, which is not compatible with the typically non-polar rubber matrices. Nevertheless, the hydroxyl groups on the surface of starch are amenable to a wide array of chemical modifications and functionalization [117-120].

The incorporation of starch in the rubber matrix can provide a reinforcing effect along with increased bio-based content and enhanced biodegradation rate. Starch itself can be used as polymer matrix, however, depending on the form of starch such as particle size (macro, - micro-nanoparticles), melt state, and relative modulus associated with its source displays different reinforcing effects. It is known that the rubbers are nonpolar entity whereas starch is highly polar which make these materials incompatible to each other. Using starch as polymer form leads to enhance biodegradation rate, reduced cost, may improve gas barrier, while starch as particles works as reinforcing agent in rubber. The particle form of starch helps to fabricate rubber composite with high crosslinking and improved mechanical strength and modulus. Independent of the form and state, miscibility of starch with rubber is crucial to extract its maximum benefit for development of rubber starch blend and composites.

View Article Online
DOI: 10.1039/D1GC01115D

In general, extensive high shear mixing produces good dispersion of polysaccharide particles in rubbers that result in good reinforcing effect including starch [121]. For instance, it was reported that the coagulation of NR-filled with 10 phr cassava starch showed improvement in mechanical properties compared to the NR/starch composites prepared by direct mixing [122]. Starch may also work as a vulcanizing agent for NR through the reaction of hydroxyl and C=C bond of NR without any chemical catalyst that ultimately reduce the cure time even at higher loading (up to 50%) [123]. The addition of 2 phr starch grafted NR (NR-g-St) which acts as a coupling agent was found to enhance the compatibility of natural fibers (NF) with NR matrix. Grafting of starch molecules with NR leads to the fabrication of molecules with polar-nonpolar combination that acts as a bridge between NR and NF molecules. This bridge enhances the interfacial interaction of NR and NF by development of hydrogen bonding between polar part of filler and coupling agent and crosslinking among nonpolar rubber and NR-g-St during curing process. Addition of NR-g-St also helps to accelerate the formation of crosslink precursor and reduce activation energy required for curing ultimately reducing the cure time from 33 min (NR/NF compound without coupling agent) to 10 min (NR/NF compound with coupling agent) [124]. The porous structure of starch and other organic fillers can trap air and sound, which can improve the acoustic properties of rubber as well [125]. Furthermore, the use of starch in rubbers could help to reduce or remove the use of expensive and environmentally non-friendly coupling agents for properties enhancement in NR or other elastomer composite formulations [126].

Further improvement in the properties of modified starch with NR can be done by enhancing the crosslinking using high energy radiation techniques. Senna et. al. [127] demonstrated that modification of starch with resorcinol and formaldehyde and its incorporation in natural rubber, which enhanced the thermal stability against unmodified starch-NR composite, however,

View Article Online
DOI: 10.1039/D1GC01115D

it was still lower than the pristine natural rubber. Thermal stability was further enhanced after irradiation due to an increased interfacial adhesion through irradiation driven free radical formation at the interface. However, the tensile strength of the modified starch filled composites (6.44 MPa) reduced to similar values as that of the NR (2.01 MPa) after irradiation. This reduction can be the consequence of starch degradation during irradiation.

Chemical modification or grafting of other polymers on to starch such as poly(methyl methacrylate) (PMMA), NR[128], polybutylacrylate[129], dicumyl peroxide driven homo-polymerization of sodium acrylate [130], etc. can improve the interfacial bonding of the constituents. For example, PMMA grafted starch was found to be able to enhance the physical entanglement which leads to an increase in tensile strength of SBR from 2.9 MPa up to 9.7 MPa [131]. Further interfacial interaction bonding between starch and SBR molecules can be improved by using suitable coupling agents such as bis(3-triethoxysilyl propyl) tetrasulfide (TESPT), 3-aminopropyl triethoxysilane (APTES), 3-Mercaptopropyl triethoxysilane (MPTES), 4,4-methylene bis (phenyl isocyanate) (MDI) etc. Li et. al. [33] reported that the use of MDI affects the interfacial interaction significantly. Due to this coupling effect of starch, the tensile strength and modulus of SBR was enhanced by 14% and 159%, respectively.

Starch nanoparticles fabricated using acid hydrolysis, micro-emulsion method[132] also have interesting properties to be used as reinforcing agent in rubbers. It contains crystalline nano-platelet structure in the size range of 6-8 nm and length and width of 20-40 nm and 15-30 nm, respectively[133]. Angellier et. al. [134] reported that the nano-sized starch fabricated from waxy maize starch can form percolating network within NR matrix via hydrogen bonding between starch nanoparticles. The authors concluded that the starch nanoparticles enhanced the storage modulus and strength at break by 75% and 4%, respectively while reducing the elongation at break by only

View Article Online
DOI: 10.1039/D1GC01115D

25%. Adsorption/desorption or in other words sliding of NR chains over starch nanoparticle's surface is responsible for nonlinear viscoelastic behavior during shear [135]. Overall, the incorporation of starch enhances the biobased content and mechanical properties of rubbers. As such, starch is a promising candidate as it provides dual effects in the rubbers system. It can work as reinforcing agent along with a coupling agent effect in rubbers (**Fig. 8**).

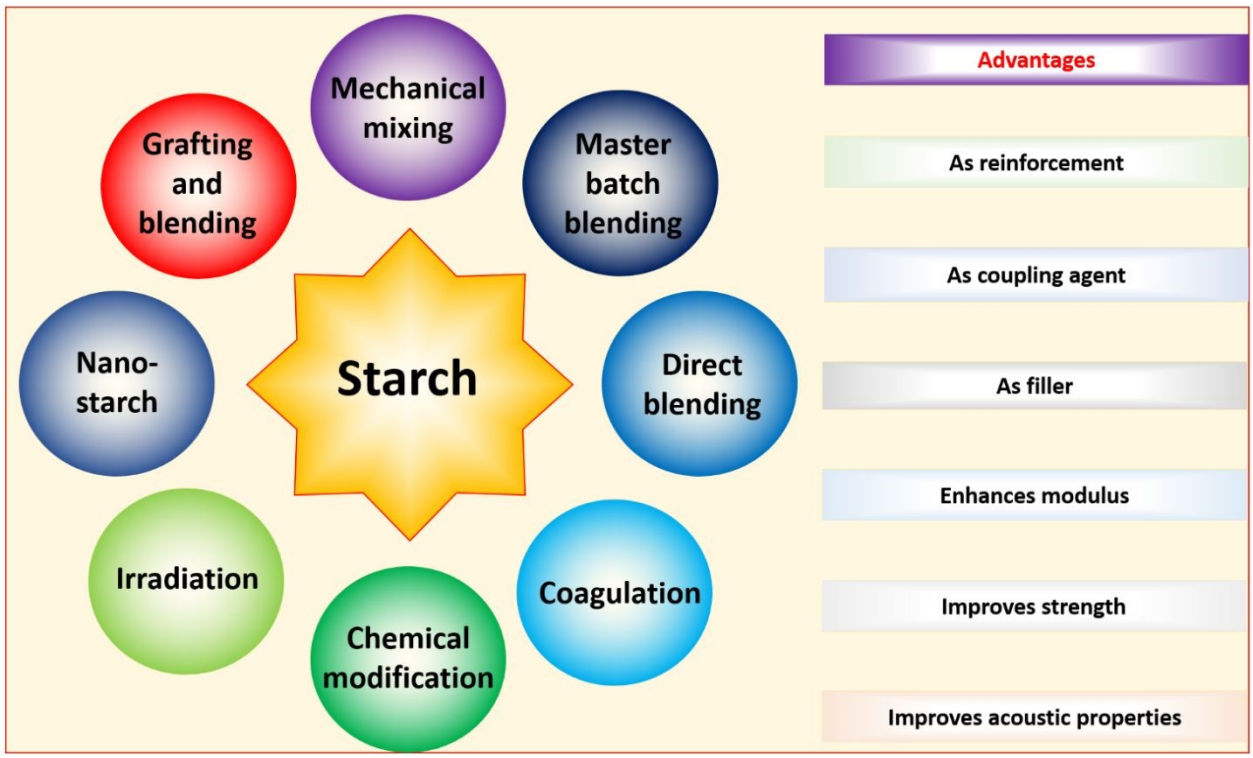

Fig. 8. Different strategies to use starch for development of rubber composite and its prospective advantages.

3.2. Chitin

Chitin is a structural long-chain polymeric polysaccharide (*N*-acetylglucosamine) that is found in many animals and plants[136]. It is one of the most abundant biopolymers in nature with amine functionality, semi-transparent, white, inexpensive and hard nitrogenous material [137]. The molecular backbone of chitin is similar to cellulose replacing the 2-hydroxy with an acetamide group [136]. Chitin is believed to be safe and biocompatible with the human body. It can be recovered

View Article Online
DOI: 10.1039/D1GC01115D

from marine organic wastes by acid hydrolysis, mechanical treatment, dissolution-regeneration method, oxidation, etc., [138]. It forms microfibrillar arrangement in living organisms embedded in a protein matrix with a length between 50 to 300 nm and diameter between 6 to 50 nm [139, 140]. Chitin and its derivatives can be useful in different applications such as paper production, pharmaceutical, and biomedical applications as it enhances the antibacterial properties [141], textile finishes photographic products, heavy metal chelating agents, waste removal, etc., [136, 142]. Chitin has the potential to be used as filler in rubbery materials and may work as compatibilizer, which helps to interweave filler to rubbery matrix ultimately improving rubber properties [143].

As discussed in the previous sections, the nano form of fillers has a high potential to enhance the properties of rubber. Chitin nanocrystals could also be utilized as a reinforcing agent [144] or Pickering emulsifier [145] in polymers. With an elastic modulus of ~150 GPa, the inherently amine functionalized and positively charged nanochitin can be an appealing reinforcing agent of rubber or other polymers [146]. The use of nanochitin as a reinforcing agent in polymers provides lightweight, biodegradable, biocompatible, higher strength composites. Nair and Dufresne [147] reported that the chemical modification of chitin by using different coupling agents, such as alkenyl succinic anhydride (ASA), phenyl isocyanate (PI), and 3-isopropenyl-R,R′- dimethyl benzyl isocyanate (TMI) does not contribute to its reinforcing effect in rubber. This was because the three-dimensional structural network of chitin was partially destroyed in the studied chemical modification processes. The same group has reported that the reinforcing effect of nanochitin derived from crab shell in NR is strongly based on its ability to form three dimensional network governed by percolation mechanism through intra- and inter-molecular hydrogen bonding [148, 149]. The incorporation of only 3% nanochitin, produced by acid hydrolysis, into C-SBR enhanced the

View Article Online
DOI: 10.1039/D1GC01115D

tensile strength by 123% (to 9.2 MPa) and elongation at break by 11% (to 396%) compared to the unfilled C-SBR [150].

Formation of self-assembly of chitin nanoparticles contributes a significant role in enhancing different properties of rubber [151]. Nanochitin having around 7.5 GPa tensile strength can easily form homogeneous dispersion and relatively enhanced interfacial interaction with rubber matrices[152]. The incorporation of 10% nanochitin increases the tensile strength of NR by up to 625 %. Hydrogen bonding and electrostatic interaction between rubber molecules and nanochitin may be responsible for the improvement in mechanical properties [140]. Deprotonated NR and 4% nanochitin formed a complex by electrostatic self-assembly, which results in higher mechanical properties (tensile strength of 25 MPa) of the composites [153].

Another approach to enhance the distribution of chitin in rubber is to develop a masterbatch with rubber and blend it with the rubber matrix. The use of the masterbatch enhances the dispersion and ease subsequent processing. In the case of ANBR, the incorporation of 2% nanochitin masterbatch resulted in 116% and 54% improvement in tensile and tear strength, respectively [154]. The tensile modulus and crosslink density were also found to be enhanced, which are attributed to the ‘caged’ or ‘trapped’ rubber chains within the three-dimensional network of rigid hydrogen-bonded network formed by nanochitin as represented in **Fig. 9**.

View Article Online
DOI: 10.1039/D1GC01115D

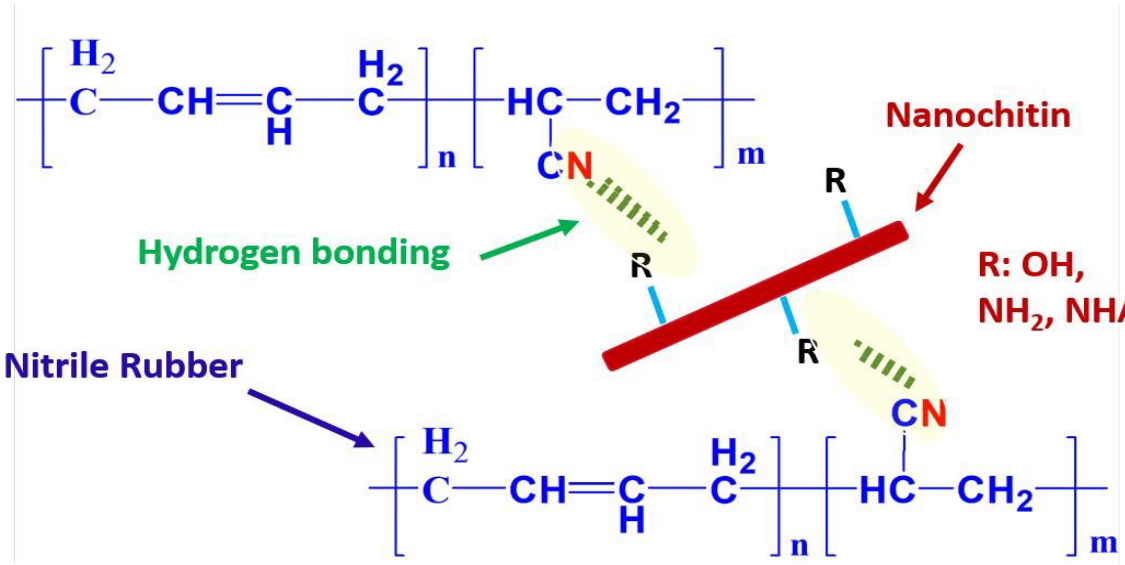

Fig. 9. Schematics for molecular interaction of nanochitin with nitrile rubber matrix (NHAc: acetyl amine group, NH_2: amine group, OH: hydroxyl group).

Some mild in situ surface interaction of chitin with rubber matrix containing reactive functionality can help improve the dispersion and mechanical properties. The reactive hydroxyl groups present on the surface of chitin may interact with the functionality present in rubber matrices. For instance, epoxidized natural rubber (ENR) that contains epoxy reactive groups can react with the residual hydroxyl groups of nanochitin to form supramolecular networks as shown in **Fig. 10**. The formation of such networks result in enhanced mechanical properties and self-healing properties (95%) as well. Using such approach, the use of 20% of nanochitin enhanced the tensile strength and modulus of the unfilled ENR by 200 % and 600 %, respectively [155].

View Article Online
DOI: 10.1039/D1GC01115D

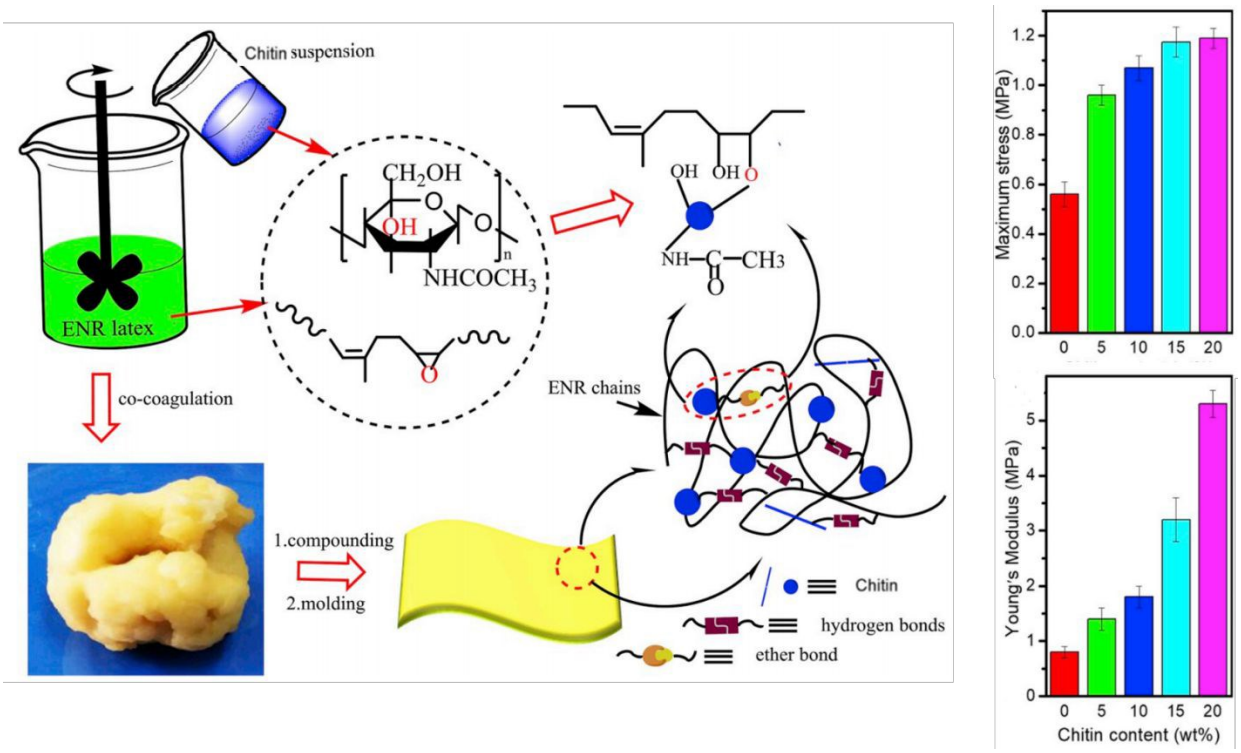

Fig. 10. Representation of the reaction of epoxy groups of epoxidized natural rubber (ENR) and residual hydroxyl functional groups of nanochitin that results in supramolecular networks and their effect on tensile strength and modulus as a function of nanochitin content. Figure adapted and reproduced with permission from ref. [155]. Copyright Elsevier, 2019.

3.3. Chitosan

Chitosan is a mucopolysaccharide biopolymer derived from chitin by alkaline deacetylation. The biodegradation of chitosan by enzymes, microorganisms, etc. makes it a promising candidate for different applications such as wound healing[156], biomedical applications [157], packaging applications[158], dye removal[159], etc. Overall, chitosan is biodegradable, antibacterial, non-toxic, biocompatible, and has film forming properties. Similar to other polysaccharides, chitosan has a melting temperature close to its thermal degradation temperature, which makes this material not suitable for melt processing[160]. In the case of producing rubber composites with chitosan, co-coagulation is a very beneficial mixing method that enhances the dispersion and provides appealing composite properties. Some studies demonstrated that the

View Article Online
DOI: 10.1039/D1GC01115D

incorporation of chitosan improves the mechanical properties of rubbers[161, 162]. The immiscibility of chitosan with rubbers makes it close to impossible to get the ultimate benefit of chitosan to develop mechanically strong rubbers[163]. Different methods can be employed to improve the compatibility of chitosan with rubbers such as maleic anhydride (MA) compatibilization [163, 164], dicumyl peroxide crosslinking [165], epoxy crosslinking [166-168], ball mill mixing [169], plasma treatment [170] etc. Poly-electrolytic derivatives of chitosan with carboxyl (COO^-) and quaternary ammonium (NR_4^+) groups can also enhance the dispersion of chitosan in rubbers [171].

The development of chitosan microspheres by ion induction and chemical crosslinking and its reinforcement of rubber can also enhance the thermal and mechanical properties [172]. It is known that chitosan is mostly soluble in low pH aqueous medium [173], which is undesirable for rubber formulations as rubber crosslinking is usually conducted at high pH. Thus, alternative ways of developing chitosan microspheres are required. For instance, chitosan gels formed by the incorporation of specific salts i.e., glycerol-phosphate complex, sodium triphosphate etc. can be used as a precursor for the chitosan microsphere [174]. The interaction between chitosan chains and phosphate complex can then occur due to ion induction or ion cross-linking. These ion crosslinked chitosan can then form microspheres upon the addition of chemical crosslinkers [175, 176]. The C-NH_2 functional group of chitosan and aldehyde group of vanillin reacts and form Schiff base, which is important to enhance the antibacterial activity. Polycationic characteristics of chitosan due to the presence of amine groups enhance the ionic crosslinks in the polymeric matrix. Nanochitosan may also act as a multi-functional crosslinking structure due to the high surface area and exposed reactive functionality [177]. Nanoparticles can be formed by gelation and crosslinking of chitosan chains in the presence of crosslinkers in solution. In the case of C-SBR, 20% nanochitosan loading improved the tensile strength to 1.3 MPa (2 times higher than neat C-SBR)

View Article Online
DOI: 10.1039/D1GC01115D

and enhanced water uptake by 75% due to the developed ionic bond crosslink in supramolecular polymer network (**Fig. 11**) [178].

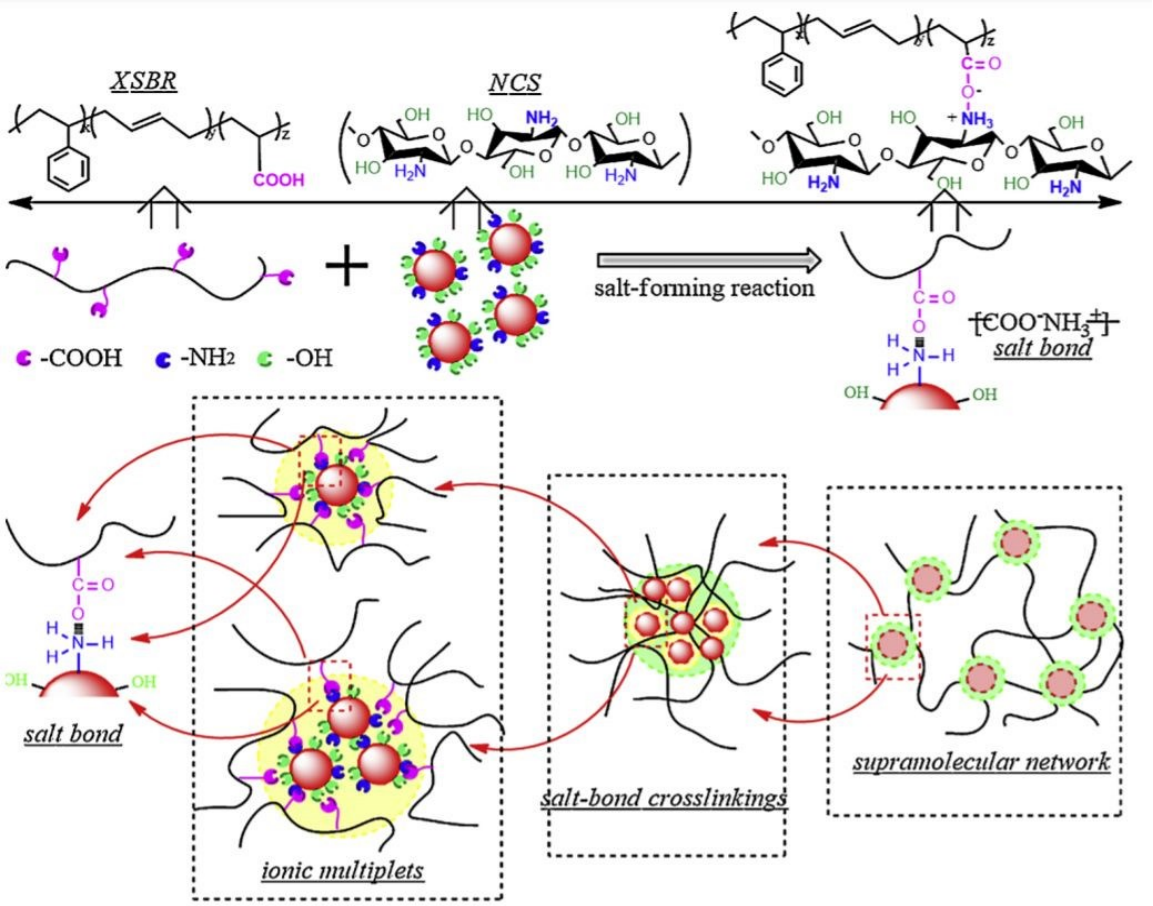

Fig. 11. Ionic crosslink formation between carboxylated styrene butadiene rubber (XSBR) and nanochitosan (NCS). Figure adapted with permission from ref. [178]. Copyright Elsevier, 2019.

3.4. Other polysaccharides

The molecular structure and design of different polysaccharides are not as uniform as other synthetic polymers, which result in variation in properties based on its source, season, or geographical location. Technology like enzymatic polymerization of sugars may yield novel controllable molecular structures (**Fig. 12**). Rubber composites developed using enzymatically polymerized glucose that is derived from sucrose [179], such as poly alpha-1,3-gulcan as reinforcing

View Article Online
DOI: 10.1039/D1GC01115D

agent, which is a water-insoluble material, can be utilized for seal, valves, footwear, tubing, gaskets, mats *etc*.,[180]. Polyalpha-1,3-glucan is an experimental engineered polysaccharide polymer synthesized via enzymatic polymerization by DuPont Nutrition and Bioscience (currently IFF). Due to the control of the enzymatic polymerization parameters, it was possible to produce a well-defined and controlled structure, architecture, and functionality. These fibrous materials can be utilized for different application such as elastomeric composites, polymer composites [181], polyurethanes, coating application etc. (**Fig. 12**). As it was produced from glucose that was derived from sucrose, it is found to be biodegradable which drive the circular economy vision.

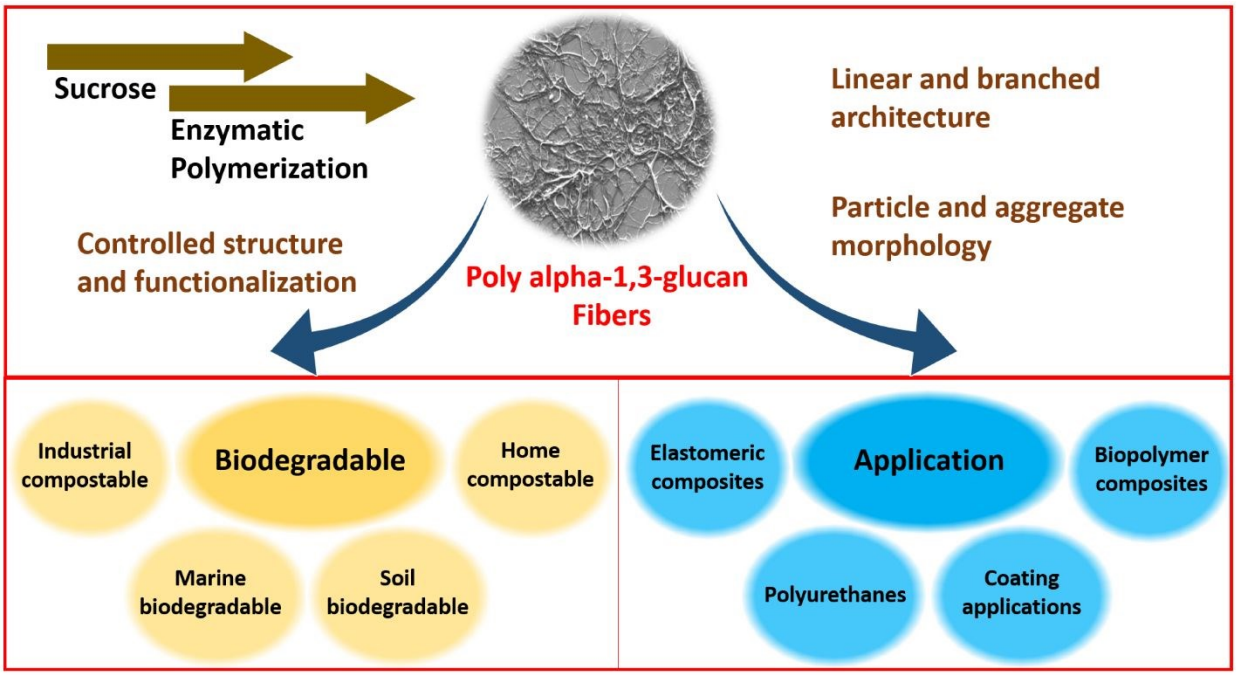

Fig. 12. Process to develop poly alpha-1,3-glucan and its application and biodegradation. SEM image adapted and reproduced from ref. [179]. Copyright ACS, 2020.

View Article Online
DOI: 10.1039/D1GC01115D

4. Lignin

4.1. Lignin structure and properties

Lignin is a highly aromatic natural polymer that is found in all sorts of lignocellulosic materials. It has several functionalities such as providing strength and rigidity to plant cell walls, improving the water transport, and protecting the cell wall polysaccharides from destructive agents and insects [182]. The ratio of cellulose, lignin, and hemicellulose varies in different lignocellulosic materials *i.e.,* trees and grasses. In woods, the percentage of lignin on a dry matter basis range from 12% to 39% [183]. Lignin has a polyphenolic amorphous structure which is made from the polymerization of p-coumaryl, coniferyl, and sinapyl alcohols resulting in the p-phenylpropane (H-monomer), guaiacyl (G-monomer), and syringyl (S-monomer) units (**Fig. 13**) [183, 184]. These monomers have different degree of methoxy ($-OCH_3$) group substitution, which provides a variety of chemical interactions in the resulting lignin. The amount of these functionality varies in the structure of lignin available in different woods and grasses. Softwood lignin (from evergreen trees) is an aromatic polymer that is composed of guaiacylpropane linked through C-C and ether bonds. In hardwood lignin (from deciduous trees) the percentage of guaiacyl and syringyl units are approximately the same. Grasses have all three types of functionality. Lignin biosynthesis is an enzymatic radical polymerization in which the monomers randomly link together to produce a three-dimensional complex structure of aryl-alkyl ether bonds [185]

View Article Online
DOI: 10.1039/D1GC01115D

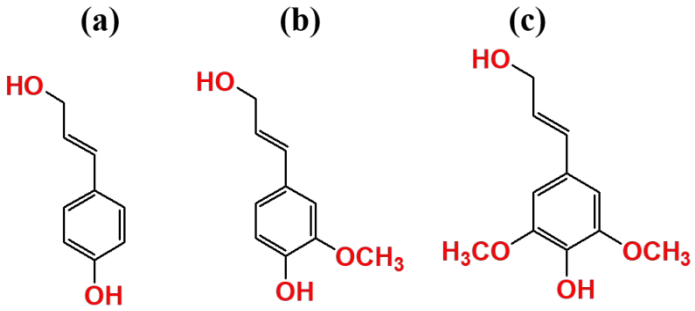

Fig. 13. Lignin basic monomer structural units: (a) 4-hydroxyphenyl, (b) Guaiacyl, and (c) Syringyl. Redrawn from ref. [184]. Copyright Elsevier, 2019.

The application of the lignin is mainly influenced by its source and extraction method. Therefore, lignin molecular characteristics such as molecular weight, chemical functionalities, and glass transition temperature should be determined to decide its end-use. Since lignin is bounded to and surrounds cellulose, some extra processing need to be conducted before recovering either the lignin or cellulose. In addition to origin-based variations between lignins, pretreatment methods also cause structural differences as they induce different types of degradation to lignin molecules [186, 187]. Kraft and sulfite processes are two common pretreatment methods in the paper industry. The sulfite process involves the reaction between sulfur dioxide and metal sulfite to produce water-soluble lignin [187]. Sulfonation of lignin during the sulfite process creates water-soluble lignin which has aliphatic sulfonic acid functionalities. Kraft process on the other hand is performed in an alkaline solution and results in lignin chains containing a small number of aliphatic thiol groups [186]. Overall, the sulfur-free lignin has great structural similarity with native lignin with moderate molecular weight change and no sulfur.

The properties of the sulfur-free lignins are different compared to sulfite and kraft lignins. Sulfur-free lignins are obtained from biomass conversion processes (mainly bio-ethanol production), solvent pulping ("organosolv") processes, and soda pulping [186]. Solvent pulping or the organosolv process is a pretreatment suggested as an alternative to kraft and sulfite pulping.

View Article Online
DOI: 10.1039/D1GC01115D

This process is claimed to be more environmentally friendly and less expensive. Organosolv lignins extracted from the spent solvent in this process are usually pure and have low molecular weights with a narrow distribution. They also have a lower glass transition temperature, flow upon heating, are highly soluble in organic solvents but insoluble in water. However, the commercial process to produce this lignin has stopped due to process economics issues. Another process to produce sulfur-free lignin is alkali/soda pulping. In this process, the lignin is precipitated and separated from the pulping mass. The lignin isolated from this process is low quality and has a wide range of variation in properties but most commonly have a low glass transition temperature, high phenolic hydroxyl functionality, and low molecular weight [186].

4.2. Lignin reinforced rubber composites

Rubber filled composites can be used for different applications because of their unique properties. Among the fillers, CB or silica is commercially used as a filler to impart better properties in the rubber products. Depending on the requirements, ingredients such as plasticizer, vulcanizing agent, accelerator, activator, and anti-degradant are incorporated into rubber compounds to achieve different functionalities in the resulting material. Since lignin is an inexpensive renewable material, it can be utilized as a reinforcing agent, antioxidant, plasticizer, UV shield, and coupling agent in rubber matrices [188]. However, the performances of the lignin reinforced rubber composites are influenced by several factors including lignin molecular weight (Mw), Mw distribution, ash content, purity, the concentration of the lignin in the matrix, preparation method, and compatibility/miscibility of the lignin with the rubber matrices. Lignin is hydrophobic material and therefore should have good miscibility with other hydrophobic polymers. However, polar groups on lignin such as hydroxyl and carbonyl groups provide the

View Article Online
DOI: 10.1039/D1GC01115D

opportunity for tailoring the polarity of the lignin to make it compatible with other hydrophilic polymer systems [187].

A large amount of hydroxyl groups present in the purified lignin can limit the interaction with rubber matrices that result in inferior performances in the resulting composites. Surface modification (*e.g.* esterification) of the lignin can be carried out to adjust the polarity and enhance its compatibility with rubber matrices [189]. Chemical modifications of the lignin and prediction of the solubility parameters of the modified lignin were found to be useful methods to achieve high performance in the lignin filled rubber composites [190]. When lignin is incorporated into rubber, the resulting composites can form spaghetti (rubber chains) and meatball (lignin particles) morphology. The lignin domain size in the rubber matrix is dependant on the lignin concentration and compatibility with the matrix. Several studies have investigated lignin as a reinforcing agent in rubber formulations, especially in NR, ANBR, SBR, polyethylene-co-vinyl acetate (EVA), and EPDM systems [188, 191, 192].

These lignin/rubber composites are mainly prepared by three methods, namely, mechanical mixing, latex mixing, and soft processing [191]. The performances of the lignin filled rubber composites are reviewed in the following section with more emphasis on reinforcing effect and compatibility. Hosseinmardi et al. [193] observed mechanical properties improvement in the NR when nanoscale organosolv lignin was incorporated. It was observed that the tensile strength of 5 wt.% lignin incorporated NR composites can increase by 39% in tensile strength compared to neat NR while retaining high elongation at break (~1800 %). Similarly, the toughness and hardness of the NR with 5 wt.% lignin were improved by 53 and 12%, respectively. These improvements are associated with favorable interaction between the lignin and rubber matrix. In another study, glycerolysate plasticizer was used as a plasticizer in the softwood lignin/NR composite [194]. The

View Article Online
DOI: 10.1039/D1GC01115D

performance of the glycerolysate plasticized lignin/NR composites was similar to those of the lignin-containing composites prepared with other commercially available plasticizers. The lignin/NR composites prepared with 5 phr lignin showed optimal performances in terms of hardness, abrasiveness, and tensile properties because of the uniform dispersion of lignin with less agglomeration in the matrix. On the contrary, glycerolysate plasticized NR composites with 10 phr kraft lignin showed optimal performances as opposed to the 5 phr observed for the formulation without a plasticizer [195]. When the lignin/NR composite was prepared with a higher amount (40 phr) of lignin (softwood or kraft), the resulting composite showed detrimental effects in the performances due to agglomeration of lignin particles in the matrix. These observations suggest that the performance of the lignin incorporated rubber composites mainly depends on the lignin type and concentration in the formulations.

The reinforcing ability and interfacial interaction of the kraft softwood lignin in three different acrylonitrile content NBR (33, 41, and 51 mol%) were systematically investigated [196]. The lignin/NBR blend showed a stress-strain curve (**Fig. 14a**) which is similar to a typically reinforced elastomer. Due to the strong reinforcing ability of the lignin, the lignin/NBR composites performance was comparable with the 50 phr CB-filled NBR system. The lignin was finely dispersed (0.2–2 μm) in the 33 mol% acrylonitrile content NBR blend whereas lignin forms an extremely interpenetrating network morphology in the 41 mol% acrylonitrile content NBR (**Fig. 14a**). Such a network structure formation in the lignin leads to form yield stress in the stress-strain curve before significant strain hardening occurs during the tensile test. In the same study, kraft lignin was fractionated using acetone/hexane (4:1) solvent to produce melt-stable lignin as a reinforcement in the 41 mol% acrylonitrile content NBR [196]. Contrary to the original kraft lignin filled NBR, organic solvent fractionated lignin filled NBR resulted in a thermoplastic elastomer

View Article Online
DOI: 10.1039/D1GC01115D

behavior as shown in the stress-strain curve (**Fig. 14b**). The morphological analysis indicates that the solvent fractionated lignin can form fine morphology with nano-scale lignin domains (<100 nm) in the resulting blend while micron-scale lignin domains were observed in the case of original kraft lignin used.

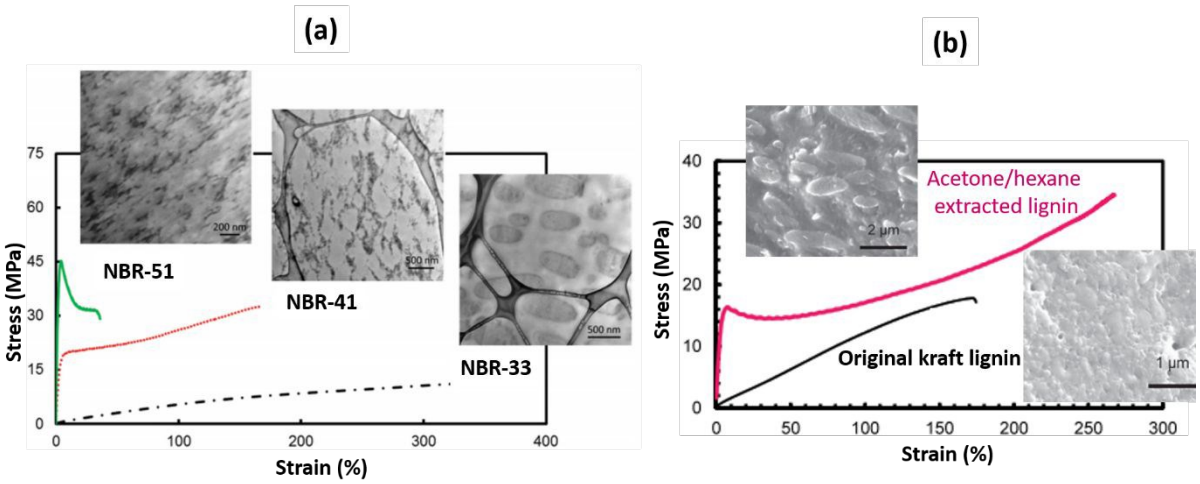

Fig. 14. (a) Mechanical properties of reactive blends of methanol extracted fraction of kraft softwood lignin with nitrile rubber (NBR) with 33 mol% acrylonitrile content (NBR-33), NBR with 41 mol% acrylonitrile content (NBR-41), and NBR with 51 mol% acrylonitrile content (NBR-51) and their corresponding transmission electron microscopy images; (b) Tensile stress-strain curves and SEM images of NBR-41/softwood Kraft lignin and NBR-41/acetone/hexane soluble fraction of the original softwood Kraft lignin blends. Figure adapted with permission from ref. [196]. Copyright Wiley, 2016.

Nano-lignin (<100 nm) incorporated rubber composite was prepared from nano-lignin dispersed poly(diallyldimethylammonium chloride) complex and NR matrix [31]. It was observed that the nano-lignin was able to disperse uniformly in the rubber matrix because of the strong interfacial adhesion between them. Consequently, the mechanical properties and thermal stability of nano-lignin incorporated NR composites were significantly improved. Similarly, the SBR/lignin-layered double hydroxide (lignin-LDH) composites showed better mechanical performances than the LDH/SBR composites, suggesting that the lignin-LDH complex could be a promising filler for rubber composites [197].

View Article Online
DOI: 10.1039/D1GC01115D

The addition of sulfur-free lignin into NR showed a significant reduction in the curing time of the rubber besides improving mechanical and physical properties [198]. A similar observation has been reported for vulcanized styrene-butadiene rubber (SBR)/sulfur-free lignin (20 phr) composites [199]. It was also shown that the lignin can act as an antioxidant to improve and maintain the mechanical properties of the vulcanized lignin/NR composites [200]. The enhanced mechanical properties of the lignin/rubber composites are perhaps through a tandem mechanism of oxidation protection and reinforcement effect. It was also observed that the thiolignin incorporated NR composites can provide dielectric properties [201]. Such a composite material could be used for energy applications.

Strain-induced crystallization (SIC) is a phenomenon that can occur in rubber materials by orienting the molecules along the stretching direction. It can provide resistance to crack growth and improved fatigue behavior in the resulting rubber products. For instance, Ikeda et al. [202] reported a soft processing method, which utilizes a rubber latex as opposed to a rubber crumb, to produce sodium lignosulfonates/NR composites. Composites (sulfur-crosslinked unfilled NR (NR-L0-S-soft), sulfur-crosslinked NR with 10 phr lignin (NR-L10-S-soft), and sulfur-crosslinked NR with 40 phr lignin (NR-L40-S-soft)) were produced and used to investigate the SIC by *in-situ* wide-angle X-ray diffraction (WAXRD)/tensile measurements. **Fig. 15** shows the tensile stress-strain curves, variations of crystallinity index (CI) against stretching ratio, and three-dimensional WAXD patterns at different stretching ratio (α = 1, 4.5, and 5.5) of the lignin/NR composites produced by a soft method. WAXD pattern (**Fig. 15c**) showed an amorphous halo ring in all the samples before stretching (α =1), suggesting the amorphous nature of the samples. On the contrary, the crystalline reflection was observed when the samples were stretched (α = 4.5 and 5.5). The crystalline reflection was attributed to the SIC which was caused by the alignment of rubber chains

View Article Online
DOI: 10.1039/D1GC01115D

during stretching. Furthermore, the crystalline reflection was increased with increasing stretching. Regardless of the stretching ratio, NR-L40-S-soft composite showed less crystalline reflection intensity and broader crystalline reflection compared to NR-L10-S-soft composites. All the samples showed similar CI (**Fig. 15b**) with a stepwise change in CI when increasing the stretching. The stepwise change in CI was attributed to the unique phase-separated morphology formation in the prepared samples. Unlike CI, the tensile properties of the prepared samples were significantly different (**Fig. 15a**). This suggest that the lignin incorporation has mainly influenced the tensile properties not SIC of the composites.

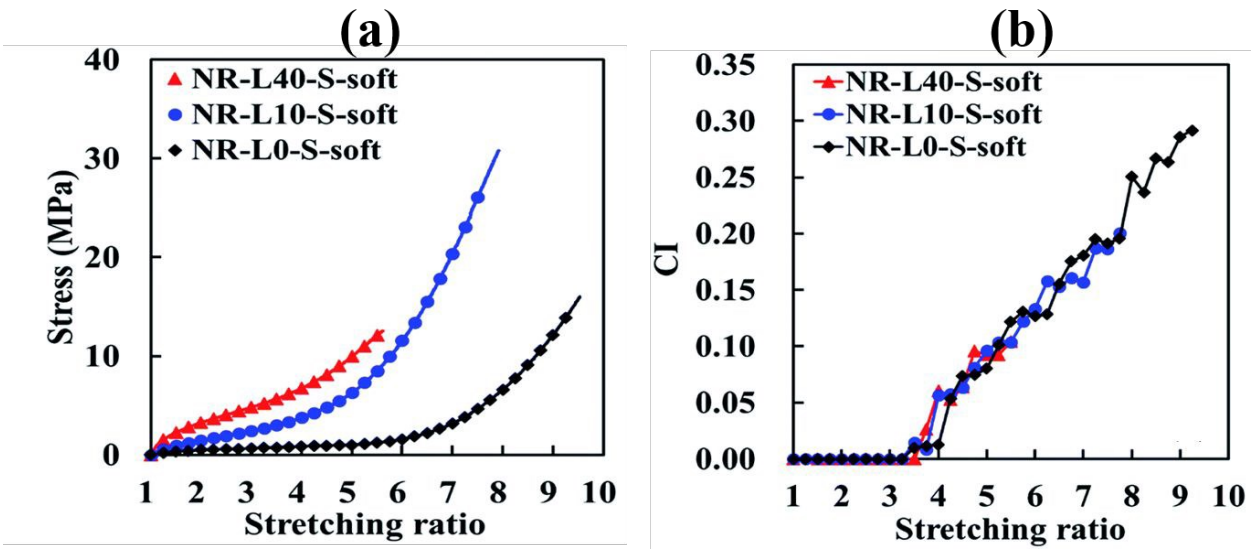

View Article Online
DOI: 10.1039/D1GC01115D

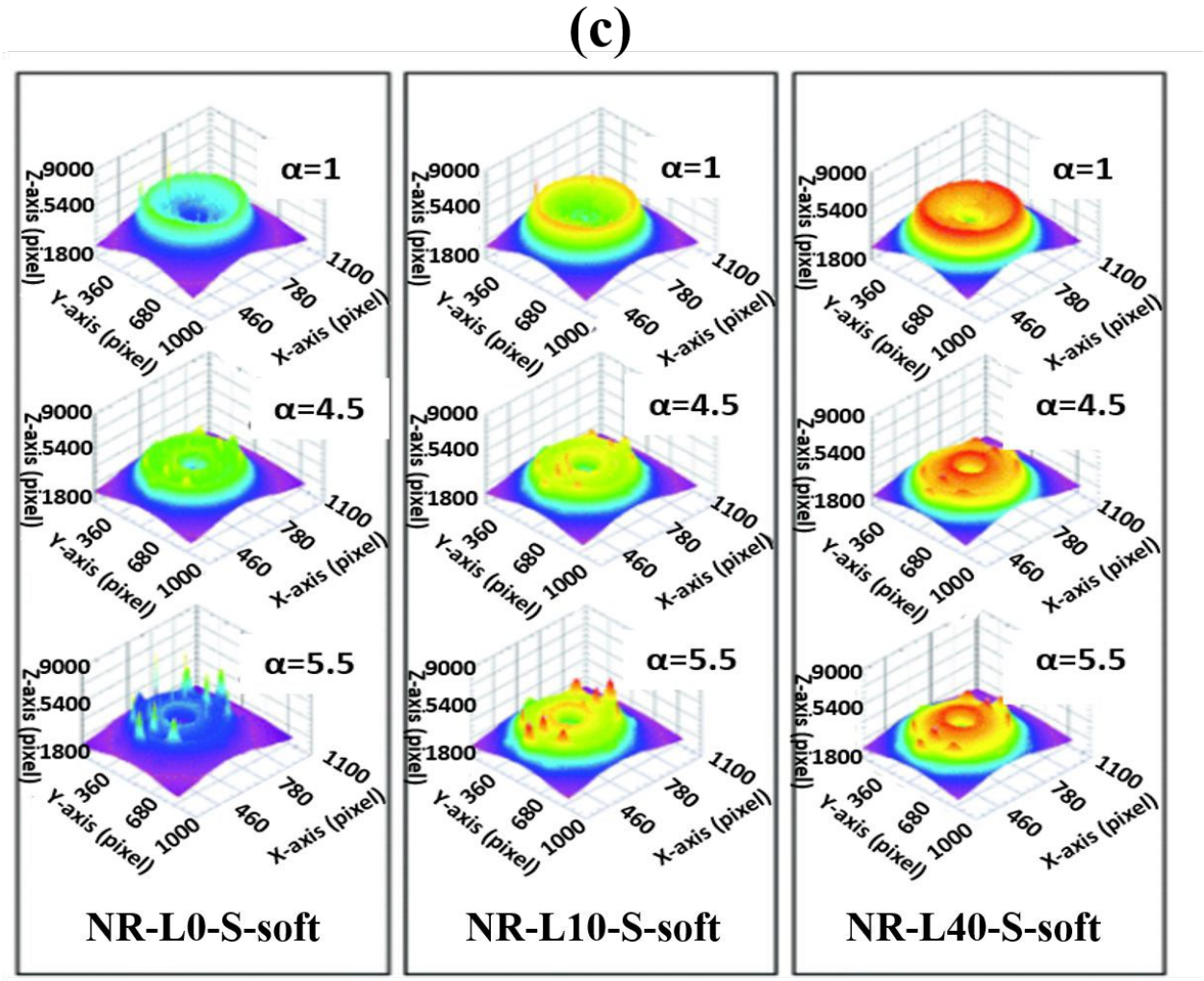

Fig. 15. Strain-induced crystallization behaviors of natural rubber/lignin soft composites (NR-L-S-soft) with 10 and 40 wt% lignin. (a) Tensile stress-strain curves, (b) variations of crystallinity index (CI) against stretching ratio, and (c) three-dimensional WAXD patterns at stretching ratio (α = 1, 4.5, and 5.5). Adapted with permission from ref. [202]. Copyright RSC, 2017.

Mechanical properties of the hexamethylenetetramine (HMT) modified commercial lignin (Protobind 3000®) reinforced SBR and NR composites were compared to corresponding rubber composites produced with CB to investigate the potential use of HMT-treated lignin as a partial replacement for CB in the rubber composites production [203]. The HMT-treated lignin/rubber composites showed poor dispersion of the lignin in the rubber matrix, which was attributed to the incompatibility between the lignin and the rubber. Consequently, the performances of the HMT-

View Article Online
DOI: 10.1039/D1GC01115D

treated lignin/rubber composites were inferior compared to their corresponding rubber composites prepared with CB. On the contrary, hydroxymethylated kraft lignin incorporated in different rubber composites showed better dispersion and good interaction with the matrix because of the weakened filler–filler interactions [204, 205]. Similarly, a high-temperature dynamic heat treatment can be used to self crosslink the lignin with ENR to improve the performances of the resulting materials as shown in **Fig. 16** [206]. The self-crosslinking of lignin/ENR composites was accomplished by the ring-opening reaction between lignin and ENR during processing [207]. The crosslinked lignin leads to form strong reinforcing effect, good interactions with ENR, and uniform dispersion of lignin in the matrix with submicron size. The observed strong reinforcing effect was mainly attributed to the lignin itself rather than the formation of strain-induced crystallization.

Additionally, self-crosslinked lignin can provide superior aging resistance compared with sulfur-cured ENR because of its ability to scavenge free radicals of phenolic hydroxyls in lignin and the consumption of epoxy groups in ENR by lignin. For this, dynamic heat treatment at high-temperature (80 - 180 °C) was employed to form submicron size lignin dispersion in the ENR with strong interactions between them [206]. The high-temperature dynamic heat-treated lignin/ENR composites showed superior mechanical performances compared to the directly mixed-rubber composites. The lignin incorporated polyethylene-co-vinyl acetate (EVA) rubber composites with enhanced performances have also been reported for durable application [208].

View Article Online
DOI: 10.1039/D1GC01115D

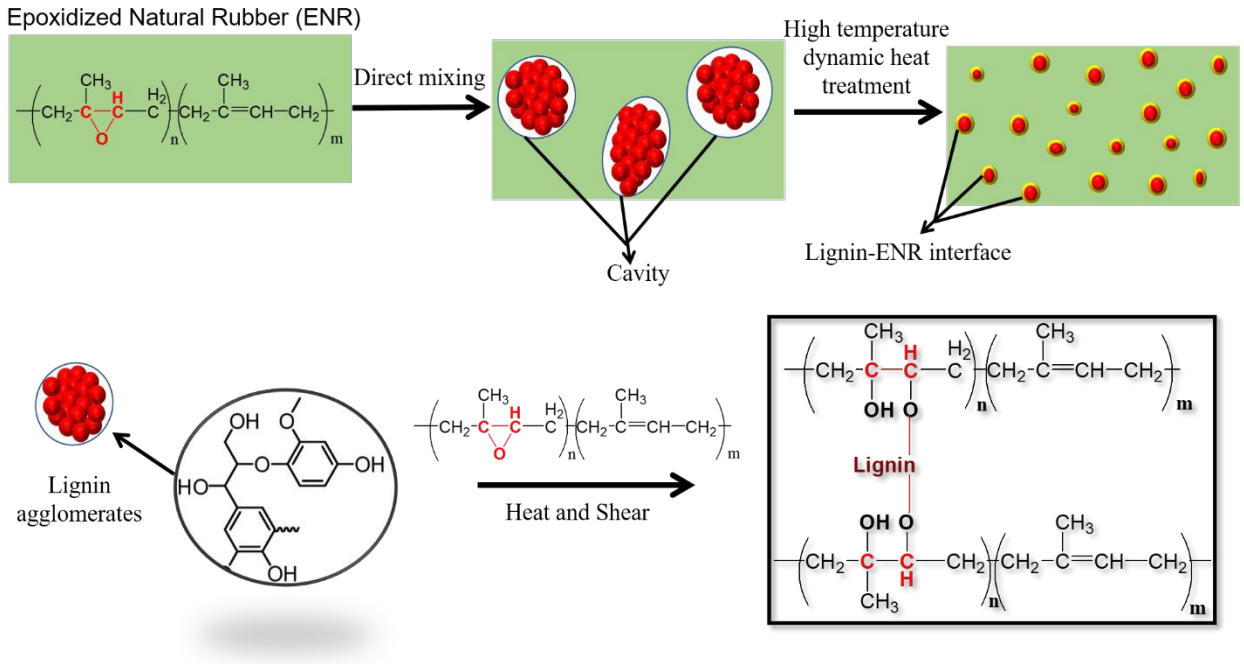

Fig. 16. Schematic illustration for the preparation of lignin/ENR composites. Figure redrawn with permission from ref. [206]. Copyright Wiley, 2015.

4.3. Lignin/conventional filler hybrid reinforced rubber composites

It has been established that synergistic effects can occur when two different fillers are incorporated into a polymer matrix. A recent article has extensively investigated the performances of the lignin/silica hybrid fillers in NR [192]. It was summarized that lignin can be a potential alternative to partially replace silica in rubber composites without negatively affecting the mechanical performances of the resulting composites. Incorporation of lignin into the rubber could reduce the Payne effect while improving the processability, anti-aging resistance, and anti-flex cracking of composites. Optimal mechanical properties were observed in the vulcanized NR composites with 30 phr silica and 20 phr lignin hybrid filler. A facile self-assembly method was used to produce a nanoscale lignin/silica hybrid as a reinforcement for the NR [209]. Unlike lignin, sphere-like morphology was observed for both lignin/silica hybrid and silica as shown in **Fig. 17 (a-d)**. The lignin/silica hybrid showed potential for the partial replacement of conventional CB in

View Article Online
DOI: 10.1039/D1GC01115D

the NR composites because of the nanoscale reinforcing effect [209]. Due to π-π interactions between the CB and kraft lignin, spherical nanostructured lignin was coated on the non-spherical aggregates of CB by precipitation method [210]. **Fig. 17 (e-h)** shows the microscopic images of spherical nano-domains of lignin, lignin coated CB hybrid, and non-spherical aggregates of CB. The lignin coated CB hybrid filler was used in the SBR matrix to reduce the CB network in the rubber compounds. The reduced filler networking in the composite led to a reduction in the viscoelastic loss of rubber compounds. Unlike unmodified lignin/CB filled rubber composites, NR/butadiene rubber matrix with hydroxymethylated kraft lignin and CB hybrid filler exhibited better tensile and compression properties because of the uniform dispersion of hydroxymethylated lignin in the rubber matrix as well as good interaction between the components [204].

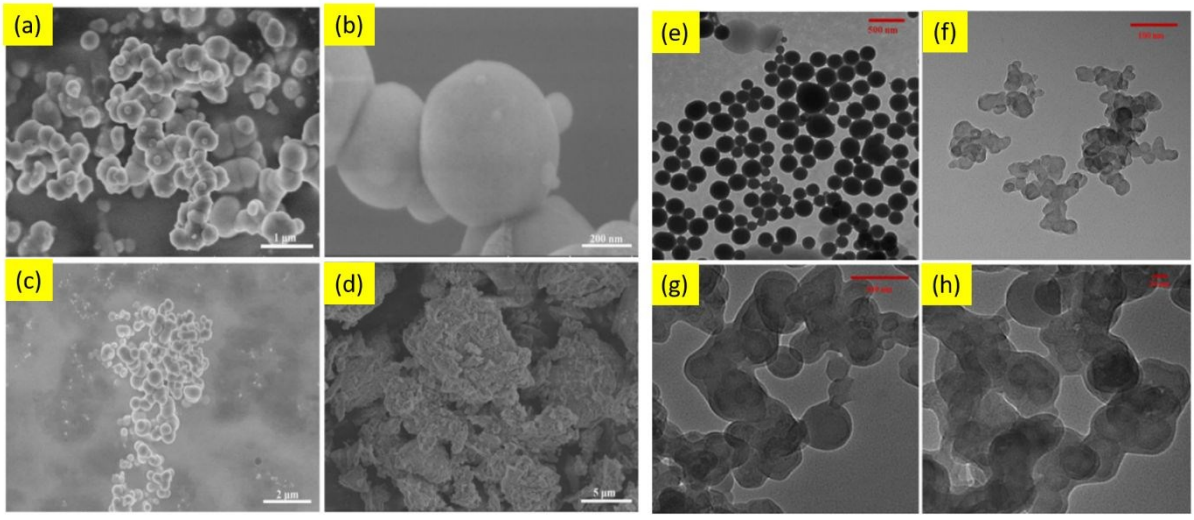

Fig. 17. SEM images of (a and b) lignin-silica hybrid material, (c) silica, and (d) lignin. Figure adapted with permission from ref. [209]. Copyright Elsevier, 2020; TEM images of (e) kraft lignin, (f) CB, (g and h) kraft lignin/CB hybrid at 1:1 by weight of lignin and CB. Figure adapted with permission from ref. [210]. Copyright Elsevier, 2014.

NBR composites with lignin/CB hybrid fillers were crosslinked by dynamic coordination sacrificial bonds and sulfur covalent bonds to develop high-performance composites as shown in **Fig. 18a** [211]. The coordination sacrificial bonds are formed between the lignin and NBR in the

View Article Online
DOI: 10.1039/D1GC01115D

presence of $ZnCl_2$ [212]. As a result, NBR composites with lignin/CB hybrid fillers showed higher strength, modulus, oil resistance, and thermal stability compared to the corresponding composites produced with only CB. Overall, this study suggests that a high-performance rubber composite can be obtained with a high lignin/CB hybrid filler loading. In another study, lignin/NBR composites were transformed from rubber-like to plastic-like material after incorporation of 1-3 wt% $ZnCl_2$ [213]. Such a transformation was attributed to the interfacial crosslinking between NBR and lignin in the presence of Zn^{2+} cations as shown in **Fig. 18b**. It was also observed that the interfacial crosslinking leads to form nanoscale lignin domain (<100nm) in the matrix. Similarly, thermoplastic-like nanocomposites were developed from lignin, NBR, and graphene oxide (GO) (1-4 wt%) formulations without any vulcanization [214]. The high surface area GO (>400 m^2/g) incorporation led to the formation of hydrogen bonding and dipolar interaction with lignin as well as NBR, resulting in nanoscale lignin dispersion in the rubber matrix with a strong reinforcing effect.

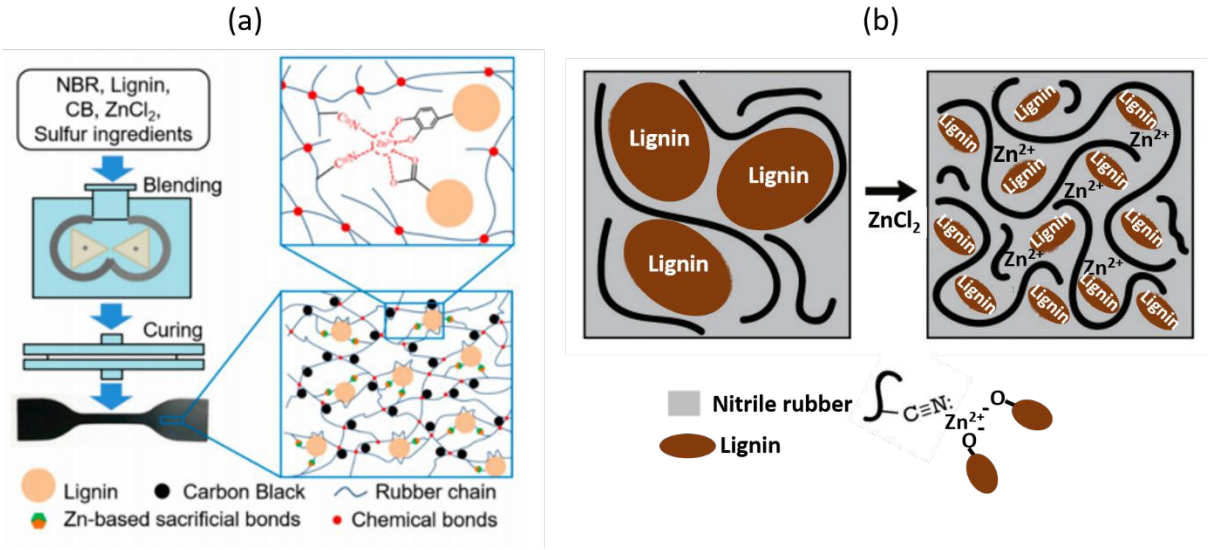

Fig. 18. (a) Constructing mechanism of lignin/CB/NBR elastomers with Zn-based coordination sacrificial bonds [211]. Open access article. Copyright MDPI, 2018; and (b) Potential structural changes in an acrylonitrile-butadiene-lignin composition caused by compounding with $ZnCl_2$. The image on the right shows that zinc cations (Zn^{+2}) can link nitrile groups of NBR with anions from

View Article Online
DOI: 10.1039/D1GC01115D

phenolic hydroxyl groups of lignin to aid interfacial crosslinking between NBR and lignin. Figure adapted with permission from ref. [213]. Copyright Wiley, 2019.

Unlike traditional filler in rubber composites, lignin has been proven to be an effective coupling agent in EPDM rubber/CB composites by Xu et al. [215]. It was observed that the alkali lignin can enhance the inter-phase cohesion between the constituents in the EPDM composites. Similar to NBR/lignin composites, maleic anhydride-grafted polyolefin elastomer/lignin composites can form synergistic coordination sacrificial bonds in the presence of $ZnCl_2$ [216]. Consequently, lignin dispersion, interfacial interaction between the components, and strain-induced crystallization were significantly improved. In another study, a high-performance multiphase NBR/lignin/CB composite was produced by dicumyl peroxide and boric acid crosslinking in the presence of polyethylene oxide (PEO) compatibilizer [190]. In the presence of peroxide, NBR was grafted on the lignin by melt free-radical polymerization to improve the interface between the components as shown in **Fig. 19a-d**. Boric acid can readily interact with lignin hydroxyl groups and PEO ether linkages to form borate esters and hydrogen bonding, respectively. The combination of these reactions in the softwood kraft lignin/NBR formulation led to a high-performance rubber compound with good tensile strength (25.2 MPa) and relatively low strain at break (9%) as shown in **Fig. 19f**. On the contrary, hardwood soda lignin was found to be less effective in terms of reactivity with NBR, PEO, and boric acid because of the predominant syringyl monomer units in the hardwood lignin. The reduced extent of reactivity in the hardwood lignin/NBR formulation resulted in inferior mechanical properties compared to the corresponding formulation produced with softwood soda lignin (**Fig. 19 e, f**).

View Article Online
DOI: 10.1039/D1GC01115D

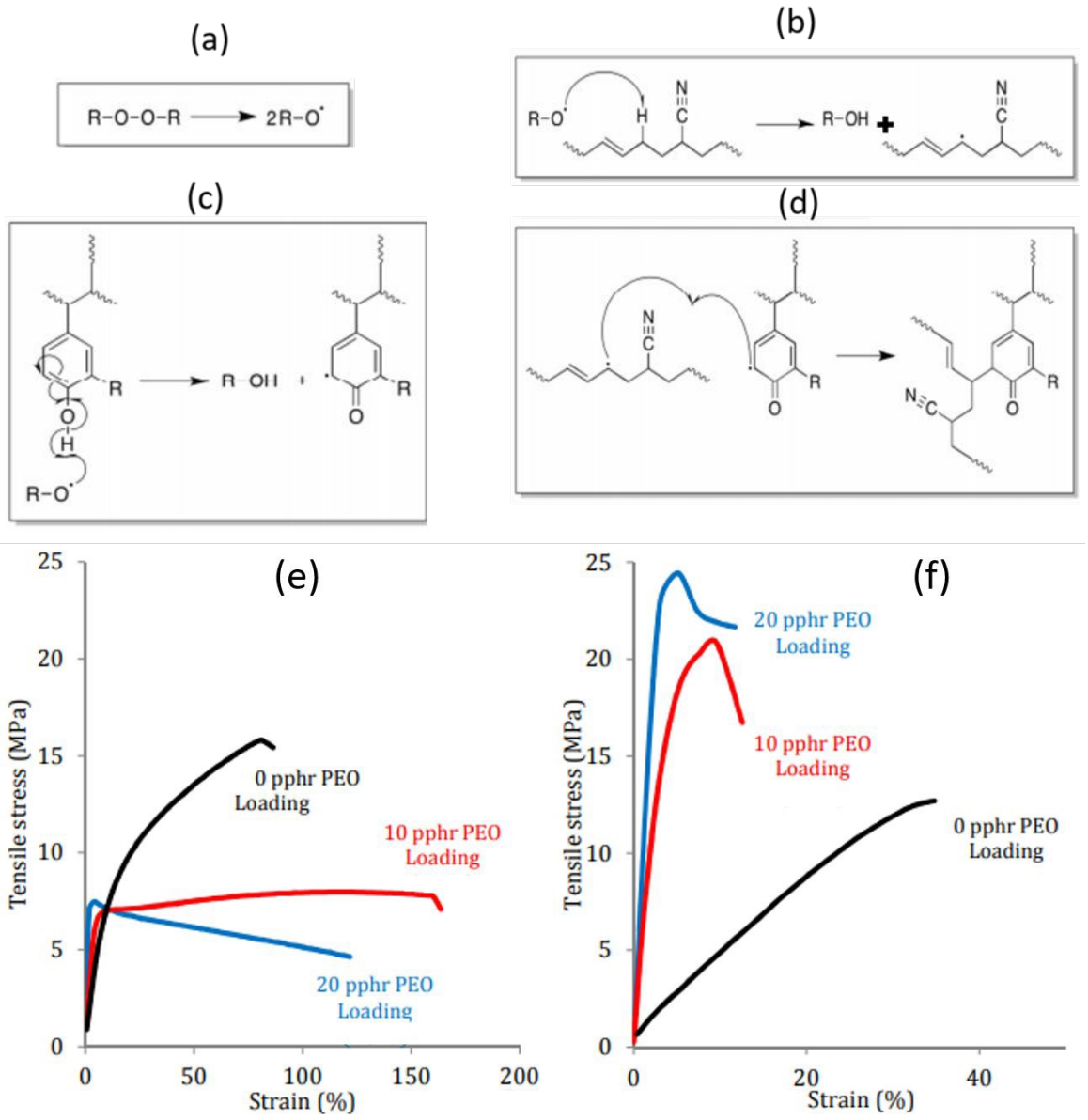

Fig. 19. (a) Free-radical formation, (b and c) proton abstraction from lignin and NBR, (d) radical termination, tensile stress-strain plots of (e) hardwood soda lignin-NBR with different parts per hundred (phr) of polyethylene oxide (PEO) loading, and (f) softwood kraft lignin–NBR containing boric acid and varying PEO content. Figure adapted with permission from ref. [190]. Copyright RSC, 2016.

5. Natural fibers reinforced rubber composites

Plant fibers/natural fibers (NFs) are renewable and biodegradable which can be obtained from the different parts of the plants as shown in **Fig. 20**. The NFs have great potential as a

View Article Online
DOI: 10.1039/D1GC01115D

reinforcement for the polymer system to produce biocomposites because NFs can offer high specific strength, lightweight, high toughness, reduced tool wear, and low respiratory irritation compared to most of the synthetic fibers [217-219]. Therefore, the NFs reinforced rubber composites can be relatively cost-effective with a low coefficient of friction, lightweight, good thermal and dimensional stability. The NFs are used as a reinforcement to partially replace silica or CB in rubber formulations [220]. Furthermore, 100% biobased composites can be produced from plant fibers reinforced NR which reduces the dependence on fossil fuels. Owing to its unique features, NFs reinforced rubber composites can be used in different applications including automotive parts [221].

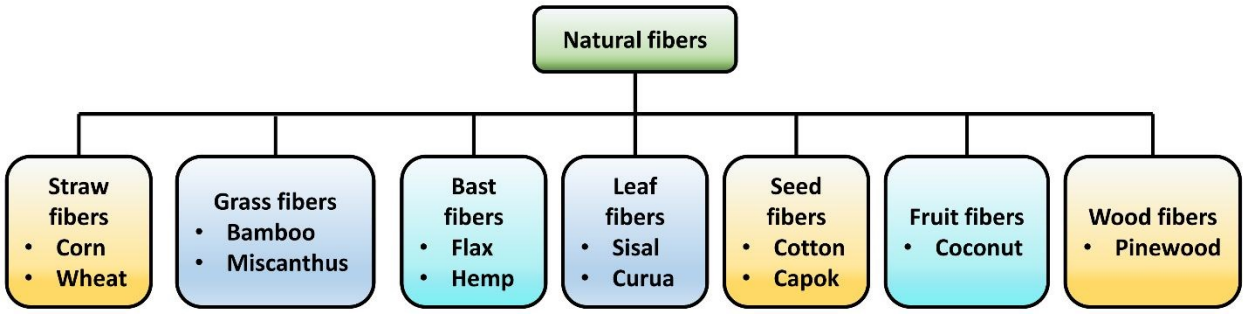

Fig. 20. Classification of natural fibers.

NFs properties such as water content, wettability with polymeric matrix, differences in the coefficients of linear thermal expansion compared to the matrix can play an important role in determining the interfacial strength of the developed composites. The performances of the NFs reinforced rubber composites can be determined by the aspect ratio of the fibers, chemical functionality of the rubber matrix, the chemical composition of the fibers, fibers orientation in the matrix, the surface texture of the fibers, volume fraction of the fibers, interfacial adhesion, type of manufacturing method, manufacturing parameters, and void content [219]. Interfacial interaction between the matrix and fibers is a key factor that determines the performances of the resulting

View Article Online
DOI: 10.1039/D1GC01115D

composites because good interfacial interaction between the fiber and matrix can provide an effective stress transfer from one phase to another [222, 223]. Therefore, various oxidative and non-oxidative chemical treatment strategies are established for NFs [224]. Surface modified NFs (e.g., jute, coir, sisal, oil palm fibers, bamboo, etc.) have been used as a reinforcement in rubber matrices to produce biocomposites with improved performances [225-227]. For instance, surface modification of the NFs can minimize the water uptake as well as enhance the interfacial interaction with rubber matrices [219]. Benzoyl peroxide, silane, and alkali-treated short NFs reinforced NR composites enhanced adhesion, tensile properties, and dynamic mechanical properties [228, 229]. The good interfacial bonding between the NR and chemically treated NFs can improve damping property because of the reduction in energy dissipation [230, 231]. The dynamic loss and storage modulus of the alkali-treated sisal/oil palm fibers/NR composites were found to increase [231].

Hussain et al. [232] studied the physicomechanical properties of the NR vulcanizates with acetyl modified long and short linen fiber wastes. It was observed that the acetyl modified linen fiber waste can improve the physicomechanical properties of the resulting composites. The alkali-treated short jute fibers were modified with acid functionalized multiwall carbon nanotubes (MWCNTs) to enhance the compatibility with NR [233]. The MWCNTs treated jute fibers exhibited hydrophobic nature to form good interaction with rubber matrix via mechanical interlocking mechanism. Consequently, mechanical properties were significantly improved in the developed composites with up to the 20 phr MWCNTs modified jute fiber loading.

In short fiber-reinforced composites, fibers with critical length can provide superior performances in the composites. For example, alkali-treated coir fibers/NR composites with critical fiber length (10 mm) displayed higher mechanical properties in both machine and transverse directions [234-236]. The alkali-treated coir fiber reinforced rubber composites indicated

View Article Online
DOI: 10.1039/D1GC01115D

less anisotropic swelling in toluene as compared to their corresponding untreated composites. Recently, the biodegradability of short flax fibers and sawdust filed NR composite was investigated in the presence of *Aspergillus niger* fungus [237]. Both crosslinked and uncrosslinked NR composites indicated surface erosion with holes and cavities after 60 days of incubation, suggesting biodegradation of the NR composites can be enhanced as a result of the fibers.

Hybrid NFs reinforced rubber composites have been widely studied because hybrid reinforcements can complement each other. Jacob et al. [238] observed that the water uptake of NR composites with sisal/oil palm hybrid fibers was mainly influenced by the fibers. Due to the higher polarity of the NFs, sisal/oil palm fibers/NR composites showed an increase in the dielectric constant values while reducing the volume resistivity [239]. Similarly, NR composites were prepared using a combination of coir/sisal hybrid fibers for potential antistatic application [240]. The NR composites with alkali, acetylation, benzoylation, peroxide, and permanganate treated coir/sisal hybrid fibers showed a reduction in the dielectric constants because of the reduced hydrophilicity of the fibers.

Often, rubber matrix modification or addition of compatibilizers into the rubber composites is conducted to improve the interaction between the fibers and matrices. Introducing compatibilizer into the composites can reduce the interfacial tension by increasing interfacial adhesion. For example, strong rubber–filler interaction was achieved in the rubber composites with the help of the maleated NR as a compatibilizer [241]. Similarly, a silane-based compatibilizer was found to enhance the tensile strength, tear strength, hardness, and tensile modulus of NR/bamboo fiber composites [242]. The scorch and cure time were increased with increasing rice husk in the ENR composites [243]. When rice husk ash was incorporated into the maleated NR and ENR, the resulting composites showed a higher tensile modulus compared to rice husk ash/NR composites [244]. The

View Article Online
DOI: 10.1039/D1GC01115D

highest crosslink density and the shortest scorch time were observed in the rice husk ash/ENR composites compared to the NR and the maleated NR composites counterparts. The observed high crosslinking density was due to ENR tended to activate the adjacent double bonds in the rubber molecules to form free radicals. Subsequently, the free radicals can crosslink with sulfur to increase the crosslinking density. The observed lower scorch time in the maleated rice husk ash/NR composite was attributed to the acidity of maleic acid and the interaction between maleic anhydride and the accelerator.

Among compatibilizers, maleic anhydride-grafted NR and ENR were mostly used with NF-filled rubber composites to improve the performances [245]. For instance, paper sludge/NR composites were compatibilized with maleated NR [246]. Due to the enhanced compatibility between the paper sludge and NR with the help of the maleated NR, better tensile modulus, tensile strength, scorch, and cure time were observed in the resulting composites compared to corresponding uncompatibilized composites. Furthermore, the palm ash/NR composites compatibilized with the maleated NR resulted in reduced damping characteristics [247]. A synergistic effect was observed in the jute fiber/NR composites developed with 2.5 phr stearic acid-modified nanoclay. Due to the synergistic effect, the resulting hybrid rubber composites showed promising improvement in the dynamic mechanical properties. In another study, maleic anhydride (2.5%) was used as a compatibilizer to enhance the interfacial adhesion between ground bagasse powder/CB/SBR composites [248]. It was observed that mechanical properties of the SBR vulcanizates can be preserved up to 50 phr of bagasse powder. Zhou et al. [221] conducted an extensive review on the effects of lignocellulosic fibers incorporation in a range of rubber matrices.

NFs are more inherently hydrophilic as compared to virgin rubbers. As a result, the NF-reinforced rubber composites are sensitive to water/moisture. The amount of water absorption has

View Article Online
DOI: 10.1039/D1GC01115D

increased with increasing fiber loading in the composites [249]. This characteristic is very often limiting the NF-reinforced composites application in many areas. However, the water absorption can be reduced by improving the interaction between the fiber and matrix, leading to encapsulation of the fiber by the rubber. For instance, NR/flax fiber composites showed less water uptake compared to NR/hemp and NR/sawdust because of the good interaction between NR and flax fibers [250]. It has been proved that the interfacial adhesion between the fibers and rubber matrix can be enhanced by fiber modification, matrix modification, adding compatibilizer, or the combination of both fiber and matrix modifications [251, 252].

Despite the fact that NF have been extensively used for composites development, the main challenge in the NF is inconsistent in their properties. The inconsistency in the NF properties is attributed to the difference in climate conditions during the growth, origin, types, and extraction methods [253]. The variabilities in the NF can influence the performance of the NF-reinforced composites applications (e.g., durable product developments). Therefore, it is important to identify and understand the NF-reinforced composites performance in order to apply for specific applications.

6. Renewable and sustainable biomass carbon (biochar)

Carbon-based materials such as graphene, graphene oxide (GO), carbon nanotubes (CNT), CB, and carbon fiber (CF) have been proven to be effective reinforcing agents for different polymer materials. The intrinsic nature of these different carbon structures promotes different interaction mechanisms with polymers due to their different carbon architecture and surface properties. Besides their mechanical strength, these carbon materials possess remarkable electrical conductivity and thermal stability, which make them popular filler materials for polymer

View Article Online
DOI: 10.1039/D1GC01115D

composites applications. Currently, there is an estabilished commercial interest for short CFs in injection moulded thermoplastic materials and CB for rubbers.

Fig. 21 presents the various forms of carbon materials that could be used as reinforcing agent of thermoplastics, thermosets, and rubbers. They display diversified physical properties depending on their structures, morphology, and arrangement (allotropes). Most of the carbon-based fillers available in the market presently are sourced from petroleum feedstock (e.g. CB and CF). While most of the crystalline carbon materials provide satisfactory performance, the cost of production of these materials can be high due to their complex synthesis processes and various stages of purification, in addition to safety concerns (e.g. GO and CNT). This has led to the exploration of eco-friendly carbon material alternatives that are derived from low-cost renewable biomass, such as biochar.

View Article Online
DOI: 10.1039/D1GC01115D

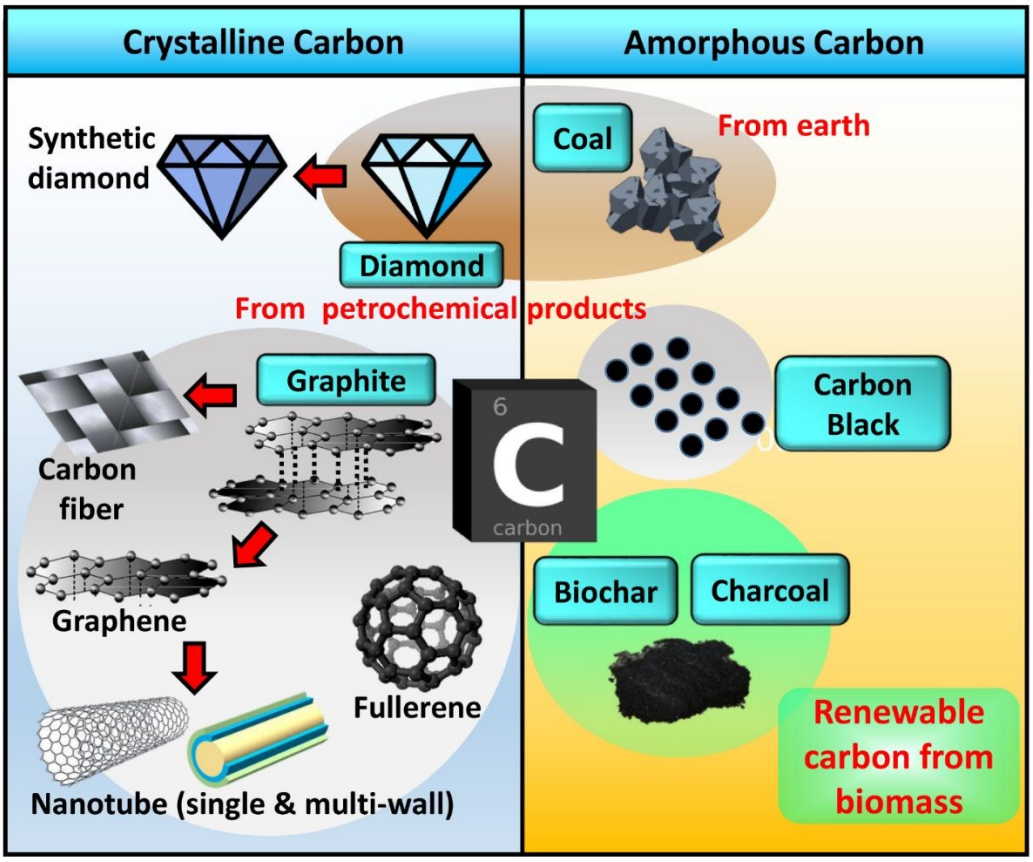

Fig. 21. Different forms of carbons and their derivation that could be potentially used in polymer composite applications.

6.1 Production and characteristic of biochar

In addition to renewable plant-based NFs, that are widely used as fillers, their carbonized form, known as biomass carbon, bioblack, or biochar are currently receiving a substantial interest and emerging as versatile sustainable biofillers that can be used for the fabrication of sustainable and green polymer biocomposites [254-256]. Biochar is an amorphous, porous carbonaceous substance that is derived from various renewable lignocellulosic feedstocks, agricultural co-products, and wastes through a thermal conversion method.

Exploration of biomass-derived carbons for various engineering applications has increased drastically in recent years. This is due to the interest in diverting various biomass and

View Article Online
DOI: 10.1039/D1GC01115D

agro-wastes produced from various agricultural activities into value-added products, which can reduce the environmental concerns. The synthesis and fabrication of nanostructured carbon from biomass possess huge potential for advanced applications such as supercapacitors, photocatalysis, electrode materials, batteries, and nanocomposites [257-259], in addition to their use as a filler or reinforcing agent of composites.

The carbonization of the biomass is usually carried out by heating biomass at >350 °C in a limited oxygen environment, known as a pyrolysis process. With appropriate instrumentation setup, the main products *i.e.,* biochar (solid), bio-oil (liquid), and pyro-gas (combustible gas) can be collected after the pyrolysis process (**Fig. 22**). These products can then be further processed and purified into value-added products for a range of industrial applications. The yield of each product can be controlled by controlling the pyrolysis process; while fast pyrolysis (high heating rate) is usually favorable for high bio-oil yield, slow pyrolysis (low heating rate) is more suitable for the production of a high yield biochar. The yield of biochar and bio-oil can be increased with the use of an appropriate catalyst as well. Recently, the use of biochar reinforced composites have been extensively studied for automotive applications [260-263]. Due to the black color of biochar, it matches well with the color design of most car's interior components. Also, the low density of biochar (1.3-1.4 g/cm^3) fits well with one of the key material innovation goal of the automotive industry, which is overall vehicle weight and carbon footprint reduction.

View Article Online
DOI: 10.1039/D1GC01115D

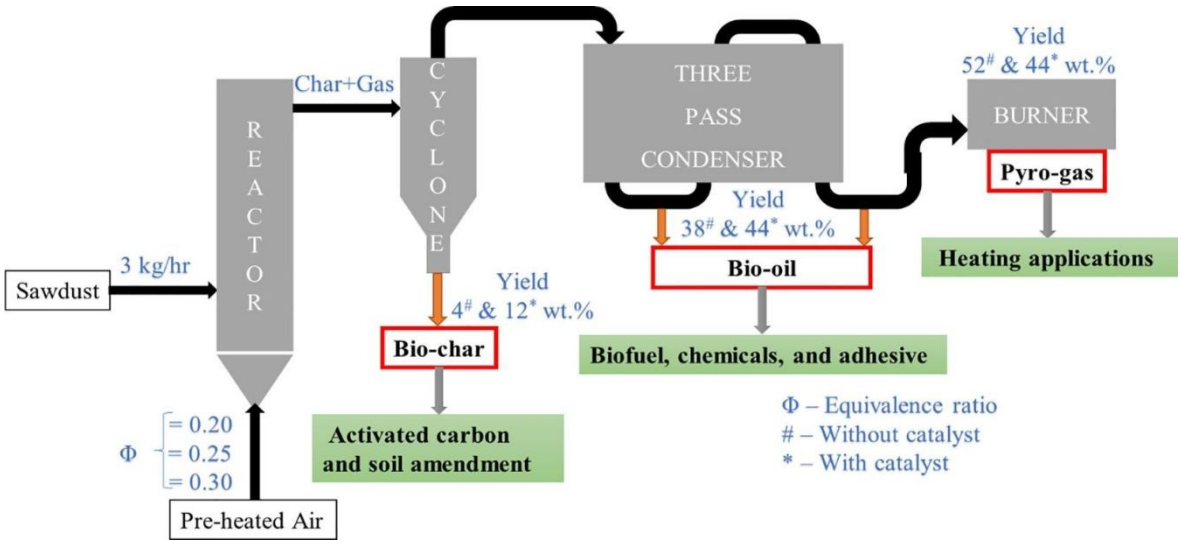

Fig. 22. The three main products i.e. Bio-char, Bio-oil, and Pyro-gas obtained through fast pyrolysis using a fluidized bed system. Figure adapted with permission from ref. [264]. Copyright Elsevier, 2020.

The mechanical strength, carbon content, surface properties of the obtained biochar can vary greatly depending on the pyrolysis conditions, *i.e.,* the heating rate and temperature. The biomass experience a huge change in physicochemical properties after it undergoes a controlled thermal-decomposition during the pyrolysis process at a high temperature. The carbon content and its carbon structure changes significantly with increasing the pyrolysis temperature. **Fig. 23a** presents the carbon structure evolution of the biochar with increasing carbonization temperatures. As the pyrolysis temperature increases, the biochar structures slowly change from amorphous char to composite char and finally to turbostratic char at above 700 °C. The pore sizes and spacing also increases linearly as the temperature increases and reach a saturation stage above 700 °C. Further increase in the pyrolysis temperature produces a higher amount of orderly-arranged carbon structures (graphitic carbon). A highly graphitic carbon structure with many pyrogenic nanopores on surfaces can be formed when the biomass is pyrolyzed above 1000 °C (activation process). Activated carbons are commonly used in filtration and absorption-based applications, such as

View Article Online
DOI: 10.1039/D1GC01115D

water filter and purification, and energy storage materials [265], due to their high and active surface area [266].

Fig. 23b shows a Raman spectra of palm kernel shell biochar pyrolyzed at different temperatures (350-750 °C) [267]. Both the disordered graphene carbon (D-band) and graphitic carbon (G-band) peaks increased with increasing pyrolysis temperature, while the oxygen and hydrogen content decreased [268]. The degree of graphitization (ratio of D-band intensity to G-band intensity, I_D/I_G) of the carbonized palm kernel shell was found to increase with increasing pyrolysis temperature [267] (**Fig. 23c**). The biochar produced from different pyrolysis temperatures, heating rate, and different biomass feedstocks yield different properties and hence affecting the performance of the overall composite when used as fillers. A high temperature pyrolyzed biochar incorporated composites showed a higher increment in modulus and stiffness than a low temperature pyrolyzed biochar due to the high graphitic carbon content [269-271].

View Article Online
DOI: 10.1039/D1GC01115D

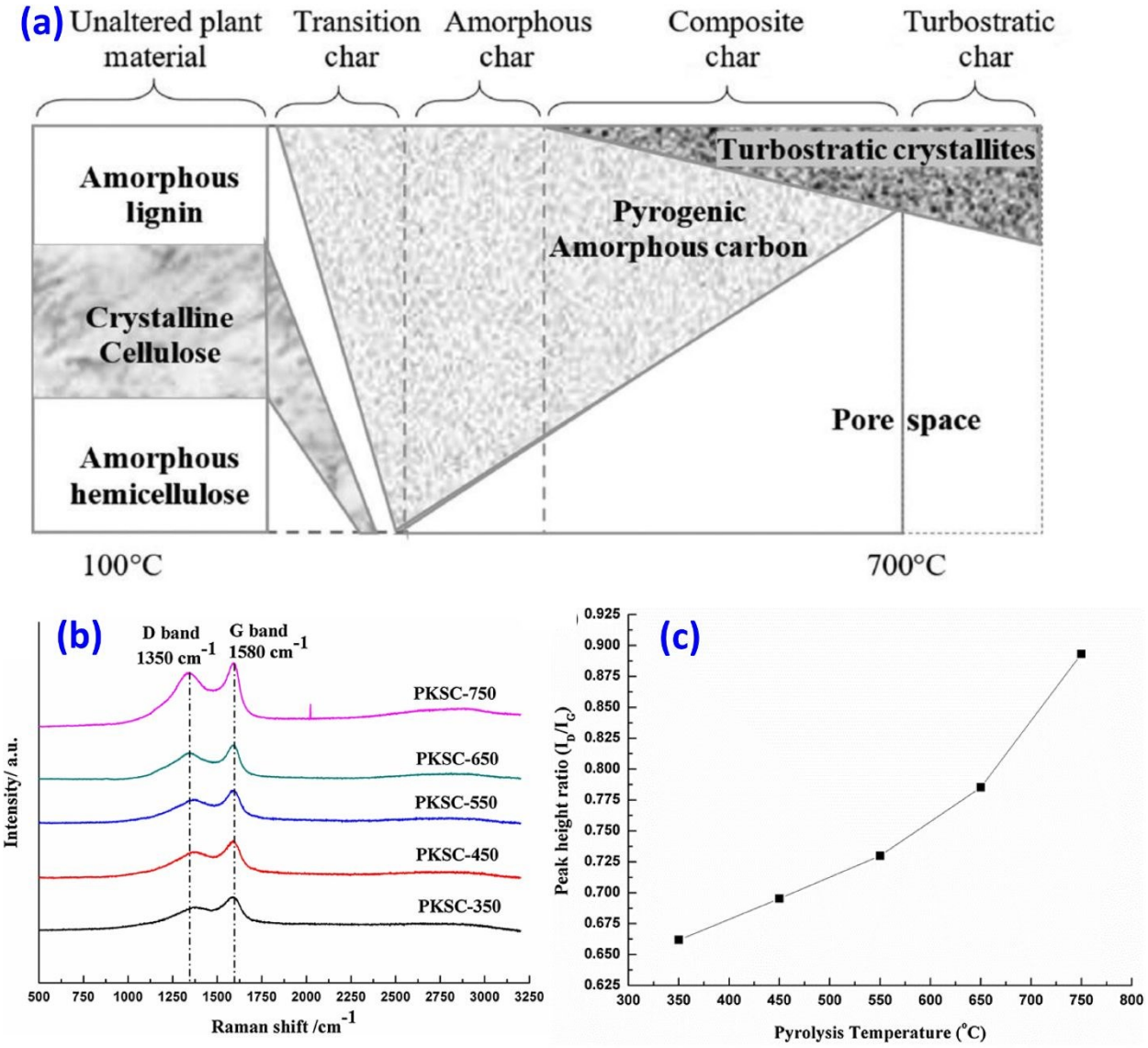

Fig. 23. (a) Biochar carbon structure transition as a function of pyrolysis temperature. Reproduced with permission from ref. [272]. Copyright De Gruyter, 2019, (b) Raman spectra analysis of palm kernel shell biochar pyrolyzed at different temperatures and (c) The degree of graphitization (I_D/I_G) as a function of pyrolysis temperature. Reproduced with permission from ref. [267]. Copyright Elsevier, 2017.

6.2 Biochar's potential in rubber composites application

The incorporation of different feedstocks of biochars have shown favorable effects on different thermoplastic polymers such as polypropylene (PP) [273, 274], poly(lactic acid) (PLA) [275, 276], polybutylene terephthalate (PBT) [277], polycarbonate [278], nylon 6 [279], nylon 6,6 [271] etc. Biochar-

View Article Online
DOI: 10.1039/D1GC01115D

based biocomposites presented comparable performance to conventional mineral-filled polymer composites [280, 281].

CB, derived from petroleum resources, has long been the standard filler used in the rubber industry due to its superior reinforcing effects. However, renewable substitutes for fossil fuel derived fillers, like CB are being explored to obtain a greener, inexpensive, sustainable, and safer next generation alternatives. Biochar owns great potential in substituting CB in the rubber and tire industries due to its resemeblence in physical properties including the color. Recently, the partial replacement of CB with sustainable biochars received substantial research interest. Studies has demonstrated that the hybridization of biochar with CB displayed promising performance as a particle replacement of CB *i.e.,* up to 30% total filler content in different rubber formulations [8, 282, 283]. For instance, a blend of biochar and corn starch in appropriate ratios exhibited better tensile properties than a CB-filled rubber [284]. The 10% hybrid biochar/soy protein-reinforced NR composites have comparable tensile properties as that of CB-reinforced NR composites [285].

Besides pyrolysis temperature, biochar from different biomass can have a different interaction with the rubber matrix. It was found that coconut shell biochar exhibited a better reinforcing effect in NR as compared to wood biochar [286]. This is attributed to the variation in the functionality and interaction between the biochar and NR. The Mooney viscosity and curing time of SBR were enhanced after the incorporation of bamboo biochar [287]. It was also found that carbonized coconut biochar was able to substitute graphite and coal-based fillers as break pad materials [288]. These biochar-based break pads showed good hardness, surface roughness, wear, and friction properties.

View Article Online
DOI: 10.1039/D1GC01115D

Biochar after pyrolysis, without further processing is usually not useful for composites applications due to its large particle size among other factors. The sharp heterogeneous edges of the biochar can act as a stress concentrator in the rubber matrix which leads to reduce the mechanical performance. Thus, it is essential to produce appropriate particle size with uniform morphology. Ball milling is one of the most widely used process to reduce the biochar particle size and generate a high surface area materials without additional chemical activation [263, 289]. Peterson and Kim recently reported that co-milling biochar with a small amount of nanosilica can further reduce the size of biochar [290, 291]. The composites prepared from SBR and co-milled biochar with 1 wt.% nanosilica exhibited great potential to replace up to 40% CB with virtually no loss in tensile strength. In addition, the toughness and elongation of the developed biocomposites displayed substantial improvement. In a separate study, the tensile strength and strain at break of biochar/NBR biocomposites were enhanced as the particle size of the biochar was reduced due to better dispersion and reinforcing ability [292]. However, no obvious modulus change was noticed with particle size variation.

Pyrolysis parameters including pyrolysis temperature, heating rate, and holding time are important parameters to optimize the performance of biochars in composite applications. Biochars produced from the dead leaf at a high temperature (1000 °C) exhibited higher porosity, smaller particle size, carbon content, and lower density as compared to the lower temperature biochars (550, 700, and 900 ^{o}C) [293]. The biochar produced at a high-temperature showed better interactions through the formation of 3D networks with rubber due to smaller particle sizes and carbon content, which greatly enhanced the mechanical properties of the NR composites [293]. In addition, it was found that both biochar/NR and CB/NR had comparable performances, suggesting biochar as a potential reinforcing filler of NR. A study showed that the performances of SBR and coconut shell

View Article Online
DOI: 10.1039/D1GC01115D

derived biochar composites are comparable to the conventional CB (N330 & N772) reinforced SBR, which indicated the excellent potential of biomass derived biochars as replacements for rubber composites [10].

Depending on the production temperature and its raw materials, biochar is usually hydrophilic due to its inherent cellulose-based biomass feedstock and residual –OH moieties remaining after the pyrolysis process. On the other hand, rubbers are very hydrophobic. Therefore, appropriate surface treatments of the biochar could be beneficial to further improve the performance of rubbers. The compatibility of biochar and SBR was enhanced after the coating of the biochar with heat-treated starch due to better hydrophobicity of the treated biochar [9]. The tensile properties and fracture toughness of the composites were improved significantly after employing the coating. The compatibility of rice bran biochar with SBR was also found to improve when biochar was surface treated with (3-Mercaptopropyl) trimethoxysilane (MPTMS) [294]. Zhang et al. [295] compared the mechanical properties of the rice bran biochar-filled C-SBR with a series of surface treatments. They found that 4,4-methylene bis(phenyl isocyanate) (MDI) treated biochar exhibited a stronger reinforcing effect in the composites compared to silane-based treatment due to the interaction of delocalized π electrons on MDI and benzene rings of C-SBR. In addition, the biochar/SBR biocomposites performance could be further enhanced in the presence of ionic liquid *i.e.*, 1-hexyl-3-methylimidazolium hexafluorophosphate (HMIMPF6) [294]. Therefore, an appropriate surface modification of biochar could maximize the performance of the rubber biocomposites which could further advance the practical use of biochar in rubber composites applications.

Qian et al. [296] reported a facile method to produce a high-performance rice husk biochar-filled NR/BR composites. The rice husk biochar was coated with phenolic formaldehyde (PF) resin

View Article Online
DOI: 10.1039/D1GC01115D

to improve its compatibility with the rubber phase. **Fig. 24** depicts the comparison of mechanical performance of the developed biochar/rubber biocomposites and commercial CB (N774)/rubber composites. It can be seen that the PF coated biochar-based rubber biocomposites (S/P-100) exhibited an enhanced tensile strength and elongation at break as compared to the CB (N774), un-coated biochar (SiCB), and rice husk ash (RHA)-based rubber composites. This shows that the mechanical properties of biochar-rubber composites can be significantly enhanced with proper surface modification.

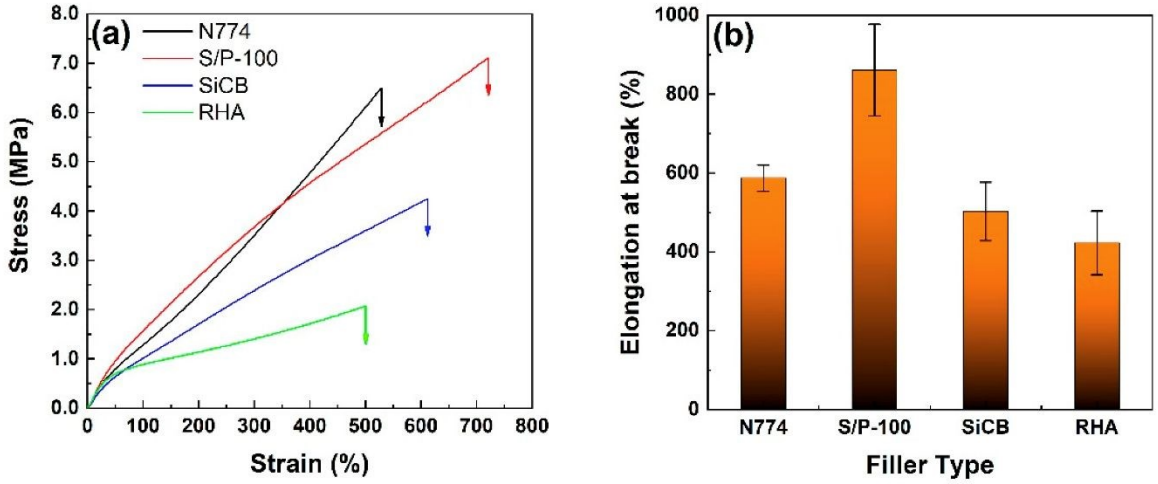

Fig. 24. (a) Stress-strain curves and (b) elongation at break of natural rubber/polybutadiene rubber composites reinforced with different fillers i.e. carbon black (N774), PF coated biochar (S/P-100), uncoated biochar (SiCB), and rice husk ash (RHA). Figure adapted with permission from ref. [296]. Copyright MDPI, 2019.

The substitution of CB with rice bran biochar in NBR composites resulted in promising mechanical properties, good thermal stability, and static friction performance in a separate study[292]. The superior anti-skid performance of biochar/NBR composites could allow it to be used in various engineering applications such as soles and tire treads. Xue et al. [297] found that the rice husk-derived biochar/NR composites can provide excellent mechanical properties when used as a filler in NR. This is because rice husk biochar contains high amount of carbon and silica with Si-O-C bonds which led to synergistic crosslinking and reinforcing effects in the developed rubber

View Article Online
DOI: 10.1039/D1GC01115D

composites. The rice husk biochar-filled rubber biocomposites prepared with approriate processing parameters and partcile size showed higher tensile strength and elongation than the CB-filled rubber composites.

Jiang et al. [298] processed industrial lignin waste into biochar through a pyrolysis process at 800 °C and utilized them as reinforcing filler in SBR (**Fig. 25**). The tensile properties of the developed lignin-based biochar/SBR biocomposites were comparable to the CB/SBR composites with up to 40 phr CB loading. This work has successfully demonstrated the undervalued lignin can be used to produce value-added products that can promote valorization of waste materials.

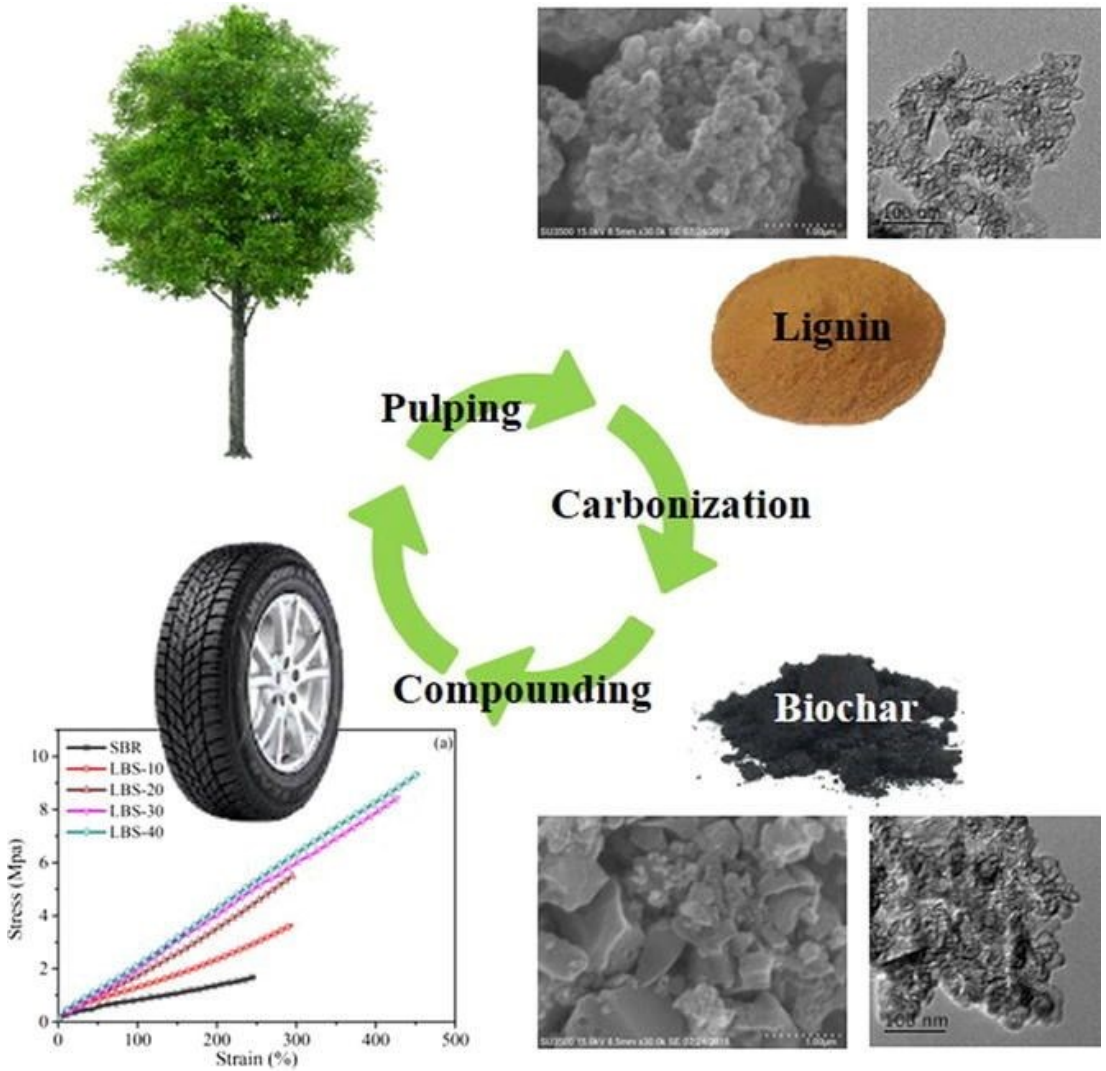

View Article Online
DOI: 10.1039/D1GC01115D

Fig. 25. Lignin waste processing and conversion into biochar (lignin-derived biochar, LB) as a renewable alternative filler to carbon black for styrene butadiene rubber (SBR) composites. Figure adapted with permission from ref. [298]. Copyright Elsevier, 2020.

Overall, biochar-filled rubber composites revealed great competitiveness in many aspects to CB-based rubber composites. Furthermore, the incorporation of biochar in polymers can impart additional functionality such as good electrical conductivity [299, 300], reduced CTE [270, 301], electromagnetic interference shielding [302], and fire retardancy [274, 276].

7. Rubber recycling

One of the most critical applications of rubber, especially NR, is tires. Approximately 70% of all natural and synthetic rubbers are used in tire manufacturing[303]. Despite the massive contribution of rubber in the global transportation sector, it comes with a significant drawback i.e., tire waste. Automotive demand and tire production is increasing every year with population growth and economic uplifting in developing countries, leading to a substantial increase in the accumulation of waste tires. The reuse and recycling of used tires from vehicles and other transportations are challenging. This is due to the essential vulcanization and crosslinking process during the tire manufacturing process. Crosslinked NR or other elastomers cannot be re-processed through re-heating, like in the case of thermoplastics. Therefore, landfilling and incineration are the most popular ways of handling end-of-life tires. It is estimated that more than 1 billion tire waste are discarded into landfills every year around the world [304-306]. The enormous amount of tire waste created strain on the existing landfills and the environment. In order to reduce the environmental impact, recycling, re-utilization, and value recovery from the used tires for various applications have attracted substantial interest. For example, shredded waste tires in asphalt pavement formulation, co-incineration to produce energy for power plants, rubberized flooring,

View Article Online
DOI: 10.1039/D1GC01115D

roofing material, sports goods, and many civil engineering applications can benefit from waste tires[307].

Currently, pyrolysis and devulcanization are the two most widely used techniques to recover value from waste tires for different applications. As presented in **Fig. 26**, pyrolysis of wastes tires can yield four different secondary products i.e., tire derive oil, pyro-gas, pyro-char, and steel wire. Each of them exhibits different physical and chemical properties that are desirable for a wide range of industries, including structural materials, energy and fuel, water treatment, etc.

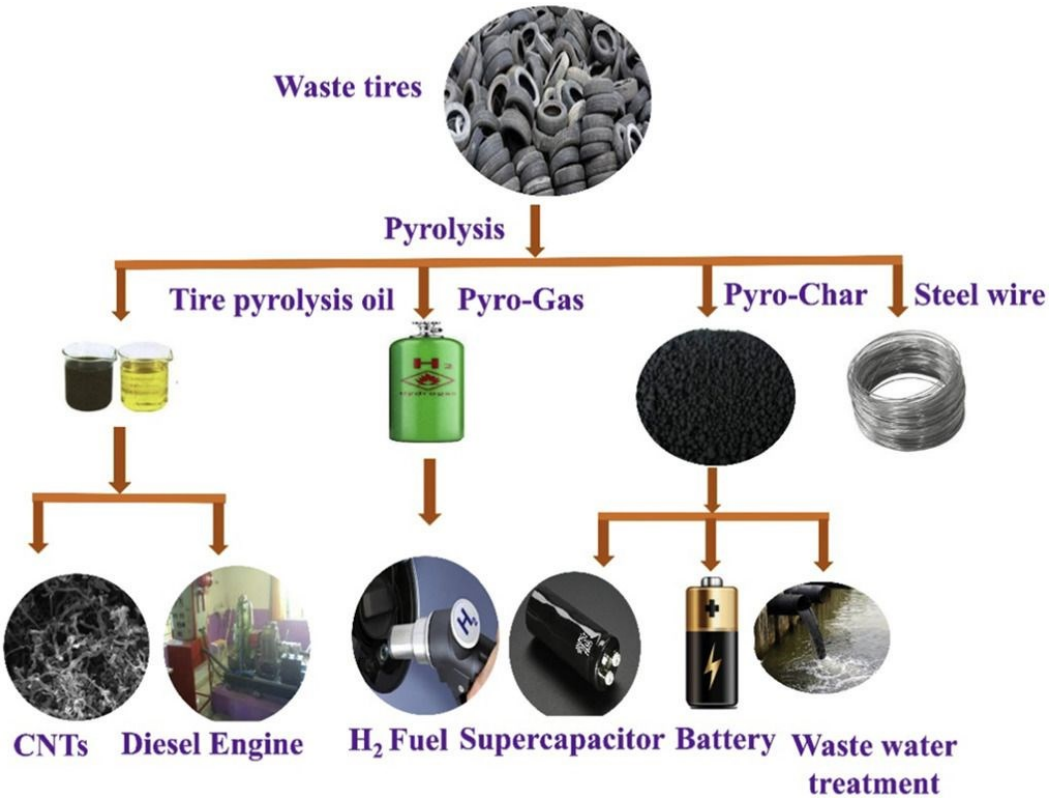

Fig. 26. Waste tire pyrolysis products and their desire application. Figure adapted from ref.[308]. Copyright Elsevier, 2019.

Devulcanization of ground tire rubber (GTR) is required for upcycling, use in a secondary application, or co-vulcanizing it in small amounts (10-20%) with virgin rubber for the fabrication

View Article Online
DOI: 10.1039/D1GC01115D

of new tires. It was reported that the incorporation of GTR with virgin rubber could accelerate the crosslinking reactions of rubber composites [309]. In addition, the thermal, acoustical and physico-mechanical properties could be enhanced. This is because of the similarity in the polarity of GTR with NR that results in good compatibility between phases leading to enhancement in properties [309]. The migration of unreacted curing additives and CB from GTR could also positively affect the mechanical performance of the GTR-based rubber composites. Several established GTR devulcanization and reclamation methods have been developed and utilized in the tire recycling industry. These include chemical reclaiming [310-312], mechanical shearing[313], ultrasound[314], microwave [315, 316], microbiological [317-319] and, thermo-mechanical [320] methods. These methods promote cleavage of sulfur-sulfur (S-S) and carbon-sulfur (C-S) crosslink bonds via different mechanisms.

The use of biofillers in rubbers necessitates re-thinking and re-design of the current recycling approaches. This is because typical rubber recycling processes involve thermal energy to devulcanize the bonds. While some biofillers (e.g., biochar) will be amenable to thermal energy, other fillers (e.g., CNCs, lignin, starch) could degrade depending on the applied thermal energy resulting in inferior recycled material quality. Among the established devulcanization techniques, supercritical carbon dioxide ($ScCO_2$) based on thermo-mechanical process could be the best option for biofiller/rubber recycling. This is because $ScCO_2$ has low viscosity, high diffusivity, and high thermal conductivity [321], and processes involving $ScCO_2$ require less thermal energy. In addition, $ScCO_2$ fluid is chemically inert, non-toxic, inexpensive, non-flammable, easy to be removed from the devulcanized rubber, and its critical point can be easily reached (31.1 °C, 7.38 MPa) [312, 322]. Meysami et al. [323] reported optimized processing conditions to effectively devulcanized scrap tire rubber with $ScCO_2$ in an industrial scale twin-screw extruder, and results showed that mild

View Article Online
DOI: 10.1039/D1GC01115D

temperatures (e.g., 100 °C) are sufficient to achieve the desired crosslink cleavage. The $ScCO_2$ environment can further protect the rubber and the biofiller from degradation during the devulcanization process at high temperatures.

7.1. Biofiller filled rubber composites on tire performance

The rubber manufacturing industry is keen on specific performance parameters, commonly known as magic triangle parameters. These paramters, (i) rolling resistance, which is associated with energy loss during continuous deformation caused by hysteresis, (ii) wear or abrasion resistance, and (iii) wet grip, associated with the friction between wet surface and rubber material, are critical drivers for tire performance [324]. These three parameters are hard to fine-tune in many practical formulations, as one parameter enhancement leads to deterioration of the other(s). Thus, the tire manufacturing industry focuses on finding a sweet spot that balances the magic triangle parameters.

Green tires development that focuses on eco-friendly tire technology in terms of raw materials, rolling resistance, and recycling are being implemented by forefront tire manufacturers like Michelin, Pirelli and Bridgestone Group [325, 326]. Silica plays an important role in green tire production as it can increase the wet grip and reduce the rolling resistance of tires. Silica and other fillers have been used in conjuncture with CB co-reinforce tire treads and improve the magic triangle performance parameters. In the case of partial replacement of CB with sustainable biofillers, it is envisaged that rolling resistance will decrease as compared to CB-filled rubber (similar to silica addition) (**Fig. 27**). This is because secondary fillers generally interrupt network formation of CB, which will form and re-form as an external force is applied (known as Payne effect). Wet traction will also be improved as biofillers or biopolymers are typically hydrophilic

View Article Online
DOI: 10.1039/D1GC01115D

and they interact better with water which can result in better wet traction. On the other hand, wear or abrasion resistance could be reduced as biofillers are soft compared to CB or silica. Outside the magic triangle parameters, biofillers provide weight reduction advantages as compared to traditional rubber fillers. Goodyear Tire and Rubber Company have developed a green tire formulation with their innovative design starch-based materials, i.e., BioTRED, to partially replace silica and CB as tire additives with the main aim of reducing tire weight and rolling resistance [327].

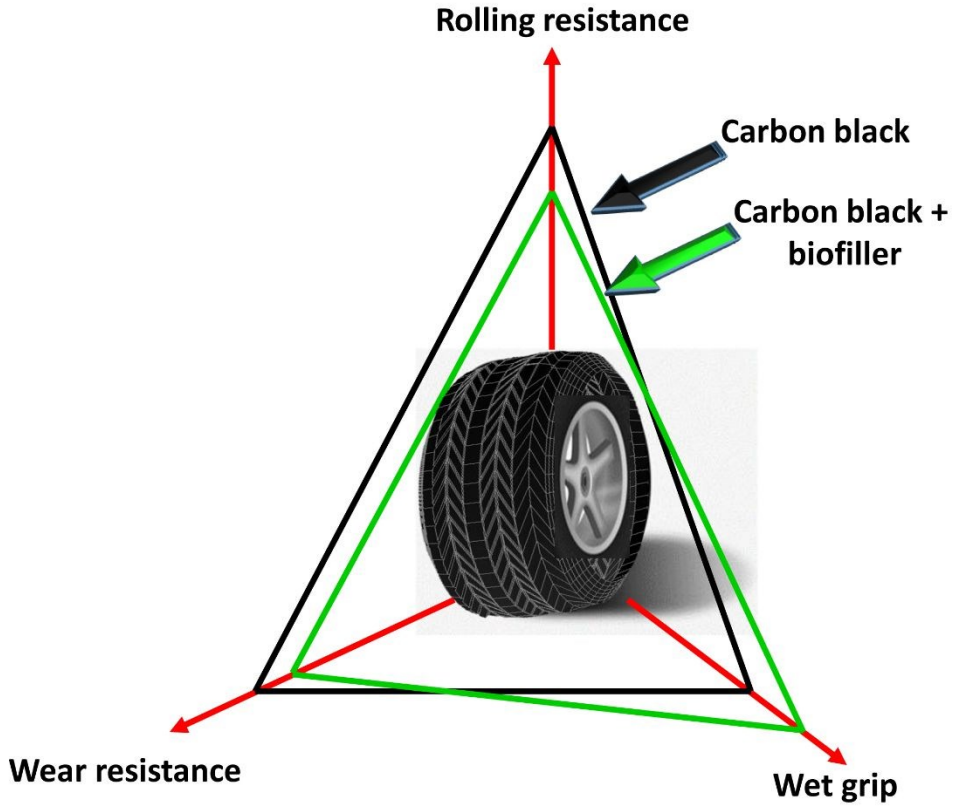

Fig. 27. Anticipation of biofiller filled rubber composites on tire magic triangle challenge as compared to traditional carbon black filler

Despite many researches on the use of sustainable biofillers for rubber composites applications, very limited studies have investigated the partial replacement of non-renewable fillers with sustainable biofiller and their influence on the key performance attributes of rubbers for tire applications. Yu et al [192] reported that the partial replacement of silica with lignin in rubber

View Article Online
DOI: 10.1039/D1GC01115D

formulations and it was found that the NR containing both lignin and silica at optimum content (20 phr lignin and 30 phr silica) exhibited desirable mechanical performance, low rolling resistance and high wet grip property. In addition, the synergistic effect of lignin and silica improves the processability, durability and reduce Payne effect of the NR compounds. In another work reported by Ren and Cornish [324], the partial replacement of silanized silica with eggshell in guayule natural rubber (GNR) composites exhibited improvement in the wet grip performance and rolling resistance reduction. This was indicative that the formulated rubber can produce a green tire with very low energy loss and leads to enhancement in both fuel economy and tire safety. Furthermore, the hybridization of eggshell and silanized silica was shown to improve the durability, such as aging, fatigue, and ozone resistance of the GNR composites.

Recently, Araujo-Morera et al. [328] reported the incorporation of ground tire rubber (GTR) in SBR on the Magic triangle of tire. They found that GTR was able to reduce the rolling resistance while maintaining both abrasion resistance and grip. Moreover, the developed GTR/SBR composites show a complete recovery of stiffness and relaxation after being damaged by cyclic deformation. The authors attributed it to the heterogeneous repairing and healing process of rubber network through the chain interdiffusion and the reversibility of the disulfide bonds.

These encouraging performance and sustainability attribute biofillers bring in rubber composites make them exciting and promising ingredient for the sustainability of rubber products and green tire evelopment. However, studies on biofillers-filled rubber composites specifically addressing the magic triangle properties are still limited. Thus, more research focusing on the impact of surface modification of biofillers on rubber performance beyond the fundamental material properties is required to understand their potential fully.

View Article Online
DOI: 10.1039/D1GC01115D

8. Other developments on environmental sustainability of rubber composites

8.1. Zinc oxide free rubber composites

Often, functional additives such as activators, accelerators, and curing agents are introduced in rubber formulations during processing. The use of these additives has been established since the discovery of NR latex. Although only a small amount (usually ~1-5 phr) of functional additives are used for each formulation. With the increasing demand of rubber products for consumer use, these additives have a huge market in the rubber industry. For example, the global production of zinc oxide (ZnO) activator is approximately 10^5 tons per year to accommodate the rubber industry for various rubber products [329]. The huge demand and usage of these traditional additives for rubber formulation have raised significant concern over their environmental impact, especially to marine life. The toxicity of ZnO to marine life is associated with the generation of reactive oxygen species (ROS) that can cause oxidative stress[330] and also the release of Zn ions that can disrupt homeostasis in organisms [331]. Therefore, in 2004, ZnO has been classified as toxic to aquatic organisms by the European Union, and it is legislated that the ZnO use in rubber products must be limited and controlled, according to the dangerous substances directive (2004/73/EC) [332, 333].

Considerable research works have been conducted on the possibility of reducing or partial replacement of ZnO content in rubber compounds to minimize its environmental effects. It was reported that zinc-m-glycerolate can be used as a replacement for ZnO as a vulcanization activator in both SBR and ethylene-propylene-diene monomer (EPDM) formulations without compromising their performances [334]. On the other hand, zinc stearate is less effective as an activator for rubber vulcanization. Heidman et al. developed a Zn-Clay hybrid that can be used as a substitute that significantly reduced the concentration of ZnO for the rubber vulcanization [335].

View Article Online
DOI: 10.1039/D1GC01115D

Clay act as a carrier to load Zn^{2+} ions through an ion-exchange process during rubber processing. A novel multifunctional additive with amine complex and fatty acids system was used for SBR vulcanization, and their properties were comparable to the conventional ZnO/stearic acid system [336]. This study found that the developed zinc-free formulations were able to obtain the sulfur vulcanization process with good properties. Zinc complexes are good substitutes for ZnO activators in sulfur vulcanization of NBR-based system, without any loss in curing rate and physical properties [332].

Roy et al. [337] synthesized magnesium oxide (MgO) nanoparticles by a sol-gel method and used it as activator to replace ZnO in NR rubber formulation. They reported that NR incorporated with 1 phr nano-MgO exhibited four times faster cure rate index as compared to the NR vulcanized with 5 phr conventional ZnO, with satisfactory mechanical and thermal properties. Das et al. [329] designed and synthesized layered double hydroxide (LDH) to replace ZnO for rubber vulcanization. The developed LDH was able to deliver Zn ions during the curing process to complete the vulcanization process and hence, ZnO-free rubber compound. Recently, plant proteins (i.e., wheat gliadin and corn zein) have been used to improve the properties of ZnO-free synthetic isoprene rubber [338]. These efforts demonstrate that there are a number of chemistries and technologies under development that can potentially replace or complement ZnO, which will reduce the current concerns associated with the leaching of Zn species from rubber goods after being disposed in the environment.

8.2. Volatile organic compounds free rubber composites

The curing/crosslinking of rubber is essential for rubber composites to achieve high elasticity with good physico-mechanical properties. Strong three-dimensional networks are formed between the crosslinking agent and the elastomer's chains during the crosslinking process.

View Article Online
DOI: 10.1039/D1GC01115D

Although several crosslinking agents are available in the market, sulfur remains the most widely adopted crosslinking agent since the discovery of the rubber crosslinking process by Charles Goodyear in 1839. Lately, there are increasing concerns about the negative impact of this crosslinking agent during rubber composites production. For instance, toxic volatile organic compounds (VOC) can be produced during the rubber crosslinking process (sulfur-based organic compounds and amines) [339]. Moreover, the sulfur crosslinking process typically forms S-S and S-C covalent bonds, while crosslinking rubber with peroxide generates C-C covalent bonds [340]. These strong covalent bonds makes the rubber-based products difficult to reprocess or recycle leading to disposal into the landfill as the only option for used rubber goods. In order to address these issues, a number of technologies, such as desulfurization and pyrolysis have been proposed and implemented to recycle rubbers. However, the recovered rubber crumb typically provides inferior mechanical properties and are not environmentally friendly [333, 341].

Other than crosslinking agents, silane-based coupling agents that are implemented to reduce aggregation of nano-silica in rubbers can also contribute to VOC emission during productions. Currently, many countries have regulations governing VOC emissions, such as the Integrated Pollution Prevention and Control Directive (Europe) and the Clean Air Act (USA). In a large-scale tire manufacturing industry, around 5–6 mL/kg of VOCs (VOC/rubber composites) can be generated from the coupling agents during the rubber processing, this is about about ~130,000 m^3 per year [342]. Thus, discovering a VOC-free crosslinking process and coupling agents is essential to mitigate environmental pollution.

Recently, Zhang et al. [340] demonstrated a new green crosslinking strategy with biobased epoxidized soybean oil in a commercial XNBR (**Fig. 28**). Effective crosslinking reactions were observed through the hydrolysis of ester crosslinking with diene groups in the XNBR. In addition,

View Article Online
DOI: 10.1039/D1GC01115D

the ester bonds can breakdown by selective cleavage that results in reprocessable and recyclable rubber products. From the same research group, a green curing process without VOC emission was reported in EPDM rubber composites [333]. An epoxy-functionalized EPDM was able to crosslink with the carboxylic groups of biobased decanedioic acid. In another study, a novel VOC-free epoxy-based coupling agent (bis-epoxypropyl polysulfide) was synthesized and used for SBR composites development in the tire industry [342]. The developed green coupling agent improved the silica dispersion and interactions between silica and rubber that lead to excellent performance in the green tires. A low VOC and alcohol compounds emission during rubber processing was developed through the modification of alkoxy-based silsesquioxane compounds [343].

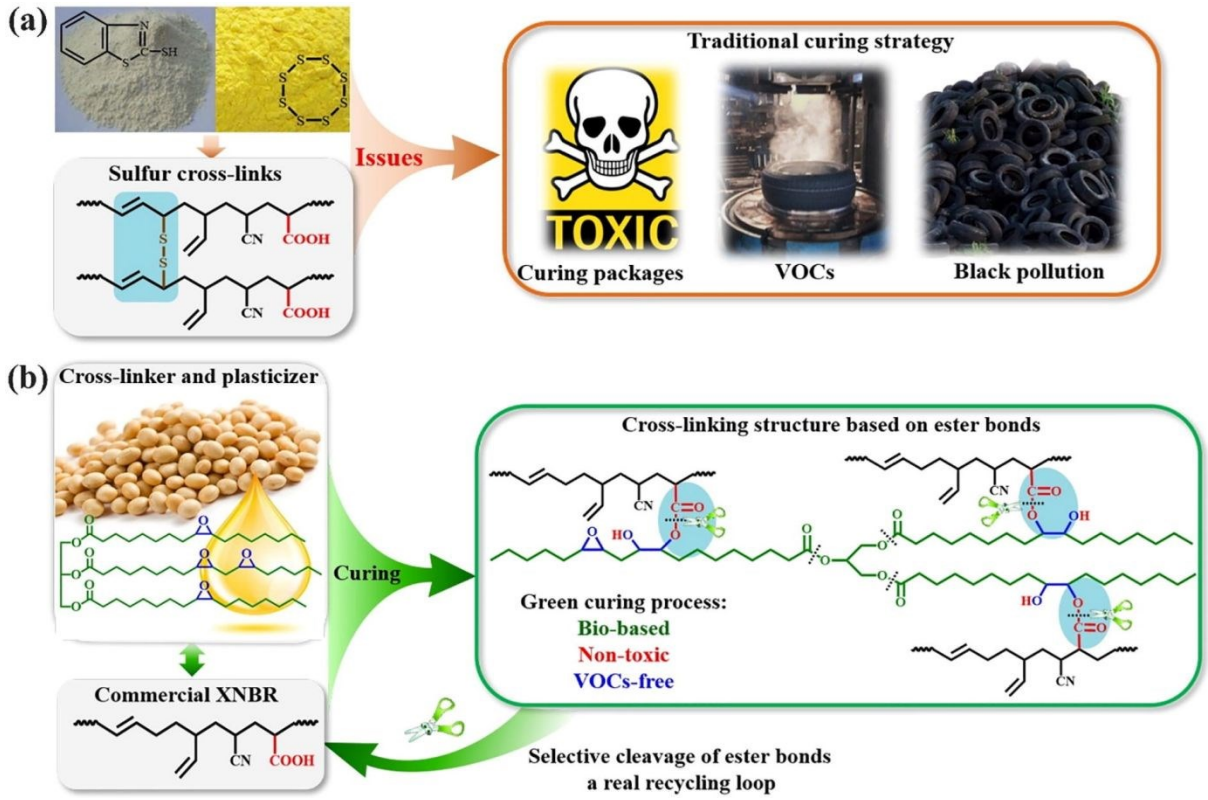

Fig. 28. (a) Schematics showing the current sulfur cross-linking strategy which is suffering from several persistent issues i.e. production of volatile organic compounds (VOCs), pollution, and etc., and (b) the design of next-generation cross-linking strategy based on epoxidized soybean oil (ESO) for carboxylated nitrile rubber (XNBR) via epoxy-acid reaction. Figure adapted with permission from ref. [340]. Copyright Elsevier, 2020.

View Article Online
DOI: 10.1039/D1GC01115D

8.3. Other biofillers

Bhagavatheswaran et al. [4] investigated the properties of chicken eggshell as a potential replacement to $CaCO_3$ in NBR composites. It was found that the biowaste eggshell-filled NBR exhibited better mechanical properties than that of $CaCO_3$/NBR at high filler loading. This can be due to the better interaction of the peptide groups from the residual proteins in the eggshell and carboxylic groups of the modified polymers through covalent and hydrogen bonding. Prochon and Ntumba [344] incorporated keratin feathers from the tanning industry wastes as fillers in carboxylated nitrile rubber (XNBR). These rubber composites were found to have good mechanical properties, oil resistance, durability to thermal aging and ease of biodegradablility. da Costa et al. [345, 346] incorporated rice husk ash in NR compounds and they found that the developed biobased rubber composites exhibited a greater rate of crosslinking and lowered apparent activation energy as compared to the commercial NR compounds containing CB and silica.

Beside the satisfactory mechanical performance, it was found that partial replacement of CB with waste-derived materials (*i.e.*, eggshells, guayule bagasse, carbon fly ash, tomato peels) could reduce the power consumption during rubber processing [347] with good mechanical performances [348]. The incorporation of different types of proteins from soy, casein, zein, gelatin, gluten, and gliadin in guayule NR was found to reduce the bulk viscosity with enhanced thermo-oxidative stability [349].

9. Conclusion and future perspectives

In alignment with global sustainable development and circular economy paradigm, there is an increasing interest for the utilization of renewable and sustainable biomass based fillers (including waste resources from agro-waste) in rubber composites applications. This paper provided a comprehensive review on the current development and improvement of renewable and

View Article Online
DOI: 10.1039/D1GC01115D

bioresource derived fillers for rubber composite applications. With appropriate processing, purification, and sometimes surface modifications, biofillers can be very effective reinforcing agents of rubber composites with a great potential to substitute or complement the incumbent petroleum derived carbon black or the undesirably high density mineral fillers.

Micro- and nanoscale cellulose (MCC, CNC and CNF) are among the most promising alternative reinforcing agents for both natural and synthetic rubbers. However, the main challenge in the use of these fillers in industrial rubber composite applications is their cost-performance balance. The current selling price of CNCs in the market can be as high as $50 USD/kg (Canadian supplier, CelluForce Inc.), and CNF can be > USD 200/kg [350, 351] even after more than a decade of intensified research and development. This is due to the highly sophisticated extraction, purification steps, scale disadvantages. Hence, facile and large scale-production and cost minimization are key factors for the extensive utilization of nanocellulose in rubber composites applications. CNCs, chitin, chitosan, NF and other polysaccharide also have the extra benefit of enhancing biodegradation when used as filler with NR due to their high degradation rate as compare to NR.

Understanding the structural characteristics of lignin is very important in the quest to utilize it for high-performance rubber composite products. With the appropriate modification and surface treatment, both lignins and NFs provided appealing composite properties, including light weighting benefits and good reinforcing effect. These composites performance can be further fine-tuned by hybridizing them with other fillers like CB. The thermal stability of the biofillers and incompatibility between biofillers (hydrophilic) and polymers (hydrophobic) remain a major challenge in developing a high performance rubber biocomposites for real-world applications.

View Article Online
DOI: 10.1039/D1GC01115D

Several compatibilization strategies (e.g., matrix modification, filler modification, etc) were established to achieve desired property set in the hydrophilic filler/rubber composites.

Renewable and low-cost biochar-filled rubber composites also revealed great competitiveness in many aspects to CB-based rubber composites. The replacement of CB with renewable environmental friendly biochar (up to 40 to 60 phr) in tires and rubber technology is possible. Through the proper manipulation of the pyrolysis process (i.e. pyrolysis temperature, heating rate, biomass feedstock, catalyst, etc.), different engineered biochars with various physical properties, graphitization levels, surface functionality, and intrinsic carbon structures can be produced. It is worthwhile to note that there is still some gaps on the correlation between the functionality of biochar and its surface interactions with different types of rubbers (both natural and synthetic). Good compatibility and dispersion of such materials in rubber could further improve the performance and advance the process of replacing the non-renewable CB with this new class of renewable biofillers derived from biomass and waste resources. Furthermore, advances in innovative strategies to synthesize and produce nano-scale biochar in different carbon structure forms can be a game-changing initiative that put forward the biobased carbon materials to the next level.

The performance of rubber composites reinforced with biofillers in tires and other rubber goods is auspicious. However, many studies are limited to fundamental material properties (e.g., tensile strength, modulus, etc.), and performance attributes that specifically address tire magic triangle properties or other key performance parameters or rubber goods are still lacking. Thus, more research is needed to design and modify biofillers that focus on specific goods, such as green tire applications. In addition, rubber recycling process investigations are limited to only CB filled

View Article Online
DOI: 10.1039/D1GC01115D

rubber goods. Research on biofiller based rubber composites as well as hybrid filler systems is needed to bring biofillers to commercial rubber products.

Despite the continuing research and innovation on various biofiller reinforced rubber composites to support sustainable development, a streamlined and cost effective green processing technology with good product performance are needed to change the future of rubber industry towards a more sustainable development.

Conflicts of interest

There are no conflicts of interest to declare.

Acknowledgements

The financial support of Natural Science and Engineering Research Council (NSERC), Canada Foundation for Innovation (CFI), and MITACS is greatly appreciated.

View Article Online
DOI: 10.1039/D1GC01115D

References

1. J. Holbery and D. Houston, *JOM*, 2006, **58**, 80-86.
2. M. Li, Y. Pu, V. M. Thomas, C. G. Yoo, S. Ozcan, Y. Deng, K. Nelson and A. J. Ragauskas, *Composites Part B: Engineering*, 2020, **200**, 108254.
3. Y. Wu, L. Cai, C. Mei, S. S. Lam, C. Sonne, S. Q. Shi and C. Xia, *Materials Today Communications*, 2020, **24**, 101008.
4. E. S. Bhagavatheswaran, A. Das, H. Rastin, H. Saeidi, S. H. Jafari, H. Vahabi, F. Najafi, H. A. Khonakdar, K. Formela, M. Jouyandeh, P. Zarrintaj and M. R. Saeb, *Journal of Polymers and the Environment*, 2019, **27**, 2478-2489.
5. Y. Fan, G. D. Fowler and M. Zhao, *Journal of Cleaner Production*, 2020, **247**, 119115.
6. I. C. B. A. (ICBA), Carbon Black User's Guide, http://www.carbon-black.org/images/docs/2016-ICBA-Carbon-Black-User-Guide.pdf, (accessed 02 July 2020, 2020).
7. A. Roychoudhury and P. P. De, *Journal of Applied Polymer Science*, 1995, **55**, 9-15.
8. S. C. Peterson, *Journal of Elastomers & Plastics*, 2013, **45**, 487-497.
9. S. C. Peterson and S. Kim, *Journal of Elastomers & Plastics*, 2019, **51**, 26-35.
10. Y. Fan, G. D. Fowler and C. Norris, *Industrial & Engineering Chemistry Research*, 2017, **56**, 4779-4791.
11. W. Bai and K. Li, *Composites Part A: Applied Science and Manufacturing*, 2009, **40**, 1597-1605.
12. S. Xu, J. Gu, Y. Luo and D. Jia, *Express Polymer Letters*, 2012, **6**.
13. G. Ulian, S. Tosoni and G. Valdrè, *Physics and Chemistry of Minerals*, 2014, **41**, 639-650.
14. D. Su and X. Li, *Experimental Mechanics*, 2014, **54**, 11-24.
15. A. Codou, J.-M. Pin, M. Misra and A. K. Mohanty, *Green Chemistry*, 2021.
16. J. F. V. Vincent and U. G. K. Wegst, *Arthropod Structure & Development*, 2004, **33**, 187-199.
17. L. H. Nelson and J. M. Henderson, *British Poultry Science*, 1975, **16**, 225-239.
18. J. Schroeter and M. Hobelsberger, *Starch - Stärke*, 1992, **44**, 247-252.
19. H. N. Dhakal and Z. Zhang, in *Biofiber Reinforcements in Composite Materials*, eds. O. Faruk and M. Sain, Woodhead Publishing, 2015, DOI: https://doi.org/10.1533/9781782421276.1.86, pp. 86-103.
20. J. Wang, Q. Li, C. Wu and H. Xu, *Polymers and Polymer Composites*, 2014, **22**, 393 - 400.
21. D. Moonchai, N. Moryadee and N. Poosodsang, 2012.
22. B. Thongma and S. Chiarakorn, 2019.
23. W.-L. Qin, T. Xia, Y. Ye and P.-P. Zhang, *Royal Society Open Science*, 2018, **5**, 171083.
24. R. Drunka, J. Grabis and A. Krumina, *Materials Science*, 2016, **22**, 138-141.
25. Y. Chun, G. Sheng, C. T. Chiou and B. Xing, *Environmental Science & Technology*, 2004, **38**, 4649-4655.
26. A. Brinkmann, M. Chen, M. Couillard, Z. J. Jakubek, T. Leng and L. J. Johnston, *Langmuir*, 2016, **32**, 6105-6114.
27. A. Ilnicka, M. Walczyk and J. P. Lukaszewicz, *Materials Science and Engineering: C*, 2015, **52**, 31-36.
28. A. S. Oladipo, O. A. Ajayi, A. A. Oladipo, S. L. Azarmi, Y. Nurudeen, A. Y. Atta and S. S. Ogunyemi, *Comptes Rendus Chimie*, 2018, **21**, 684-695.
29. Q. Yan and Z. Cai, *Molecules*, 2020, **25**, 2167.
30. T. Skripkina, E. Podgorbunskikh, A. Bychkov and O. Lomovsky, *Coatings*, 2020, **10**, 1115.
31. C. Jiang, H. He, H. Jiang, L. Ma and D. Jia, *Express Polymer Letters*, 2013, **7**.
32. W. Chen, J. Gu and S. Xu, *Express Polymer Letters*, 2014, **8**.
33. M.-C. Li and U. R. Cho, *Materials Letters*, 2013, **92**, 132-135.

View Article Online
DOI: 10.1039/D1GC01115D

34. C. S. Barrera and K. Cornish, *Industrial Crops and Products*, 2016, **86**, 132-142.
35. P. Intharapat, A. Kongnoo and K. Kateungngan, *Journal of Polymers and the Environment*, 2013, **21**, 245-258.
36. B. Karaağaç, *Polymer Composites*, 2014, **35**, 245-252.
37. L. Jong, *Industrial Crops and Products*, 2015, **65**, 102-109.
38. J. Bras, M. L. Hassan, C. Bruzesse, E. A. Hassan, N. A. El-Wakil and A. Dufresne, *Industrial Crops and Products*, 2010, **32**, 627-633.
39. R. C. Reis-Nunes, V. Compañ and E. Riande, *Journal of Polymer Science Part B: Polymer Physics*, 2000, **38**, 393-402.
40. W. von Langenthal and J. Schnetger, in *Ullmann's Encyclopedia of Industrial Chemistry*, 2011, DOI: 10.1002/14356007.a23_421.pub2.
41. M. Sheridan, *The Vanderbilt Rubber Handbook*, RT Vanderbilt Company Inc, Norwalk, CT, 2010.
42. D. Vasseur, P. Labrunie and X. Saintigny, *Google Patents, Tread of a tyre with improved grip on wet ground*, 2013.
43. A. Steyermark, *Kirk-Othmer encyclopedia of chemical technology, vol. 21:* , Elsevier, 1984.
44. C. M. Long, M. A. Nascarella and P. A. Valberg, *Environmental Pollution*, 2013, **181**, 271-286.
45. U. Heinrich, R. Fuhst, S. Rittinghausen, O. Creutzenberg, B. Bellmann, W. Koch and K. Levsen, *Inhalation Toxicology*, 1995, **7**, 533-556.
46. S. Kawanishi, S. Ohnishi, N. Ma, Y. Hiraku and M. Murata, *International Journal of Molecular Sciences*, 2017, **18**, 1808.
47. Y.-P. Wu, Q. Qi, G.-H. Liang and L.-Q. Zhang, *Carbohydrate polymers*, 2006, **65**, 109-113.
48. R. C. R. Nunes and E. B. Mano, *Polymer Composites*, 1995, **16**, 421-423.
49. S. Chuayjuljit, S. Su-Uthai, C. Tunwattanaseree and S. Charuchinda, *Journal of Reinforced Plastics and Composites*, 2009, **28**, 1245-1254.
50. F. Deng, X. Ge, Y. Zhang, M.-C. Li and U. R. Cho, *Journal of Applied Polymer Science*, 2015, **132**.
51. S. K. Basu and B. J. Helmer, *Patents, Cellulose esters in pneumatic tires*, 2013.
52. N. V. Weingart and A. M. Randall, *Google Patents, Rubber Compositions Including Cellulose Esters And Inorganic Oxides*, 2015.
53. A. Y. Coran, K. Boustany and P. Hamed, *Rubber Chemistry and Technology*, 1974, **47**, 396-410.
54. B. Westerlind, S. Hirose, S. Yano, H. Hatekayama and M. Rigdahl, *International Journal of Polymeric Materials and Polymeric Biomaterials*, 1987, **11**, 333-353.
55. P. Flink and B. Stenberg, *British Polymer Journal*, 1989, **21**, 259-267.
56. G. Ahlblad, A. Kron and B. Stenberg, *Polymer International*, 1994, **33**, 103-109.
57. G. Ahlblad, T. Reitberger, B. Stenberg and P. Danielsson, *Polymer International*, 1996, **39**, 261-269.
58. R. C. Reis Nunes, M. López-González and E. Riande, *Journal of Polymer Science Part B: Polymer Physics*, 2005, **43**, 2131-2140.
59. P. Flink, B. Westerlind, M. Rigdahl and B. Stenberg, *Journal of Applied Polymer Science*, 1988, **35**, 2155-2164.
60. A. F. Martins, S. M. de Meneses, L. L. Y. Visconte and R. C. R. Nunes, *Journal of Applied Polymer Science*, 2004, **92**, 2425-2430.
61. V. L. C. Lapa, J. C. Miguez Suarez, L. L. Y. Visconte and R. C. R. Nunes, *Journal of Materials Science*, 2007, **42**, 9934-9939.
62. T. Li, C. Chen, A. H. Brozena, J. Y. Zhu, L. Xu, C. Driemeier, J. Dai, O. J. Rojas, A. Isogai, L. Wågberg and L. Hu, *Nature*, 2021, **590**, 47-56.
63. C. Calvino, N. Macke, R. Kato and S. J. Rowan, *Progress in Polymer Science*, 2020, **103**, 101221.
64. O. Nechyporchuk, M. N. Belgacem and J. Bras, *Industrial Crops and Products*, 2016, **93**, 2-25.

View Article Online
DOI: 10.1039/D1GC01115D

65. A. Blanco, M. C. Monte, C. Campano, A. Balea, N. Merayo and C. Negro, in *Handbook of Nanomaterials for Industrial Applications*, ed. C. Mustansar Hussain, Elsevier, 2018, DOI: https://doi.org/10.1016/B978-0-12-813351-4.00005-5, pp. 74-126.
66. M. A. S. Azizi Samir, F. Alloin and A. Dufresne, *Biomacromolecules*, 2005, **6**, 612-626.
67. G. Siqueira, S. Tapin-Lingua, J. Bras, D. da Silva Perez and A. Dufresne, *Cellulose*, 2011, **18**, 57-65.
68. X. Xu, F. Liu, L. Jiang, J. Y. Zhu, D. Haagenson and D. P. Wiesenborn, *ACS Applied Materials & Interfaces*, 2013, **5**, 2999-3009.
69. X. Cao, C. Xu, Y. Wang, Y. Liu, Y. Liu and Y. Chen, *Polymer Testing*, 2013, **32**, 819-826.
70. A. Šturcová, G. R. Davies and S. J. Eichhorn, *Biomacromolecules*, 2005, **6**, 1055-1061.
71. Y. Habibi, L. A. Lucia and O. J. Rojas, *Chemical Reviews*, 2010, **110**, 3479-3500.
72. J. M. Jardin, Z. Zhang, G. Hu, K. C. Tam and T. H. Mekonnen, *International Journal of Biological Macromolecules*, 2020, **152**, 428-436.
73. A. Dufresne, in *Monomers, Polymers and Composites from Renewable Resources*, eds. M. N. Belgacem and A. Gandini, Elsevier, Amsterdam, 2008, DOI: https://doi.org/10.1016/B978-0-08-045316-3.00019-3, pp. 401-418.
74. X. Cao, C. Xu, Y. Liu and Y. Chen, *Carbohydrate Polymers*, 2013, **92**, 69-76.
75. Y. Chen, Y. Zhang, C. Xu and X. Cao, *Carbohydrate Polymers*, 2015, **130**, 149-154.
76. P. M. Visakh, S. Thomas, K. Oksman and A. P. Mathew, *Composites Part A: Applied Science and Manufacturing*, 2012, **43**, 735-741.
77. D. Lasrado, S. Ahankari and K. Kar, *Journal of Applied Polymer Science*, 2020, **137**, 48959.
78. J. Cao, X. Zhang, X. Wu, S. Wang and C. Lu, *Carbohydrate Polymers*, 2016, **140**, 88-95.
79. X. Wu, C. Lu, Y. Han, Z. Zhou, G. Yuan and X. Zhang, *Composites Science and Technology*, 2016, **124**, 44-51.
80. U. Kulshrestha, T. Gupta, P. Kumawat, H. Jaiswal, S. B. Ghosh and N. N. Sharma, *Polymer Testing*, 2020, **90**, 106676.
81. J. Sun, X. Liu, L. Wang and X. Shi, *Journal of Sol-Gel Science and Technology*, 2018, **85**, 213-220.
82. C. Zhang, Y. Dan, J. Peng, L.-S. Turng, R. Sabo and C. Clemons, *Advances in Polymer Technology*, 2014, **33**.
83. H. Eslami, C. Tzoganakis and T. H. Mekonnen, *Composites Part C: Open Access*, 2020, **1**, 100009.
84. D. Pasquini, E. d. M. Teixeira, A. A. d. S. Curvelo, M. N. Belgacem and A. Dufresne, *Industrial Crops and Products*, 2010, **32**, 486-490.
85. A. E. Way, L. Hsu, K. Shanmuganathan, C. Weder and S. J. Rowan, *ACS Macro Letters*, 2012, **1**, 1001-1006.
86. Y. Chen, G. Li, Q. Yin, H. Jia, Q. Ji, L. Wang, D. Wang and B. Yin, *Polymers for Advanced Technologies*, 2018, **29**, 1507-1517.
87. Q. Yin, D. Wang, H. Jia, Q. Ji, L. Wang, G. Li and B. Yin, *Industrial Crops and Products*, 2018, **113**, 240-248.
88. M. Tian, X. Zhen, Z. Wang, H. Zou, L. Zhang and N. Ning, *ACS Applied Materials & Interfaces*, 2017, **9**, 6482-6487.
89. M. Maiti, R. V. Jasra, S. K. Kusum and T. K. Chaki, *Industrial & Engineering Chemistry Research*, 2012, **51**, 10607-10612.
90. R. Gu, M. Sain and S. Konar, *Journal of Materials Science*, 2014, **49**, 3125-3134.
91. B. S. Zhang, Z. X. Zhang, X. F. Lv, B. X. Lu and Z. X. Xin, *Polymer Engineering & Science*, 2012, **52**, 218-224.
92. R. Blanchard, E. O. Ogunsona, S. Hojabr, R. Berry and T. H. Mekonnen, *ACS Applied Polymer Materials*, 2020, **2**, 887-898.
93. L. Goetz, A. Mathew, K. Oksman, P. Gatenholm and A. J. Ragauskas, *Carbohydrate Polymers*, 2009, **75**, 85-89.

View Article Online
DOI: 10.1039/D1GC01115D

94. L. Goetz, M. Foston, A. P. Mathew, K. Oksman and A. J. Ragauskas, *Biomacromolecules*, 2010, **11**, 2660-2666.
95. F. Jiang, C. Pan, Y. Zhang and Y. Fang, *Applied Surface Science*, 2019, **480**, 162-171.
96. C. E. Hoyle and C. N. Bowman, *Angewandte Chemie International Edition*, 2010, **49**, 1540-1573.
97. B. Parambath Kanoth, M. Claudino, M. Johansson, L. A. Berglund and Q. Zhou, *ACS Applied Materials & Interfaces*, 2015, **7**, 16303-16310.
98. M. Fumagalli, J. Berriot, B. de Gaudemaris, A. Veyland, J.-L. Putaux, S. Molina-Boisseau and L. Heux, *Soft Matter*, 2018, **14**, 2638-2648.
99. S. Fukui, T. Ito, T. Saito, T. Noguchi and A. Isogai, *Cellulose*, 2019, **26**, 463-473.
100. S. Fukui, T. Ito, T. Saito, T. Noguchi and A. Isogai, *Composites Science and Technology*, 2018, **167**, 339-345.
101. T. Noguchi, M. Endo, K. Niihara, H. Jinnai and A. Isogai, *Composites Science and Technology*, 2020, **188**, 108005.
102. A. Sinclair, X. Zhou, S. Tangpong, D. S. Bajwa, M. Quadir and L. Jiang, *ACS Omega*, 2019, **4**, 13189-13199.
103. H. Eslami, C. Tzoganakis and T. H. Mekonnen, *Cellulose*, 2020, **27**, 5267-5284.
104. S. Eyley and W. Thielemans, *Nanoscale*, 2014, **6**, 7764-7779.
105. E. Abraham, M. S. Thomas, C. John, L. A. Pothen, O. Shoseyov and S. Thomas, *Industrial Crops and Products*, 2013, **51**, 415-424.
106. M. Mariano, N. El Kissi and A. Dufresne, *Carbohydrate Polymers*, 2016, **137**, 174-183.
107. Y. Chen, C. Xu and X. Cao, *Polymer Composites*, 2015, **36**, 623-629.
108. S. Yasin, M. Hussain, Q. Zheng and Y. Song, *Journal of Colloid and Interface Science*, 2021, **588**, 602-610.
109. R. C. R. Nunes, in *Chemistry, Manufacture and Applications of Natural Rubber*, eds. S. Kohjiya and Y. Ikeda, Woodhead Publishing, 2014, DOI: https://doi.org/10.1533/9780857096913.2.284, pp. 284-302.
110. K. Fein, D. W. Bousfield and W. M. Gramlich, *Carbohydrate Polymers*, 2020, **250**, 117001.
111. A. Ali Shah, F. Hasan, Z. Shah, N. Kanwal and S. Zeb, *International Biodeterioration & Biodegradation*, 2013, **83**, 145-157.
112. F. Bosco, D. Antonioli, A. Casale, V. Gianotti, C. Mollea, M. Laus and G. Malucelli, *Bioremediation Journal*, 2018, **22**, 43-52.
113. E. Abraham, P. A. Elbi, B. Deepa, P. Jyotishkumar, L. A. Pothen, S. S. Narine and S. Thomas, *Polymer Degradation and Stability*, 2012, **97**, 2378-2387.
114. X. Wu, C. Lu, H. Xu, X. Zhang and Z. Zhou, *ACS Applied Materials & Interfaces*, 2014, **6**, 21078-21085.
115. X. Wu, C. Lu, X. Zhang and Z. Zhou, *Journal of Materials Chemistry A*, 2015, **3**, 13317-13323.
116. E. Ogunsona, E. Ojogbo and T. Mekonnen, *European Polymer Journal*, 2018, **108**, 570-581.
117. E. Ojogbo, R. Blanchard and T. Mekonnen, *Journal of Polymer Science Part A: Polymer Chemistry*, 2018, **56**, 2611-2622.
118. E. Ojogbo, V. Ward and T. H. Mekonnen, *Carbohydrate Polymers*, 2020, **229**, 115422.
119. E. Ojogbo, E. O. Ogunsona and T. H. Mekonnen, *Materials Today Sustainability*, 2020, **7-8**, 100028.
120. E. Ojogbo, J. Jardin and T. H. Mekonnen, *Industrial Crops and Products*, 2020, DOI: https://doi.org/10.1016/j.indcrop.2020.113153, 113153.
121. *US Pat.*, 3830762, 1974.
122. N. Q. Duy, A. A. Rashid and H. Ismail, *Polymer-Plastics Technology and Engineering*, 2012, **51**, 940-944.
123. I. M. Alwaan, *Journal of Applied Polymer Science*, 2018, **135**, 46347.

View Article Online
DOI: 10.1039/D1GC01115D

124. M. Chalid, Y. A. Husnil, S. Puspitasari and A. Cifriadi, *Polymers*, 2020, **12**, 3017.
125. A. T. Le, A. Gacoin, A. Li, T. H. Mai and N. El Wakil, *Composites Part B: Engineering*, 2015, **75**, 201-211.
126. A. N. Roziafanto, S. Puspitasari, A. Cifriadi, D. Hasnasoraya and M. Chalid, *Macromolecular Symposia*, 2020, **391**, 1900142.
127. M. M. Senna, R. M. Mohamed, A. N. Shehab-Eldin and S. El-Hamouly, *Journal of Industrial and Engineering Chemistry*, 2012, **18**, 1654-1661.
128. S.-A. Riyajan, Y. Sasithornsonti and P. Phinyocheep, *Carbohydrate Polymers*, 2012, **89**, 251-258.
129. C. Liu, Y. Shao and D. Jia, *Polymer*, 2008, **49**, 2176-2181.
130. C. Ji, S.-S. Song, L.-Q. Zhang and Y.-P. Wu, *Carbohydrate Polymers*, 2011, **86**, 581-586.
131. M.-C. Li, X. Ge and U. R. Cho, *Macromolecular Research*, 2013, **21**, 519-528.
132. X. Wang, L. Zhang and D. Yue, *Integrated Ferroelectrics*, 2012, **137**, 149-155.
133. J.-L. Putaux, S. Molina-Boisseau, T. Momaur and A. Dufresne, *Biomacromolecules*, 2003, **4**, 1198-1202.
134. H. Angellier, S. Molina-Boisseau and A. Dufresne, *Macromolecular Symposia*, 2006, **233**, 132-136.
135. P. Mélé, H. Angellier-Coussy, S. Molina-Boisseau and A. Dufresne, *Biomacromolecules*, 2011, **12**, 1487-1493.
136. T. D. Rathke and S. M. Hudson, *Journal of Macromolecular Science, Part C*, 1994, **34**, 375-437.
137. M. Barikani, E. Oliaei, H. Seddiqi and H. Honarkar, *Iranian Polymer Journal*, 2014, **23**, 307-326.
138. X. Yang, J. Liu, Y. Pei, X. Zheng and K. Tang, *ENERGY & ENVIRONMENTAL MATERIALS*, 2020, **3**, 492-515.
139. J. F. Revol and R. H. Marchessault, *International Journal of Biological Macromolecules*, 1993, **15**, 329-335.
140. Y. Liu, M. Liu, S. Yang, B. Luo and C. Zhou, *ACS Sustainable Chemistry & Engineering*, 2018, **6**, 325-336.
141. N. Zhang and H. Cao, *Materials*, 2020, **13**, 1039.
142. D. K. Singh and A. R. Ray, *Journal of Macromolecular Science, Part C*, 2000, **40**, 69-83.
143. S. Poompradub, in *Chemistry, Manufacture and Applications of Natural Rubber*, eds. S. Kohjiya and Y. Ikeda, Woodhead Publishing, 2014, DOI: https://doi.org/10.1533/9780857096913.2.303, pp. 303-324.
144. A. Morin and A. Dufresne, *Macromolecules*, 2002, **35**, 2190-2199.
145. Y. Tian, K. Liang, X. Wang and Y. Ji, *ACS Sustainable Chemistry & Engineering*, 2017, **5**, 3305-3313.
146. J. Araki, Y. Yamanaka and K. Ohkawa, *Polymer Journal*, 2012, **44**, 713-717.
147. K. Gopalan Nair, A. Dufresne, A. Gandini and M. N. Belgacem, *Biomacromolecules*, 2003, **4**, 1835-1842.
148. K. Gopalan Nair and A. Dufresne, *Biomacromolecules*, 2003, **4**, 666-674.
149. K. Gopalan Nair and A. Dufresne, *Biomacromolecules*, 2003, **4**, 657-665.
150. M. Liu, Q. Peng, B. Luo and C. Zhou, *European Polymer Journal*, 2015, **68**, 190-206.
151. B. Ding, S. Huang, K. Shen, J. Hou, H. Gao, Y. Duan and J. Zhang, *Carbohydrate Polymers*, 2019, **225**, 115230.
152. Y. Liu, F. Wu, X. Zhao and M. Liu, *ACS Sustainable Chemistry & Engineering*, 2018, **6**, 10595-10605.
153. J. Hu, X. Tian, J. Sun, J. Yuan and Y. Yuan, *Journal of Applied Polymer Science*, 2020, **137**, 49173.
154. M. Dominic C.D, R. Joseph, P. M. Sabura Begum, A. Raghunandanan, N. T. Vackkachan, D. Padmanabhan and K. Formela, *Carbohydrate Polymers*, 2020, **245**, 116505.
155. J. Nie, W. Mou, J. Ding and Y. Chen, *Composites Part B: Engineering*, 2019, **172**, 152-160.

View Article Online
DOI: 10.1039/D1GC01115D

156. M. Ishihara, K. Nakanishi, K. Ono, M. Sato, M. Kikuchi, Y. Saito, H. Yura, T. Matsui, H. Hattori, M. Uenoyama and A. Kurita, *Biomaterials*, 2002, **23**, 833-840.
157. X. Liang, X. Wang, Q. Xu, Y. Lu, Y. Zhang, H. Xia, A. Lu and L. Zhang, *Biomacromolecules*, 2018, **19**, 340-352.
158. S. T. Sam, M. A. Nuradibah, H. Ismail, N. Z. Noriman and S. Ragunathan, *Polymer-Plastics Technology and Engineering*, 2014, **53**, 631-644.
159. J. Johns and V. Rao, *International Journal of Polymeric Materials and Polymeric Biomaterials*, 2011, **60**, 766-775.
160. V. M. Correlo, L. F. Boesel, M. Bhattacharya, J. F. Mano, N. M. Neves and R. L. Reis, *Materials Science and Engineering: A*, 2005, **403**, 57-68.
161. V. Rao and J. Johns, *Journal of Applied Polymer Science*, 2008, **107**, 2217-2223.
162. J. Johns and V. Rao, *International Journal of Polymer Analysis and Characterization*, 2008, **13**, 280-291.
163. J. Johns and V. Rao, *Journal of Adhesion Science and Technology*, 2012, **26**, 793-812.
164. J. Johns and V. Rao, *Fibers and Polymers*, 2009, **10**, 761-767.
165. J. Johns and V. Rao, *International Journal of Polymer Analysis and Characterization*, 2009, **14**, 508-526.
166. H. Ismail, S. M. Shaari and N. Othman, *Polymer Testing*, 2011, **30**, 784-790.
167. S.-A. Riyajan and W. Sukhlaaied, *Materials Science and Engineering: C*, 2013, **33**, 1041-1047.
168. C. Xu, J. Nie, W. Wu, Z. Zheng and Y. Chen, *ACS Sustainable Chemistry & Engineering*, 2019, **7**, 15778-15789.
169. S. Boonrasri, P. Sae–Oui and P. Rachtanapun, *Molecules*, 2020, **25**, 2777.
170. S. Yorsaeng, O. Pornsunthorntawee and R. Rujiravanit, *Plasma Chemistry and Plasma Processing*, 2012, **32**, 1275-1292.
171. A. Arakkal, I. Aazem, G. Honey, A. Vengellur, S. G. Bhat and G. C. S. Sailaja, *Journal of Applied Polymer Science*, 2021, **138**, 49608.
172. L. Ming-zhe, W. Li-feng, F. Lei, L. Pu-wang and L. Si-dong, *Micro & Nano Letters*, 2017, **12**, 386-390.
173. M. Fan, Q. Hu and K. Shen, *Carbohydrate Polymers*, 2009, **78**, 66-71.
174. P. Rahmanian-Devin, V. Baradaran Rahimi and V. R. Askari, *Advances in Pharmacological and Pharmaceutical Sciences*, 2021, **2021**, 6640893.
175. P. Aramwit, S. Ekasit and R. Yamdech, *Biomedical Microdevices*, 2015, **17**, 84.
176. W. Zeng, J. Huang, X. Hu, W. Xiao, M. Rong, Z. Yuan and Z. Luo, *International Journal of Pharmaceutics*, 2011, **421**, 283-290.
177. A. Gupta and B. S. Kim, *Nanomaterials*, 2019, **9**, 225.
178. C. Xu, J. Nie, W. Wu, L. Fu and B. Lin, *Carbohydrate Polymers*, 2019, **205**, 410-419.
179. N. Behabtu and S. Kralj, *ACS Sustainable Chemistry & Engineering*, 2020, **8**, 9947-9954.
180. A. Adibi, J. Kim, J. Mok, C. Lenges, L. Simon, T. H. Mekonnen, *Carbohydrate Polymers*, 2021, **267**, 118234.
181. T. H. Mekonnen, N. Behabtu and C. Lenges, *Carbohydrate Polymers*, 2020, **241**, 116252.
182. V. K. Thakur, M. K. Thakur, P. Raghavan and M. R. Kessler, *ACS Sustainable Chemistry & Engineering*, 2014, **2**, 1072-1092.
183. R. Muthuraj, A. Horrocks and B. Kandola, *Journal of Materials Science*, 2020, 1-18.
184. R. Muthuraj, M. Hajee, A. Horrocks and B. K. Kandola, *International journal of biological macromolecules*, 2019, **132**, 439-450.
185. S. Brudin and P. Schoenmakers, *Journal of separation science*, 2010, **33**, 439-452.
186. J. H. Lora and W. G. Glasser, *Journal of Polymers and the Environment*, 2002, **10**, 39-48.

View Article Online
DOI: 10.1039/D1GC01115D

187. W. O. Doherty, P. Mousavioun and C. M. Fellows, *Industrial crops and products*, 2011, **33**, 259-276.
188. N. A. Mohamad Aini, N. Othman, M. H. Hussin, K. Sahakaro and N. Hayeemasae, *Frontiers in Materials*, 2020, **6**.
189. D. Barana, M. Orlandi, L. Zoia, L. Castellani, T. Hanel, C. Bolck and R. Gosselink, *ACS sustainable chemistry & engineering*, 2018, **6**, 11843-11852.
190. T. Bova, C. D. Tran, M. Y. Balakshin, J. Chen, E. A. Capanema and A. K. Naskar, *Green Chemistry*, 2016, **18**, 5423-5437.
191. K. Roy, S. C. Debnath and P. Potiyaraj, *Journal of Polymers and the Environment*, 2020, 1-21.
192. P. Yu, H. He, Y. Jia, S. Tian, J. Chen, D. Jia and Y. Luo, *Polymer Testing*, 2016, **54**, 176-185.
193. A. Hosseinmardi, N. Amiralian, A. N. Hayati, D. J. Martin and P. K. Annamalai, *Industrial Crops and Products*, **159**, 113063.
194. J. Datta, P. Parcheta and J. Surówka, *Industrial Crops and Products*, 2017, **95**, 675-685.
195. J. Datta and P. Parcheta, *Iranian Polymer Journal*, 2017, **26**, 453-466.
196. C. D. Tran, J. Chen, J. K. Keum and A. K. Naskar, *Advanced Functional Materials*, 2016, **26**, 2677-2685.
197. S. Xiao, J. Feng, J. Zhu, X. Wang, C. Yi and S. Su, *Journal of Applied Polymer Science*, 2013, **130**, 1308-1312.
198. B. Košíková, A. Gregorova, A. Osvald and J. Krajčovičová, *Journal of applied polymer science*, 2007, **103**, 1226-1231.
199. B. Košíková and A. Gregorová, *Journal of applied polymer science*, 2005, **97**, 924-929.
200. D. Barana, S. D. Ali, A. Salanti, M. Orlandi, L. Castellani, T. Hanel and L. Zoia, *ACS Sustainable Chemistry & Engineering*, 2016, **4**, 5258-5267.
201. S. Botros, M. Eid and Z. Nageeb, *Journal of applied polymer science*, 2006, **99**, 2504-2511.
202. Y. Ikeda, T. Phakkeeree, P. Junkong, H. Yokohama, P. Phinyocheep, R. Kitano and A. Kato, *RSC advances*, 2017, **7**, 5222-5231.
203. P. Frigerio, L. Zoia, M. Orlandi, T. Hanel and L. Castellani, *BioResources*, 2014, **9**, 1387-1400.
204. N. A. Mohamad Aini, N. Othman, M. H. Hussin, K. Sahakaro and N. Hayeemasae, *Processes*, 2019, **7**, 315.
205. C. Jiang, H. He, X. Yao, P. Yu, L. Zhou and D. Jia, *Journal of Applied Polymer Science*, 2018, **135**, 45759.
206. C. Jiang, H. He, X. Yao, P. Yu, L. Zhou and D. Jia, *Journal of Applied Polymer Science*, 2015, **132**.
207. C. Jiang, H. He, X. Yao, P. Yu, L. Zhou and D. Jia, *Journal of applied polymer science*, 2014, **131**.
208. J. Dörrstein, R. Scholz, D. Schwarz, D. Schieder, V. Sieber, F. Walther and C. Zollfrank, *Composite Structures*, 2018, **189**, 349-356.
209. B. Xue, X. Wang, L. Yu, B. Di, Z. Chen, Y. Zhu and X. Liu, *International Journal of Biological Macromolecules*, 2020, **145**, 410-416.
210. K. Bahl, T. Miyoshi and S. C. Jana, *Polymer*, 2014, **55**, 3825-3835.
211. H. Wang, W. Liu, J. Huang, D. Yang and X. Qiu, *Polymers*, 2018, **10**, 1033.
212. H. Wang, W. Liu, Z. Tu, J. Huang and X. Qiu, *Industrial & Engineering Chemistry Research*, 2019, **58**, 23114-23123.
213. S. H. Barnes, M. Goswami, N. A. Nguyen, J. K. Keum, C. C. Bowland, J. Chen and A. K. Naskar, *Macromolecular Rapid Communications*, 2019, **40**, 1900059.
214. G. G. Jang, N. A. Nguyen, C. C. Bowland, H. C. Ho, J. K. Keum and A. K. Naskar, *Composites Science and Technology*, 2020, **199**, 108352.
215. G. Xu, G. Yan and J. Zhang, *Polymer Bulletin*, 2015, **72**, 2389-2398.
216. J. Huang, W. Liu and X. Qiu, *ACS Sustainable Chemistry & Engineering*, 2019, **7**, 6550-6560.

View Article Online
DOI: 10.1039/D1GC01115D

217. R. Muthuraj, M. Misra, F. Defersha and A. K. Mohanty, *Composites Part A: Applied Science and Manufacturing*, 2016, **83**, 120-129.
218. R. Muthuraj, M. Misra and A. Mohanty, in *Biocomposites*, Elsevier, 2015, pp. 93-140.
219. R. Muthuraj and T. Mekonnen, *Macromolecular Materials and Engineering*, 2018, **303**, 1800366.
220. K. Prukkaewkanjana, S. Thanawan and T. Amornsakchai, *Polymer Testing*, 2015, **45**, 76-82.
221. Y. Zhou, M. Fan, L. Chen and J. Zhuang, *Composites Part B: Engineering*, 2015, **76**, 180-191.
222. R. Muthuraj, M. Misra and A. K. Mohanty, *RSC advances*, 2017, **7**, 27538-27548.
223. R. Muthuraj, M. Misra and A. K. Mohanty, *Journal of Applied Polymer Science*, 2018, **135**, 45726.
224. A. Nair and R. Joseph, in *Chemistry, manufacture and applications of natural rubber*, Elsevier, 2014, pp. 249-283.
225. N. Arumugam, K. T. Selvy, K. V. Rao and P. Rajalingam, *Journal of applied polymer science*, 1989, **37**, 2645-2659.
226. H. Ismail, M. Edyham and B. Wirjosentono, *Polymer testing*, 2002, **21**, 139-144.
227. V. Murty and S. De, *Journal of applied polymer science*, 1984, **29**, 1355-1368.
228. N. Lopattananon, K. Panawarangkul, K. Sahakaro and B. Ellis, *Journal of Applied Polymer Science*, 2006, **102**, 1974-1984.
229. S. Joseph, S. P. Appukuttan, J. M. Kenny, D. Puglia, S. Thomas and K. Joseph, *Journal of Applied Polymer Science*, 2010, **117**, 1298-1308.
230. V. G. Geethamma, G. Kalaprasad, G. Groeninckx and S. Thomas, *Composites Part A: Applied Science and Manufacturing*, 2005, **36**, 1499-1506.
231. M. Jacob, B. Francis, S. Thomas and K. T. Varughese, *Polymer Composites*, 2006, **27**, 671-680.
232. A. Hussain, A. Abdel-Kader and A. Ibrahim, *Nat. Sci*, 2010, **8**, 82-93.
233. L. Tzounis, S. Debnath, S. Rooj, D. Fischer, E. Mäder, A. Das, M. Stamm and G. Heinrich, *Materials & Design*, 2014, **58**, 1-11.
234. V. G. Geethamma, R. Joseph and S. Thomas, *Journal of Applied Polymer Science*, 1995, **55**, 583-594.
235. S. Joseph, K. Joseph and S. Thomas, *International Journal of Polymeric Materials and Polymeric Biomaterials*, 2006, **55**, 925-945.
236. M. J. John, K. T. Varughese and S. Thomas, *Journal of Natural Fibers*, 2008, **5**, 47-60.
237. M.-D. Stelescu, E. Manaila, G. Craciun and C. Chirila, *Materials*, 2017, **10**, 787.
238. M. Jacob, K. Varughese and S. Thomas, *Biomacromolecules*, 2005, **6**, 2969-2979.
239. M. Jacob, K. T. Varughese and S. Thomas, *Journal of Materials Science*, 2006, **41**, 5538-5547.
240. A. P. Haseena, G. Unnikrishnan and G. Kalaprasad, *Composite Interfaces*, 2007, **14**, 763-786.
241. A. T. Collier, *Journal*, 1911.
242. H. Ismail, S. Shuhelmy and M. R. Edyham, *European Polymer Journal*, 2002, **38**, 39-47.
243. Z. M. Ishak and A. A. Bakar, *European Polymer Journal*, 1995, **31**, 259-269.
244. C. Pattamaprom, K. Bandidchutikun, S. Sotananan and S. Phrommedetch, *Thammasat Int. J. Sc. Technol*, 2008, **13**, 36-43.
245. W. Wongsorat, N. Suppakarn and K. Jarukumjorn, *Journal of Composite Materials*, 2014, **48**, 2401-2411.
246. H. Ismail, A. Rusli and A. A. Rashid, *Polymer testing*, 2005, **24**, 856-862.
247. H. Ismail and F. Haw, *Journal of applied polymer science*, 2008, **110**, 2867-2876.
248. E. Khalaf, H. Farag and E. Abdel-Bary, *Polymers and Polymer Composites*, 2020, **28**, 663-677.
249. F. Chigondo, P. Shoko, B. C. Nyamunda and M. Moyo, 2013.
250. E. Manaila, G. Craciun and D. Ighigeanu, *Polymers*, 2020, **12**, 2437.
251. H. Osman, H. Ismail and M. Mustapha, *Journal of Composite Materials*, 2010, **44**, 1477-1491.
252. M. Jacob, K. T. Varughese and S. Thomas, *Biomacromolecules*, 2005, **6**, 2969-2979.

View Article Online
DOI: 10.1039/D1GC01115D

253. K. Adekunle, S.-W. Cho, C. Patzelt, T. Blomfeldt and M. Skrifvars, *Journal of Reinforced Plastics and Composites*, 2011, **30**, 685-697.
254. M. Picard, S. Thakur, M. Misra, D. F. Mielewski and A. K. Mohanty, *Scientific Reports*, 2020, **10**, 3310.
255. O. Das, A. K. Sarmah and D. Bhattacharyya, *Science of The Total Environment*, 2015, **512-513**, 326-336.
256. Q. Zhang, W. Yi, Z. Li, L. Wang and H. Cai, *Polymers*, 2018, **10**, 286.
257. E. O. Ogunsona, T. Grovu and T. H. Mekonnen, *Sustainable Materials and Technologies*, 2020, **26**, e00208.
258. B.P. Chang, A. Gupta, T.H. Mekonnen, Chemosphere, 2021, 282, 131062.
259. S. Zhang, S.-F. Jiang, B.-C. Huang, X.-C. Shen, W.-J. Chen, T.-P. Zhou, H.-Y. Cheng, B.-H. Cheng, C.-Z. Wu, W.-W. Li, H. Jiang and H.-Q. Yu, *Nature Sustainability*, 2020, **3**, 753-760.
260. D. Tadele, P. Roy, F. Defersha, M. Misra and A. K. Mohanty, *Clean Technologies and Environmental Policy*, 2020, **22**, 639-649.
261. A. Mohanty, M. Misra, E. O. Ogunsona, A. J. Anstey, S. E. T. GALVEZ, A. M. F. M.-S. CODOU and D. F. JUBINVILLE, *Journal*, 2020.
262. A. Mohanty, M. Misra, B. Atul and A. Rodriguez-uribe, *Journal*, 2019.
263. T. Wang, A. Rodriguez-Uribe, M. Misra and A. K. Mohanty, *2018*, 2018, **13**, 20.
264. S. K. Karmee, G. Kumari and B. Soni, *Bioresource Technology*, 2020, **318**, 124071.
265. Q. Ma, Y. Yu, M. Sindoro, A. G. Fane, R. Wang and H. Zhang, *Advanced Materials*, 2017, **29**, 1605361.
266. J.-H. Park, Y. S. Ok, S.-H. Kim, J.-S. Cho, J.-S. Heo, R. D. Delaune and D.-C. Seo, *Chemosphere*, 2016, **142**, 77-83.
267. Z. Ma, Y. Yang, Q. Ma, H. Zhou, X. Luo, X. Liu and S. Wang, *Journal of Analytical and Applied Pyrolysis*, 2017, **127**, 350-359.
268. Q. Fang, B. Chen, Y. Lin and Y. Guan, *Environmental Science & Technology*, 2014, **48**, 279-288.
269. E. Behazin, M. Misra and A. K. Mohanty, *Composites Part B: Engineering*, 2017, **118**, 116-124.
270. M. A. Abdelwahab, A. Rodriguez-Uribe, M. Misra and A. K. Mohanty, *Molecules*, 2019, **24**, 4026.
271. T. Balint, B. P. Chang, A. K. Mohanty and M. Misra, *Molecules*, 2020, **25**, 1455.
272. B. Sajjadi, W.-Y. Chen and N. O. Egiebor, *Reviews in Chemical Engineering*, 2019, **35**, 735.
273. O. Das, N. K. Kim, A. L. Kalamkarov, A. K. Sarmah and D. Bhattacharyya, *Polymer Degradation and Stability*, 2017, **144**, 485-496.
274. O. Das, D. Bhattacharyya, D. Hui and K.-T. Lau, *Composites Part B: Engineering*, 2016, **106**, 120-128.
275. Z. Li, C. Reimer, M. Picard, A. K. Mohanty and M. Misra, *Frontiers in Materials*, 2020, **7**.
276. M. R. Snowdon, F. Wu, A. K. Mohanty and M. Misra, *RSC Advances*, 2019, **9**, 6752-6761.
277. B. P. Chang, A. K. Mohanty and M. Misra, *Journal of Applied Polymer Science*, 2019, **136**, 47722.
278. J. Andrzejewski, M. Misra and A. K. Mohanty, *Journal of Applied Polymer Science*, 2018, **135**, 46449.
279. E. O. Ogunsona, M. Misra and A. K. Mohanty, *Composites Part A: Applied Science and Manufacturing*, 2017, **98**, 32-44.
280. P. Myllytie, M. Misra and A. K. Mohanty, *ACS Sustainable Chemistry & Engineering*, 2016, **4**, 102-110.
281. E. O. Ogunsona, M. Misra and A. K. Mohanty, *Polymer Degradation and Stability*, 2017, **139**, 76-88.
282. S. C. Peterson, *Journal of Composites Science*, 2020, **4**, 147.
283. S. C. Peterson, S. R. Chandrasekaran and B. K. Sharma, *Journal of Elastomers & Plastics*, 2016, **48**, 305-316.

View Article Online
DOI: 10.1039/D1GC01115D

284. S. C. Peterson, *Journal of Elastomers & Plastics*, 2012, **44**, 43-54.
285. L. Jong, *Polymer Composites*, 2013, **34**, 697-706.
286. L. Jong, S. C. Peterson and M. A. Jackson, *Journal of Polymers and the Environment*, 2014, **22**, 289-297.
287. X. Meng, Y. Zhang, J. Lu, Z. Zhang, L. Liu and P. K. Chu, *Journal of Applied Polymer Science*, 2013, **130**, 4534-4541.
288. M. Sutikno, P. Marwoto and S. Rustad, *Carbon*, 2010, **48**, 3616-3620.
289. S. C. Peterson, M. A. Jackson, S. Kim and D. E. Palmquist, *Powder Technology*, 2012, **228**, 115-120.
290. S. C. Peterson and S. Kim, *Journal of Polymers and the Environment*, 2020, **28**, 317-322.
291. S. C. Peterson, *Journal of Composites Science*, 2019, **3**, 107.
292. M.-C. Li, Y. Zhang and U. R. Cho, *Materials & Design*, 2014, **63**, 565-574.
293. M. Lay, A. Rusli, M. K. Abdullah, Z. A. Abdul Hamid and R. K. Shuib, *Composites Part B: Engineering*, 2020, **201**, 108366.
294. Y. Zhang, D. Fei, G. Xin and U.-R. Cho, *Journal of Composite Materials*, 2016, **50**, 2987-2999.
295. Y. Zhang, X. Li, X. Ge, F. Deng and U. R. Cho, *Macromolecular Research*, 2015, **23**, 952-959.
296. M. Qian, W. Huang, J. Wang, X. Wang, W. Liu and Y. Zhu, *Polymers*, 2019, **11**, 1763.
297. B. Xue, X. Wang, J. Sui, D. Xu, Y. Zhu and X. Liu, *Industrial Crops and Products*, 2019, **141**, 111791.
298. C. Jiang, J. Bo, X. Xiao, S. Zhang, Z. Wang, G. Yan, Y. Wu, C. Wong and H. He, *Waste Management*, 2020, **102**, 732-742.
299. M. Giorcelli and M. Bartoli, *Polymers*, 2019, **11**, 1916.
300. N. Nan, D. B. DeVallance, X. Xie and J. Wang, *Journal of Composite Materials*, 2016, **50**, 1161-1168.
301. M. Abdelwahab, A. Codou, A. Anstey, A. K. Mohanty and M. Misra, *Composites Part A: Applied Science and Manufacturing*, 2020, **129**, 105695.
302. S. Li, A. Huang, Y.-J. Chen, D. Li and L.-S. Turng, *Composites Part B: Engineering*, 2018, **153**, 277-284.
303. M. Myhre and D. A. MacKillop, *Rubber Chemistry and Technology*, 2002, **75**, 429-474.
304. J. D. Martínez, N. Puy, R. Murillo, T. García, M. V. Navarro and A. M. Mastral, *Renewable and Sustainable Energy Reviews*, 2013, **23**, 179-213.
305. A. S. R. Subramanian, T. Gundersen and T. A. Adams, *Energy*, 2021, **223**, 119990.
306. F. Alkadi, J. Lee, J.-S. Yeo, S.-H. Hwang and J.-W. Choi, *International Journal of Precision Engineering and Manufacturing-Green Technology*, 2019, **6**, 211-222.
307. H. Yaqoob, Y. H. Teoh, F. Sher, M. A. Jamil, D. Murtaza, M. Al Qubeissi, M. UI Hassan and M. A. Mujtaba, *Sustainability*, 2021, **13**, 3214.
308. C. Sathiskumar and S. Karthikeyan, *Sustainable Materials and Technologies*, 2019, **22**, e00125.
309. Ł. Zedler, X. Colom, M. R. Saeb and K. Formela, *Composites Part B: Engineering*, 2018, **145**, 182-188.
310. S. Rooj, G. C. Basak, P. K. Maji and A. K. Bhowmick, *Journal of Polymers and the Environment*, 2011, **19**, 382-390.
311. S. K. Mandal, N. Alam and S. C. Debnath, *Rubber Chemistry and Technology*, 2012, **85**, 629-644.
312. M. Kojima, M. Tosaka and Y. Ikeda, *Green Chemistry*, 2004, **6**, 84-89.
313. X.-X. Zhang, C.-H. Lu and M. Liang, *Journal of Applied Polymer Science*, 2007, **103**, 4087-4094.
314. A. Tukachinsky, D. Schworm and A. I. Isayev, *Rubber Chemistry and Technology*, 1996, **69**, 92-103.
315. K. Aoudia, S. Azem, N. Aït Hocine, M. Gratton, V. Pettarin and S. Seghar, *Waste Management*, 2017, **60**, 471-481.

View Article Online
DOI: 10.1039/D1GC01115D

316. X. Colom, M. Marín-Genescà, R. Mujal, K. Formela and J. Cañavate, *Journal of Composite Materials*, 2018, **52**, 3099-3108.
317. V. Tatangelo, I. Mangili, P. Caracino, G. Bestetti, E. Collina, M. Anzano, P. Branduardi, R. Posteri, D. Porro, M. Lasagni and A. Franzetti, *Polymer Degradation and Stability*, 2019, **160**, 102-109.
318. Y. Li, S. Zhao and Y. Wang, *Journal of Polymers and the Environment*, 2012, **20**, 372-380.
319. Y. Li, S. Zhao and Y. Wang, *Journal of Polymer Research*, 2012, **19**, 9864.
320. L. Asaro, M. Gratton, S. Seghar and N. Aït Hocine, *Resources, Conservation and Recycling*, 2018, **133**, 250-262.
321. I. Mangili, E. Collina, M. Anzano, D. Pitea and M. Lasagni, *Polymer Degradation and Stability*, 2014, **102**, 15-24.
322. E. Markl and M. Lackner, *Materials*, 2020, **13**, 1246.
323. M. Meysami, C. Tzoganakis, P. Mutyala, S. H. Zhu and M. Bulsari, *International Polymer Processing*, 2017, **32**, 183-193.
324. X. Ren and K. Cornish, *Industrial Crops and Products*, 2019, **138**, 111440.
325. G. F. C. Rodrigues and N. P. Oliveira, in *Water, Energy and Food Nexus in the Context of Strategies for Climate Change Mitigation*, eds. W. Leal Filho and J. B. S. de Andrade Guerra, Springer International Publishing, Cham, 2020, DOI: 10.1007/978-3-030-57235-8_21, pp. 271-285.
326. H.-R. Hein, K. Akutagawa, H. Heguri and N. Yamagishi, *ATZ worldwide eMagazine*, 2011, **113**, 36-41.
327. P. H. Sandstrom, *Google Patents, Rubber containing starch reinforcement and tire having component thereof*, 2002.
328. J. Araujo-Morera, M. Hernández Santana, R. Verdejo and M. A. López-Manchado, *Polymers*, 2019, **11**, 2122.
329. A. Das, D.-Y. Wang, A. Leuteritz, K. Subramaniam, H. C. Greenwell, U. Wagenknecht and G. Heinrich, *Journal of Materials Chemistry*, 2011, **21**, 7194-7200.
330. D. Wang, L. Zhao, H. Ma, H. Zhang and L.-H. Guo, *Environmental Science & Technology*, 2017, **51**, 10137-10145.
331. M. Chevallet, G. Veronesi, A. Fuchs, E. Mintz, I. Michaud-Soret and A. Deniaud, *Biochimica et Biophysica Acta (BBA) - General Subjects*, 2017, **1861**, 1566-1577.
332. M. Przybyszewska, M. Zaborski, B. Jakubowski and J. Zawadiak, *Express Polym. Lett*, 2009, **3**, 256-266.
333. G. Zhang, X. Zhou, K. Liang, B. Guo, X. Li, Z. Wang and L. Zhang, *ACS Sustainable Chemistry & Engineering*, 2019, **7**, 11712-11720.
334. G. Heideman, J. W. M. Noordermeer, R. N. Datta and B. van Baarle, *Rubber Chemistry and Technology*, 2005, **78**, 245-257.
335. G. Heideman, J. W. M. Noordermeer, R. N. Datta and B. van Baarle, *Rubber Chemistry and Technology*, 2004, **77**, 336-355.
336. G. Heideman, J. W. M. Noordermeer, R. N. Datta and B. van Baarle, *Rubber Chemistry and Technology*, 2006, **79**, 561-588.
337. K. Roy, M. N. Alam, S. K. Mandal and S. C. Debnath, *Journal of Applied Polymer Science*, 2015, **132**.
338. B. L. DeButts, N. Chauhan and J. R. Barone, *Journal of Applied Polymer Science*, 2019, **136**, 48141.
339. G. Zhang, K. Liang, H. Feng, J. Pang, N. Liu, X. Li, X. Zhou, R. Wang and L. Zhang, *Industrial & Engineering Chemistry Research*, 2020, **59**, 10447-10456.
340. G. Zhang, H. Feng, K. Liang, Z. Wang, X. Li, X. Zhou, B. Guo and L. Zhang, *Science Bulletin*, 2020, **65**, 889-898.

View Article Online
DOI: 10.1039/D1GC01115D

341. J. Shi, H. Zou, L. Ding, X. Li, K. Jiang, T. Chen, X. Zhang, L. Zhang and D. Ren, *Polymer Degradation and Stability*, 2014, **99**, 166-175.
342. N. Ye, J. Zheng, X. Ye, J. Xue, D. Han, H. Xu, Z. Wang and L. Zhang, *Composites Part B: Engineering*, 2020, **202**, 108301.
343. W. L. Hergenrother, C. J. Lin, T. E. Hogan and A. S. Hilton, *Journal*, 2012.
344. M. Prochoń and Y. H. T. Ntumba, *Rubber Chemistry and Technology*, 2015, **88**, 258-275.
345. H. M. da Costa, L. L. Y. Visconte, R. C. R. Nunes and C. R. G. Furtado, *Journal of Applied Polymer Science*, 2003, **90**, 1519-1531.
346. H. M. da Costa, L. L. Y. Visconte, R. C. R. Nunes and C. R. G. Furtado, *Journal of Applied Polymer Science*, 2003, **87**, 1405-1413.
347. C. S. Barrera and K. Cornish, *Industrial Crops and Products*, 2017, **107**, 217-231.
348. C. S. Barrera and K. Cornish, *Journal of Polymers and the Environment*, 2015, **23**, 437-448.
349. D. Lhamo and C. McMahan, *Rubber Chemistry and Technology*, 2017, **90**, 387-404.
350. C. A. de Assis, M. C. Iglesias, M. Bilodeau, D. Johnson, R. Phillips, M. S. Peresin, E. M. Bilek, O. J. Rojas, R. Venditti and R. Gonzalez, *Biofuels, Bioproducts and Biorefining*, 2018, **12**, 251-264.
351. N. M. Clauser, F. E. Felissia, M. C. Area and M. E. Vallejos, *Chemical Engineering Research and Design*, 2021, **167**, 1-14.